Checks and Balances of T cells in Inflammatory Environments

by

Rebekah E. Dadey

B.S., Pennsylvania State University, 2015

Submitted to the Graduate Faculty of the

School of Medicine in partial fulfillment

of the requirements for the degree of

Doctor of Philosophy

University of Pittsburgh

2021

UNIVERSITY OF PITTSBURGH

SCHOOL OF MEDICINE

This dissertation was presented

by

Rebekah E. Dadey

It was defended on

July 1, 2021

and approved by

Greg Delgoffe, PhD., Associate Professor, Department of Immunology

Dennis Kostka, PhD., Associate Professor, Department of Developmental Biology

Amanda Poholek, PhD., Assistant Professor, Department of Immunology

Anuradha Ray, PhD., Professor, Department of Immunology

Dissertation Director: Dario A.A. Vignali PhD, Frank Dixon Chair in Cancer Immunology, Distinguished Professor and Vice Chair, Department of Immunology

Checks and Balances of T cells in Inflammatory Environments

Rebekah E. Dadey, PhD

University of Pittsburgh, 2021

The immune system is composed of many checks and balances that are critical to limiting disease and maintaining homeostasis. T cells are critical regulators of this balance. For example, $CD8^+$ T cells can limit diseases such as cancer and infection through induction of apoptosis in malignant and infected cells, respectively. Conversely, Regulatory T cells (Tregs), a subset of $CD4^+$ T cells, are a suppressive population that can limit overt T cell activation and prevent autoimmunity.

However, these checks and balances can be potentially damaging if they are off-balance. $CD8^+$ can inappropriately induce cell death of various cells which can induce disease. For example, cytotoxicity towards pancreatic beta cells, can induce autoimmune diabetes. Likewise, Tregs can detrimentally suppress T cell activation and function in the tumor microenvironment (TME) to limit clearance of the tumor. Therefore, identifying these mechanisms and regulation of these mechanisms of inappropriate function in inflammatory environments will be critical to limit disease.

Therefore, I examined how this balance may be maintained through epigenetic regulation in the TME and production of cytotoxic molecules in the TME and diabetic islet. Specifically, in **Chapter 3**, I demonstrate that Tregs alter their epigenome to aid in their suppression of the anti-tumor response. In **Chapter 4**, I show that Tregs do not require TNF-related apoptosis-inducing ligand (TRAIL) as a means of suppression in the TME

nor diabetic islet but rather are capable of using other suppressive molecules in its absence. In **Chapter 5**, I demonstrate $CD8^+$ T cell-restricted deletion of *Tnfsf10* leads to almost complete protection from autoimmune diabetes. Understanding this regulation of checks and balances may aid in future therapeutic approaches to cancer and autoimmune disease.

In addition to my thesis study, **Appendix A** shows data in which I examined various models of tumor growth in a mouse model with genetic deletion of Neuropilin-1 (Nrp1) on Tregs and **Appendix B** shows data in which I examined the role of Nrp1 on Tregs in fetal maternal tolerance. Finally **Appendix C** identifies publications that I have contributed to and awards that I have received during my graduate training.

Table of Contents

List of Tables

List of Figures

Preface

It has been an incredibly difficult road to my PhD but I have learned so much and matured into the scientist and person I want to be. Moreover, I would not have gotten this far without the many people who have encouraged and mentored me along the way. First, I am thankful to my mentor, Dario Vignali; my training and development would not have been possible without his encouragement and mentorship. I am grateful for all his help and support throughout the years. I am hopeful to continue our conversations and to update him with my successes in the future.

Next, I am so thankful to my thesis committee members, Greg Delgoffe, Dennis Kostka, Amanda Poholek, and Anuradha Ray. They have been instrumental in providing guidance to my experiments, encouragement when I was struggling, and my overall development as a scientist. I am especially grateful to Amanda Poholek; she always had her door open for me and encouraged me when I needed it the most.

I am also grateful to three mentors in the lab, Creg Workman, Kate Vignali, and Tullia Bruno. Creg has been my personal in-lab cheerleader for many years and has been someone that I can meet with when I have any questions. He has always pushed me to do better, and I am very appreciative of his support. Kate has been very kind to me and has helped me with lab work in many ways and I am grateful for her help. Tullia Bruno has been a great mentor to me and I am thankful for her. She has always encouraged me and was a mentor to me when I needed it the most. She has always tried to push me in the right direction, while reminding me that life is always more important than your job.

Andrea Workman and I have become close in my last year of graduate school. She helped and is helping me through the worst time in my life and I am forever grateful for her friendship, kindness, and understanding.

I do not believe I would have been able to make it through my graduate school career without Angela Gocher. She has been the best person, scientist, and friend. Anyone who has the pleasure of working with her knows her for her kind huge heart, relentless perseverance, and extremely bright mind. She never judges anyone for “dumb” questions and is always willing to help or lend an ear, even with her extremely busy schedule. I am so eternally grateful for her friendship and will miss working alongside her every day, but I am excited to see how far she goes in her career.

I would like to thank those that have contributed to the data and data analysis throughout the years such as Ting Wang and Tao Sun from the laboratory of Dr Wei Chen (Department of Biostatistics, University of Pittsburgh School of Public Health), Tracy Tabib from the laboratory of Dr. Robert Lafyatis (Division of Rheumatology and Clinical Immunology, Department of Medicine, University of Pittsburgh School of Medicine), Tony Cillo, and Dhivyaa Rajasundaram (Department of Pediatrics, UPMC Children’s Bioinformatics Core) for the ATAC and RNAseq analysis.

There are many others in the lab that I cannot thank enough. First, Stephanie Grebinoski has been instrumental in the autoimmune diabetes work and many of these studies would have been impossible with her. She is also a very kind person and a great friend. Gracie Liu has been so helpful since my start in the lab and I admire her for her intelligence and critical thinking skills. Sayali Onkar has been an extremely supportive voice and has been such a great person to vent any frustrations to; I will miss our

conversations and hope they will continue after our graduate program. Erin Brunazzi for all the murine and emotional support. Deepali Sawant, Sherry Zhang, Abby Overacre-Delgoffe, Ellen Scott, Hiroshi Yano, Cheng Ye, Feng Shan, Uzo Uche, Elisa Ruffo, Chris Chuckran, Aarika Yates, and many others have been wonderful co-workers and good friends to me throughout the years.

I definitely would not been able to get through this graduate program without my family. First, I am grateful to Debbie and Bruce Johnson for being so kind and supportive. Next, my parents have been extremely supportive. They have called me in my times of struggle and encouraged me over and over again, which I am so grateful for. My older brother Nathan has supported me constantly. I am so grateful that he is someone I can always look up to and count on.

I wish words were enough to say how thankful I am to my fiancé, Brian Johnson. He has been there for me every day, through every single tear, through every breakdown. I know I would have quit graduate school if it was not for him. He was there for me during the struggles in the lab, development and explosion of my mental health struggles, and the worst loss I will ever have in my lifetime. Through all of this, he was always gentle, kind, and understanding and never harsh or judgmental. I am so grateful for him and I hope that I can somehow repay him some day for his kindness.

Finally, I have to thank my little brother Alex. I wish I had a whole dissertation to describe how much he means to me. He was the best person that anyone could ever know. He would call me to check in every week and would genuinely care how I was doing. He supported me through every minute of graduate school and reminded me that life and love is way more important than another experiment. There is not a minute of my

life that I don’t think of him. I miss him greatly and will never forget him. If I could dedicate this dissertation to someone, it would absolutely be him.

1.0 Introduction

Portions of this chapter (1.1.3 and 1.3) were taken from my previous publication ***Dadey, R.E.,*** *Workman, C.J., Vignali, D.A.A. "Regulatory T cells in the Tumor Microenvironment" Adv Exp Med Biol. 2020;1273:105-134. doi: 10.1007/978-3-030-49270-0_6, under copyright permission of Springer Nature (license number 4992560654498). Section 1.5.2 was taken from my previous publication* ***Dadey, R.E.****, Grebinoski, S., Zhang, Q., Brunazzi, E.A., Burton, A., Workman, C.J., Vignali, D.A.A. "Regulatory T Cell-Derived TRAIL Is Not Required for Peripheral Tolerance" Immunohorizons. 2021:Jan22;5(1):48-58. doi: 10.4049/immunohorizons.2000098 under our own Copyright (open access).*

Regulatory T cells and $CD8^+$ T cells are critical mediators in maintaining homeostasis and limiting pathogen infection, respectively. However, these cells can also contribute to the progression of disease in cancer and autoimmune diabetes. Therefore, studies to understand their function and regulation in cancer and autoimmune disease will lead to better therapeutic strategies and ultimately favorable disease outcomes.

1.1 Regulatory T cells

Regulatory T cells (Tregs) are an immunosuppressive subset of $CD4^+$ T cells that suppress activated immune cells and limit autoimmunity. Tregs are also an effective

barrier to the anti-tumor response [1,2]. There are two types of Tregs commonly identified in vivo: thymically-derived Tregs (tTregs), and peripherally-derived Tregs (pTregs), the latter of which are induced from a $CD4^+$ Forkhead box protein $P3^-$ ($Foxp3^-$) precursor (pTregs) [3]. The majority of the in vivo pool of Tregs are likely thymically-derived, and therefore will be focused on in the text, unless otherwise stated [4].

1.1.1 Hallmarks and markers of Tregs

Tregs are incredibly unique and have many characteristics that are critical for their function. Expression of Foxp3 and CD25 are two key markers of Tregs.

1.1.1.1 FOXP3

Foxp3 is a transcriptional activator and repressor either through direct DNA binding or binding to other transcription factors to alter their interactions with DNA [5]. Some examples of genes regulated by Foxp3 and critical in Treg function are *Il2ra* (encodes CD25), *Tnfrsf18* (encodes GITR/TNFRSF18), and *Nrp1* (encodes Neuropilin-1, Nrp1) [6,7]. Foxp3 can also transcriptionally repress $CD4^+$ $Foxp3^-$ T conventional (Tconv) genes such as *Ifng* (encodes Interferon-γ) and *Il2* (encodes IL-2), enhancing a suppressive phenotype [8]. While regulation of these genes by Foxp3 plays an important role in Treg development, maintenance, and function, ectopic expression of *Foxp3* will confer a suppressive phenotype but does not confer all signature Treg genes [9-12]. Consequently, other key molecules may regulate Treg function.

1.1.1.2 CD25 and IL-2

In addition using the high expression level in identifying Tregs, CD25 (IL-2Rα) also plays a critical role in the development, maintenance, and function of Tregs. CD25, or IL-2Rα, is one component of the IL-2 receptor, consisting of CD25, CD122 (IL-2Rβ), and CD132 (common gamma chain, γc). IL-2 binding to its receptor induces a signaling cascade that results in the Janus kinase (JAK)-mediated tyrosine phosphorylation and activation of signal transducer and activator of transcription 5 (STAT5). Phosphorylated STAT5 homodimers translocate to the nucleus to facilitate the induction of *Foxp3* expression through binding to the promoter, conserved non-coding sequence 2 (CNS2), and the distal enhancer CNS4 [13-15]. Induction of Foxp3 via STAT5 is critical for Treg development and homeostasis [16-18]. STAT5 also induces expression *of Il2ra*, to enforce a positive feedback loop, as well as other key Treg functional genes, such as *Ctla4*, *Tnfrsf18*, and *Icos* [17]. Importantly, the IL-2/STAT5 pathway is not only required for Treg development and stability but also necessary for Treg function.

As Tregs are unable to make their own IL-2, they rely on other cells as their source of IL-2 [17]. There has been speculation that due to their high CD25 expression, Tregs can sequester IL-2 away from other cells as a form of suppression [19]. However, it has been highly contended whether this occurs in vivo. Nonetheless, Treg expression of CD25 and dependence on IL-2 is a key marker of Tregs.

1.1.2 Treg Function

There are four main mechanisms of Treg suppression: [i] production of inhibitory cytokines such as IL-10, IL-35, and TGFβ [20-22] [ii] cytolysis with molecules such as

Granzyme, Perforin, and TRAIL (elaborated on in Section 1.5.2) [23-26] [iii] targeting dendritic cell (DC) function and inhibitory receptor expression of CTLA-4 and LAG3 [27,28-30] and [iv] metabolic disruption by CD39 and CD73, and sequestering IL-2 via high CD25 expression (Fig 1) [19,31-37].

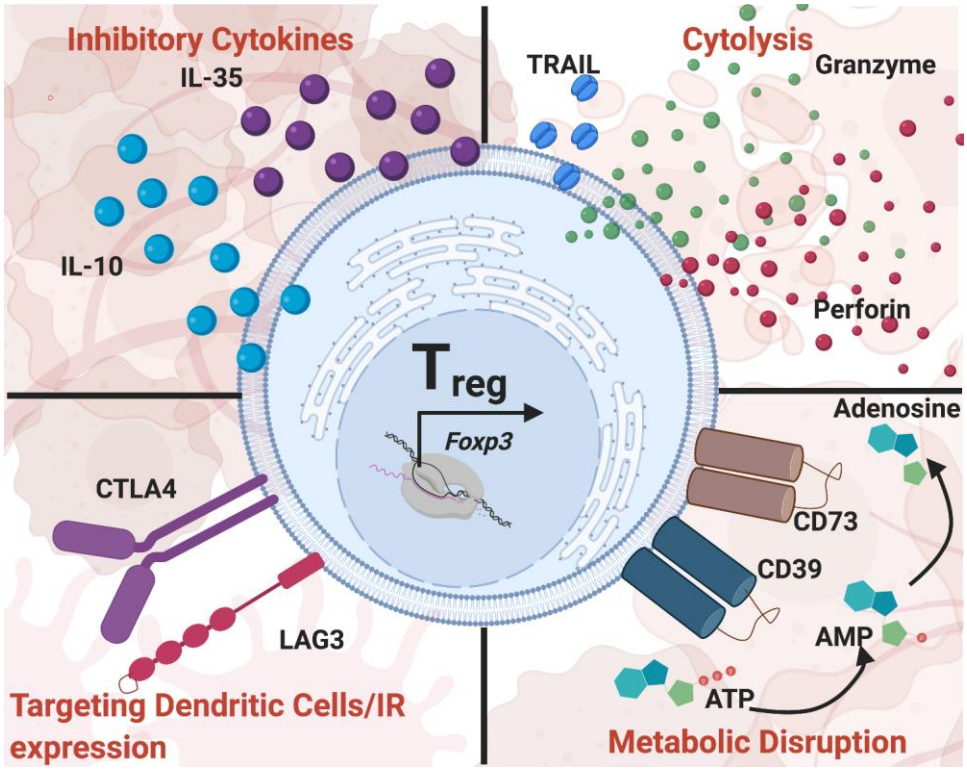

Figure 1 Mechanisms of Treg Suppression

1.2 CD8$^+$ T cells

CD8$^+$ T cells can effectively control infection and cancer development to limit pathology. However, CD8$^+$ T cells can also can be toxic if they are unproperly activated

resulting in overt tissue damage and can also promote or exacerbate lead to autoimmune disease.

1.2.1 $CD8^+$ T cell Function

$CD8^+$ T cells can be cytotoxic in four main ways (Fig 2). $CD8^+$ T cells can kill through [i] cytolysis with molecules such as Granzyme, Perforin [ii] binding of FasL to Fas expressing target cells and [iii] production of inflammatory cytokines such as IFNγ and TNFα [38]. TRAIL also has a role in $CD8^+$ T cell-mediated killing and will be discussed in Section 1.5.2. Granzyme, Perforin, FasL, and TRAIL can induce cellular apoptosis in responding cells, while IFNγ and TNFα can recruit macrophages and limit viral replication in responding cells [38]. $CD8^+$ T cells also possess an ability to differentiate into memory precursors and memory T cells; however, herein will focus on their cytotoxic potential.

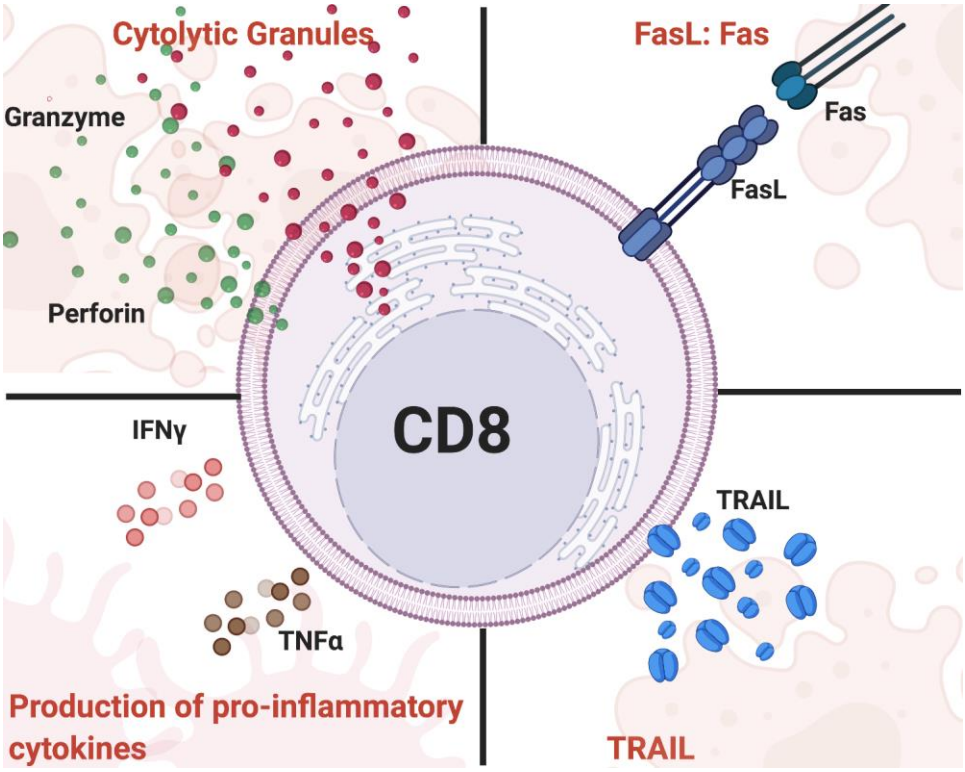

Figure 2 Mechanisms of CD8⁺ T cell Function

1.3 Cancer

Cancer is one of the top leading causes of death globally. Over 19.3 million new cancer cases and 9.96 million deaths are estimated for 2021 worldwide [39]. In the United States alone, over 1.9 million projected new cases and 608,570 fatalities are expected in 2021 [40,41]. Cases and fatalities are expected to continue increasing by 2040 [40,42,43]. Cancer is also an enormous financial burden on the health care system. Cancer costs in the United States are projected to be as high as $175 billion in 2020, with cancer patients paying four times higher expenditures than those without cancer [44,45].

1.3.1 Cancer Development and Hallmarks

Cells are regulated by signals that control cell growth, proliferation, and cell death. However, DNA mutations can accumulate due to environmental cues, oncoviral infection, or inherited mutations [46]. These mutations can affect genes involved in cell growth and DNA damage repair, which can facilitate rapid replication, proliferation, and ignorance of cell growth signals [46,47]. Cancer cells also acquire abilities to evade apoptosis, induce angiogenesis, metastasize, change their metabolism, promote genome instability, promote inflammation, and avoid detection by the immune response [47,48]. Accumulation of these hallmarks in cancer cells provide a platform for uncontrolled growth in the target environment and metastasized locations.

Cancer mutations and acquisition of cancer hallmarks can arise in any cell type, which can lead to over 100 unique cancer types and environments [49]. Accumulation of tumors in the primary organ or metastasized sites can lead to organ failure and death; therefore, efforts to limit tumor growth and metastasis are key to cancer treatments.

1.3.2 Immunoediting

Cancer cells have many hallmarks that enable them to rapidly proliferate; however, this proliferation is not uncontrolled. The immune system can recognize and eliminate tumors, also known as immunosurveillance [50]. However, during this immune-mediated elimination, tumor cell variants evolve to limit detection from the immune response, yielding an equilibrium state. Finally, outgrowth of the variant tumor cells will dominate the microenvironment and and lead to immune escape. These active phases of immune

elimination, equilibrium, and escape have been coined as the “Three E’s of cancer immunoediting” [50]. These stages are discussed below.

First, seminal studies have demonstrated the importance of immune elimination by examination of immune-mediated molecules Interferon Gamma (IFNγ), Perforin, and TRAIL, which control tumor development, growth, and metastasis [51-56]. IFNγ was one of the first immune-mediated molecules that was shown to have an anti-tumor effect in mice; blocking of IFNγ or IFNγ receptor function lead to uncontrolled tumor growth [57-59]. Similar results of uncontrolled tumor development and growth were seen in the mice lacking cytotoxic molecules Perforin and TRAIL. T cells also have a critical role in immunosurveillance, as *Tcrb*$^{-/-}$ mice had increased incidence of particular cancers compared to wild-type (WT) mice [60]. Cytotoxic CD8^{+} T cells are thought to play a role in regulating tumor cell growth, as detailed in Section 1.3.4 [61]. Immunosurveillance is also demonstrated in humans by development of tumors in patients undergoing immunosuppressive therapy [50,62-64].

Although the immune system has developed many mechanisms to eliminate tumor cells, malignant cells can escape these immunosurveillance mechanisms thus developing cancer. Transformation into malignant cells is most likely due to the development of mutations in cells; in this phase, the immune system will aid in clearance of tumor cells while the tumor evolves under this selection pressure and gains mutations to avoid immune detection [50]. This equilibrium can last many years [65]. However, variant tumor cells will eventually escape immune detection. This may be due to intrinsic changes to the tumor such as downregulation of tumor antigens, defective death receptor signaling, downregulation of costimulatory molecules, production of suppressive cytokines or

extrinsic changes such as recruitment of suppressor T cells, including Regulatory T cells (Tregs), outlined in Section 1.3.3 [50,66].

1.3.3 Tregs in the TME

Tregs play a deleterious role by suppressing anti-tumor responses [1,67-69]. High numbers of Tregs are found in a variety of human and murine tumors [36,70]. In human tumors, an increased Treg to $CD8^+$ T cell ratio correlates with worse prognosis in many cancer types [71]. Further, systemic ablation of Tregs in mice results in complete tumor clearance, although these mice eventually succumb to lethal autoimmunity [72-77]. Therefore, targeting Treg function specifically in the TME but not in the periphery may prove efficacious for cancer treatment.

1.3.4 $CD8^+$ T cells in the TME

$CD8^+$ T cells are critical for inducing tumor cell apoptosis and limiting tumor growth [78-83]. Higher $CD8^+$ tumor infiltration generally leads to a better prognosis [84,85]. However, $CD8^+$ T cell function in the TME is often hindered due to chronic antigen activation which leads to decreased effector function, decreased proliferation, and expression of inhibitory molecules such as PD-1 and LAG-3, also known as T cell exhaustion [86,87]. Efforts to circumvent T cell exhaustion are critical to improving the anti-tumor response.

1.3.5 Immunotherapy

Immunotherapy enhances the immune response to limit tumor growth and escape. Many therapies have sought to enhance $CD8^+$ T cell function due to their chronic activation and exhaustion in the TME, although targeting other cells are also currently under investigation.

The idea for immunotherapy can be traced back to the 19th century but has only recently garnered rapid interest for the treatment of cancer [88,89].

1.3.5.1 Early Immunotherapy

One of the first documented cases of immunotherapy is from William B. Coley who observed that patients with a superficial skin infection caused by *Streptococcus pyogenes* had tumor regression [90]. From this observation, Coley inoculated patients with extracts from heat-inactivated *S. pyogenes* and *Serratia marcescens*, coined "Coley's Toxins" to promote sarcoma tumor regression [91]. Although this was ultimately not adopted as a standard practice due to lack of reproducibility, these observations gave a platform for future studies.

1.3.5.2 Current Immunotherapies

Modern day immunotherapy was advanced by seminal studies demonstrating molecules cytotoxic T-lymphocyte-associated protein 4 (CTLA4), lymphocyte activation gene 3 protein (LAG3), and programmed cell death protein (PD-1) negatively regulated T cell activation [92-100].

CTLA4

Activation of T cells requires binding of TCR to the peptide-Major Histocompatibility Complex (MHC) class I or II. However, T cells also require activation of the costimulatory pathway. The costimulatory molecule CD28 is expressed by T cells and interacts with B7-1 (CD80) or B7-2 (CD86) on APCs. CD28 co-stimulation provides T cells with additional signals for activation and survival [101].

CTLA4 is a highly similar molecule to CD28 and also binds CD80 and CD86. CTLA4 does not provide T cells with the same activation signals but rather is a negative regulator of T cell activation via inhibition of CD28 co-stimulation, IL-2 production, and cell cycle progression [27]. Activated T cells upregulate CTLA4, and CTLA4 competes with CD28 for binding to CD80 and CD86. *Ctla4* knock-out mice develop severe lymphoproliferative disease and succumb to the severe autoimmunity within 3-4 weeks of age [93,102]. Further, Tregs constitutively express CTLA4 and use it as a means of suppression [103,104]. For example, CTLA4 restricts expression of CD80 and CD86 on DCs to limit activation of other cells through trogocytosis [105-107].

In addition to causing downregulation of CD80 and CD86, CTLA4 on Tregs can bind to these molecules to induce expression of indoleamine 2,3,-dioxygenase (IDO) [108-110]. IDO catalyzes the breakdown of the amino acid tryptophan to suppressive metabolites including kynurenines and suppresses T cells in two ways: [i] less available tryptophan will limit the ability of T cells to use this essential amino acid for the cell cycle and other functions [111-113], and [ii] tryptophan metabolites such as kynurenine, quinolinic acid, and picolinic acid suppress T cell proliferation and function and can induce apoptosis [109,114].

Treating mice with established tumors with anti-CTLA4 results in tumor clearance, which could be due to re-invigoration of T cells or Treg depletion through antibody-

dependent cellular cytotoxicity (ADCC) [93,115]. Currently there is one approved human monoclonal antibody that targets CTLA4, ipilimumab. In clinical trials, ipilimumab improved overall survival in metastatic melanoma with an overall response rate (ORR) of 10.9% alone [116,117]. Due to the success of these trials, ipilimumab was approved by the U.S. Food and Drug Administration (FDA) for metastatic melanoma treatment in 2011. Ipilimumab has also been approved for use in combination with anti-PD-1 (nivolumab) for melanoma, renal cell carcinoma, and metastatic colorectal cancer [118]. A new anti-CTLA4 anti-human antibody with a non-fucosylated Fc region, which increases availability for ADCC, and a pro-drug anti-CTLA4 are currently under investigation (NCT03110107) [119,120].

PD-1

Programmed cell death protein 1 (PD-1) is upregulated on activated and exhausted T cells in chronic viral infections, cancers, and other inflammatory states [121]. Ligation of PD-1 to programmed death-ligand 1 (PD-L1), delivers an intrinsic signal to dampen immune activation and function, including decreased cytokine production,[122,123] decreased TCR signaling, and stimulation [123,124]. PD-1 is necessary to limit aberrant T cell activation, although tumor cells and other cells in the TME can express PD-L1 to dampen T cell response in the TME [125]. Therefore, it may prove important to limit this pathway for full activation of the T cell response to tumors.

Targeting PD-1 has proved efficacious for a multitude of human cancers. I discuss here two antibodies against PD-1, but antibodies targeting its ligand, such as atezolizumab, have also been approved for cancer treatment [125]. The first anti-PD1 trial showed the drug nivolumab was efficacious in a Phase III trial of advanced melanoma

[126,127]. This treatment is now FDA approved for use in melanoma, lung cancer, renal cancer, Hodgkin lymphoma, urothelial carcinoma, colorectal cancer, and hepatocellular carcinoma, and more cancer types may be added in the future [125]. Pembrolizumab was the next approved anti-PD-1 therapy and is also approved for many cancers, including metastatic melanoma, head and neck squamous cell carcinoma, and advanced cervical cancer. Pembrolizumab also demonstrated advanced efficacy in the clinic [128-130].

However, a large proportion of patients treated with anti-PD1 (13%–87%) do not respond to therapy, depending on the tumor type [131]. Therefore, many more studies are necessary to improve response to immunotherapy.

LAG3

Lymphocyte activation-gene 3 (LAG3) or CD223 is an inhibitory receptor that is highly homologous to CD4 and is upregulated upon activation [132-134]. Like CD4, LAG3 binds to MHCII but with a much higher affinity resulting in the negative regulation of T cell activation [28-30]. Targeting LAG3 along with PD-1 has had significant efficacy in limiting tumor growth in murine models [135].

Naïve Tregs express low levels of LAG3, which is upregulated upon stimulation and required for full Treg suppression [134,136]. In addition, LAG3 binding to MHC II on DCs limits DC activation to further suppress T cell activation [137]. LAG3 may affect Treg function but also may re-invigorate exhausted $CD8^+$ T cells. Further studies are required to understand these differences. Therapies targeting LAG3 are currently in clinical trials as a single and combinatory treatment [30,138].

1.3.5.3 Future Immunotherapies

In 2013, Science declared Immunotherapy the “Breakthrough of the Year” and in 2018, James Allison and Tasuku Honjo were awarded the Nobel Prize in Physiology or Medicine for their work with CTLA4 and PD-1 respectively [92,139]. The success of these molecules in the clinic has catapulted the interest to understand why only a percentage of patients respond to anti-CTLA4 or anti-PD1 blockade, if response can be enhanced, and if targeting other molecules that play a role in the TME can synergize to provide a therapeutic benefit.

1.4 Type 1 Diabetes (T1D)

Type 1 diabetes (T1D) is a polygenic autoimmune disease characterized by immune-mediated destruction of insulin-producing pancreatic beta (β) cells. T1D can also include auto-antibody-negative patients, also known as “idiopathic diabetes” but this is a small percentage of patients and will not be discussed herein [140]. Loss of insulin production by immune-targeting leads to hyperglycemia, which if left untreated, can lead to ketoacidosis, chronic microvascular and macrovascular effects, and death [141,142]. Exogenous supplemented insulin can control hyperglycemia in those diagnosed with T1D, although patients are required to administer recombinant insulin regularly. It is estimated that there is $16 billion combined health care expenditures and lost income for T1D healthcare in the United States annually [143,144]. T1D patients pay more than $6,000 compared to non-T1D patients for yearly medical expenditures including hospital visits and prescription drugs [145]. Moreover, T1D patients must regulate their blood glucose

levels with continuous blood glucose monitoring, physical activity, and dietary management [141,142].

T1D, formerly known as juvenile diabetes, is among the most common endocrine and metabolic disorder among children [142]. Presentation of symptoms most often occur around 5-7 years of age and around puberty; however, diagnosis is also prevalent in adults [141,146]. It is estimated that more than one million Americans are currently living with T1D, including 200,000 adolescents [41,147]. The number of people living with T1D is expected to increase up to 5 million by 2050 [148].

1.4.1 T1D Risk and Development

T1D is a disease characterized by genetic and environmental risk factors, which are discussed below; these triggers are thought to activate the immune response, initiate β cell death and subsequent hypoglycemia. Disease pathogenesis is characterized by three stages of disease development, ultimately leading to overt diabetes.

1.4.1.1 Pre-Stage Risk for Development of Diabetes

First, genetic and environmental risk pre-dispose patients to T1D development [149-151]. The genetic risk factor can be demonstrated by the genetic concordance for identical twins (30-70%), for siblings (6-7%) and children with parents with diabetes and (1-9%) [149]. HLA haplotypes such as HLA-DR3-DQ2 and HLA-DR4-DQ8 are responsible for approximately 50% of disease heritability [149]. In addition, over 50 genetic loci have been

attributed to disease susceptibility, including genes involved in T cell function such the IL-2 pathway and β cell survival [149,152,153].

Environmental triggers may also contribute to disease; exposure to enteroviruses, such as Coxsackie B virus, that infect or perturb β cells, are one the most commonly studied risk [154]. Reports of T1D have shown that infections were higher in newly diagnosed T1D patients compared to controls [155-158]. Moreover, IFNα, a cytokine produced during viral infection, is upregulated in T1D patients and can even induce T1D in patients with cancer or viral infections undergoing IFNα therapy [159-164]. Other environmental factors such as diet, vitamin D insufficiency, and decreased gut-microbiome diversity are also risk factors for T1D [149].

Environmental triggers may activate the immune system or alter β cells in genetically predisposed individuals, induce initial β cell death and antigen release, induce autoantibody production, and further destruction of β cells [146,149,154]. Initiation of how immune cells trigger β cell attack is unclear but may be mediated by $CD8^+$ and $CD4^+$ T cells; this will be expanded upon in Section 1.4.4.

1.4.1.2 Stages of T1D Development

Stage 1 of T1D is characterized by development of two or more autoantibodies, with normal blood sugar levels, and sufficient amounts of β cells producing insulin [165]. Stage 2 is characterized by presence of two or more autoantibodies with abnormal blood sugar. In Stage 2, there is progressive β cells loss and less regulation of blood glucose. Stage 3 is usually when patients present in the clinic with symptoms of high blood sugar,

low β cell number, and are typically diagnosed with T1D. Due to symptoms manifesting in Stage 3 patients, treatments to prevent progression to overt diabetes remain difficult.

1.4.2 Therapies for T1D

Currently, the only approved treatment for T1D is addition of exogenous insulin. Some blocking antibodies such as Rituximab (anti-CD20), Teplizumab (non-mitogenic anti-CD3), Abatacept (CTLA4-Immunoglobulin) and Alefacept (anti-CD2) have had some efficacy; however, none of these have demonstrated insulin independence or proceeded to Stage 3 clinical trials [149]. β cell and pancreas transplant have been considered as a treatment but are considered high risk, require long-term immunosuppressants, or may not work for a majority of patients [149,166,167]. Many other treatments are currently under investigation; however, the current limited treatment options are a large barrier in prevention of T1D.

1.4.3 Tregs in Autoimmune Diabetes

Tregs are critical for limiting multiple models of autoimmunity such as the Non-Obese Diabetic (NOD) mouse, a spontaneous model of autoimmune diabetes that is similar to human disease [168]. Treg depletion in NOD mice rapidly results in overt diabetes [169,170]. Tregs in patients with T1D were reported to be less suppressive, more apoptotic, and produce more proinflammatory cytokines than those without T1D, which may contribute to disease [171,172]. Efforts to examine how Treg function can be improved in the diabetic islet could prove efficacious for T1D treatment.

1.4.4 CD8$^+$ T cells in Autoimmune Diabetes

A hallmark of T1D is the infiltration of immune cells in and around the pancreatic islets, referred to as insulitis [173]. CD8$^+$ T cells represent a large proportion of these infiltrating immune cells in recent onset and long-term T1D patients and NOD mice [174-176]. CD8$^+$ T cells are thought to play an important role in autoimmune diabetes as demonstrated by limited disease in NOD mice treated with anti-CD8, in mice deficient in MHC class I β2-microglobulin deficient mice, and adoptive transfer of T cells into MHCI deficient recipients [177-180]. CD8$^+$ T cells are thought to be the main initiators in β cell death in the islet; however, CD4$^+$ T cell help is contended [181,182]. CD8$^+$ T cells are thought to initiate β cell death through production of Perforin and Granzyme [183-186]. However, deletion of these molecules do not protect 100% of mice from diabetes, indicating other molecules may also play a role [187].

1.5 Mechanisms of T cell function

Tregs and CD8$^+$ T cells can be detrimental in various inflammatory environments, therefore, efforts to understand how these cells perform their functions in the TME and autoimmune environment will be critical for limiting disease and maintaining homeostasis. Two cellular mechanisms, chromatin accessibility of the Treg genome and expression of cytotoxic molecule TRAIL may play key roles in the function of these cells in inflammatory environments.

1.5.1 Epigenetics and Chromatin Accessibility

DNA is the hereditary code for all living organisms. DNA is tightly packaged around nucleosome proteins called histones which condense to become heterochromatin [188]. Histone modifications such as methylation and acetylation represent heritable epigenetic marks that modulate chromatin and DNA accessibility [188,189]. DNA accessibility can be increased over gene enhancers, promoters, and gene bodies to facilitate transcription factors and other molecules to bind and initiate transcription [188].

Epigenetic modifications regulate cellular development, function, and phenotype [190]. Therefore, analyzing the chromatin accessibility of the genome of Tregs may provide clues on cellular changes in various environments and external stimuli.

1.5.2 TRAIL

TRAIL (*Tnfsf10*/CD253/Apo2L) is a homotrimeric type II transmembrane tumor necrosis factor (TNF) superfamily member [191-193]. TRAIL, discovered due to its sequence similarity to Fas, is a molecule that induces extrinsic apoptosis [194,195]. TRAIL initiates apoptosis by binding to agonistic murine Death Receptor 5 (DR5) (*Tnfrsf10b*) or human Death Receptor 4/TRAIL Receptor 1 (DR4/TRAILR1, *Tnfrsf10a*) and DR5/TRAIL Receptor 2 (TRAILR2, *Tnfrsf10b*) (Fig 3) [196,197]. Receptor-ligand interaction recruits adaptor molecule FADD which recruits and activates initiator caspases such as caspase 8 and 10 [198,199]. The initiator caspases then cleave and activate an executioner caspase, such as caspase 3, which degrades cellular components ultimately leading to cellular apoptosis [200]. TRAIL can induce cell death as either a membrane bound or soluble

mediator as it can be cleaved by intracellular aspartic and/or cysteine proteases [197,201,202]. TRAIL expression is regulated by cell stimulation and IFNα, IFNβ and IFNγ on multiple cells types including T cells, NK cells, monocytes, macrophages and dendritic cells [203-212].

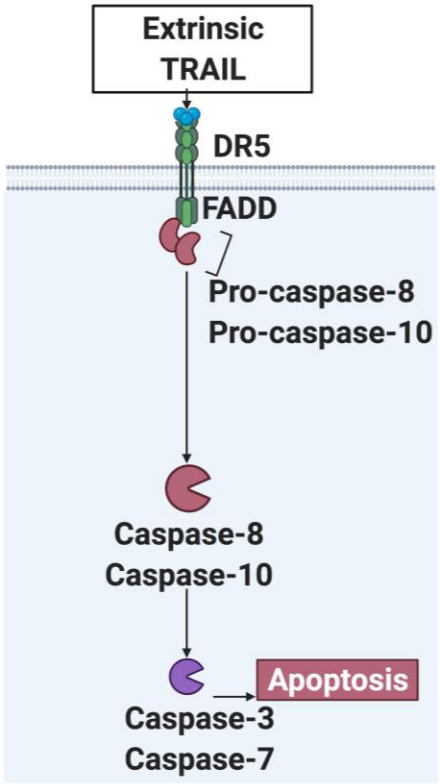

Figure 3 TRAIL signaling pathway

TRAIL was initially discovered as a molecule that specifically targets malignant cells and spares non-malignant cells. TRAIL-, or DR5-, deficient mice are more susceptible to tumor growth and metastasis, implicating an important role for TRAIL in controlling tumor growth [56,213-220]. TRAIL tumor-specific killing is primarily mediated by NK

cells and $CD8^+$ T cells in the tumor microenvironment (TME), although other cells express TRAIL in the TME [207,220,221]. Moreover, while TRAIL is a molecule that targets cell death, TRAIL can also regulate proliferation [222].

1.6 Questions to Address

Tregs and $CD8^+$ T cell function have important roles in maintaining homeostasis and limiting disease; however, their function in inflammatory environments can be detrimental. For example, Tregs can limit the anti-tumor response while $CD8^+$ T cells can aid in β cell death in autoimmune diabetes. Therefore, I will address three questions to examine their function in the tumor and autoimmune environments and if this can be altered: (i) what is the chromatin accessibility of Tregs in the TME and is this altered with immunotherapy (ii) does TRAIL contribute to Treg suppressive function in the TME and autoimmune diabetes and (iii) does TRAIL contribute to $CD8^+$ T cell cytotoxicity in autoimmune diabetes? To address these questions, I utilized transplantable tumor models and the autoimmune diabetes NOD mouse model.

2.0 Materials and Methods

Note: most of the materials and methods were taken from my previous publication ***Dadey, R.E.***, *Grebinoski, S., Zhang, Q., Brunazzi, E.A., Burton, A., Workman, C.J., Vignali, D.A.A. "Regulatory T Cell-Derived TRAIL Is Not Required for Peripheral Tolerance" Immunohorizons. 2021:Jan22;5(1):48-58. doi: 10.4049/immunohorizons.2000098 under our own Copyright (open access).*

2.1 Mice

Foxp3$^{Cre\text{-}YFP}$ mice on a C57BL/6 background were obtained from A.Y. Rudensky (Memorial Sloan Kettering) [223]. *Foxp3*^{Cre} mice on a BALB/c background were obtained from S. Sakaguchi (Osaka University) [106]. NOD/ShiLtJ (The Jackson Laboratory, stock #001976), NOD mice were purchased from the Jackson Laboratory. Foxp3$^{Cre\text{-}GFP}$.NOD mice were obtained from J.A. Bluestone (University of California San Francisco) [224]. E8I$^{Cre\text{-}GFP}$ C57BL/6 mice were given curtesy of the Littman and Taniguchi Labs and were bred onto a NOD background at St. Jude Children's Research Hospital. Microsatellite analysis revealed 99.6% NOD, having one heterozygous SNP on chromosome 16. All animal experiments were performed in the American Association for the Accreditation of Laboratory Animal Care–accredited, specific pathogen–free facilities in Division of Laboratory Animal Resources, University of Pittsburgh School of Medicine (UPSOM). Female and male mice of 4-6 weeks of age were used for B6 and BALB/c experiments.

All tumor phenotype and functional experiments were performed at 12 days post tumor inoculation unless otherwise specified. Female and male NOD mice were followed for diabetes incidence up to 30 weeks of age. All NOD.*Tnfsf10*$^{L/L}$ Foxp3$^{Cre\text{-}GFP}$ phenotype and functional experiments were performed with female mice at 10 weeks unless otherwise specified. All NOD.*Tnfsf10*$^{L/L}$ E8I$^{Cre\text{-}GFP}$ mice experiments were performed at 12 weeks unless otherwise specified. Animal protocols were approved by the Institutional Animal Care and Use of Committees of University of Pittsburgh.

2.2 Generation of the *Tnfsf10*$^{L/L}$ mouse

The *Tnfsf10*$^{L/L}$ targeting construct was generated by Amanda Burton with help from Kate Vignali using standard recombineering methods [225]. Initially, 26.7 kb of the *Tnfsf10* locus were retrieved from a BAC plasmid and a Loxp-Neo-Loxp cassette inserted 313bp upstream of exon 2. The Neo was removed via Cre-mediated recombination leaving a single Loxp and a *Stu*I restriction site (inserted into the intron of the retrieved *Tnfsf10* locus). A Frt-Neo-Frt-Loxp cassette was then inserted 573bp downstream of exon 5 to establish an alternate exon 2 containing: a *Spe*I restriction site, the splice acceptor from exon 2, 'self-cleaving' T2A peptide sequence, a truncated version (non-functioning) of the human nerve growth factor receptor (hNGFR) and the SV40 polyadenylation sequence. The linearized targeting construct was electroporated into JM8A3.N1 embryonic stem cells (C57BL/6N background) and neomycin-resistant clones were screened by southern blot analysis using *Stu*I and *Spe*I restriction digests for the 5' and 3' ends, respectively. Correctly targeted clones were 100% normal diploid by karyotype analysis and were

injected into C57BL/6 blastocysts. Chimeric mice were mated to C57BL/6 mice and transmission of the targeted allele verified by PCR. The mice were crossed with actin flipase mice to remove the Neo cassette. The mice were backcrossed >10 generations onto the BALB/c or NOD background and verified by microsatellite analysis. Genotyping primers are 5' GCCCACGGGTGTAAAGAGCAGTTC 3', 5' GGTGGAACAGCTGACAGACATGATAAGATAC 3', and 5' GTCTCCCCAGTCCAATCACTGCTAC 3'. Primers for detection of exon 1 of *Tnfsf10* are forward 5' GCACTCCGCCTTCTAACTGT 3' and reverse 5' GTGCTGACTGAAGCTGAGGT 3', exon 2 forward 5' GACGGATGAGGATTTCTGGGAC 3' and reverse 5' TTCAATGAGCTGATACAGTTGCC' and exon 5 forward 5' ATGGAAAGACCTTAGGCCAGA 3' and reverse 5' TAGATGTAATACAGGCCCTCCTGC 3'.

2.3 Measurement of diabetes and insulitis

Measurement of diabetes and insulitis were performed as previously described [226-228]. Briefly, diabetes incidence was monitored weekly through presence of glucose in the urine with Diastix (Bayer). Mice positive for glucose on Diastix were then measured for blood glucose with a Breeze2 glucometer (Bayer). Mice were considered diabetic and were marked for sacrifice when blood glucose was ≥ 400 mg/dL.

Pancreata for histology and Vectra staining/IHC were prepared as previously described at the University of Pittsburgh Biospecimen Core [226]. Briefly, pancreata were embedded in a paraffin block and cut into 4 μm-thick sections with 150μm steps between

sections and stained with hematoxylin and eosin or the Vectra panel. An average of 60 to 80 islets per mouse were scored in a blinded manner. Two methods of insulitis measurement were used as previously described [229]. Vectra and IHC staining was performed at University of Colorado Denver, Cancer Center. Slides were stained for Foxp3 (570), Cleaved Caspase 3 (c-casp3) (520), CD8 (690), DR5 (650), Insulin (540), CD45 (480), CD4 (780), and DAPI.

2.4 Islet isolation and lymphocyte preparation

Islets were prepared as previously described [226,230]. Briefly, 3 mL of collagenase [600 U/mL in complete Hanks' based salt solution (HBSS) with 10% fetal bovine serum (FBS)] was perfused through the pancreatic duct. Pancreata were then incubated for 30 minutes at 37°C. Pancreata were then washed two times, resuspended in phenol-free HBSS supplemented with 10% FBS, and islets were isolated by hand under a dissecting microscope. Isolated islets were dissociated with 1 mL dissociation buffer (Life Technologies) for 15 minutes at 37°C with vortexing every 5 minutes. Cells were washed, resuspended, counted, and used.

2.5 Experimental Autoimmune Encephalomyelitis (EAE) induction

Induction of EAE was performed as described previously [231,232]. Briefly, Incomplete Freund's Adjuvant (Difco) was supplemented with 5mg/mL *Mycobacterium tuberculosis*

(Difco) to make Complete Freund's Adjuvant (CFA). MOG peptide (AAPPTEC) was diluted to 1 mg/mL in PBS and mixed with CFA at a 1:1 ratio. Mice were injected with 100 uL of the emulsion on both hind flanks subcutaneously (s.c.). Pertussis toxin (200 ng/200 μL PBS, Sigma) was injected intraperitoneally (i.p.) on day 0 and day 2 of initial MOG/CFA injection. Animals were scored blinded for clinical symptoms as follows: 0, no change; 1, limp tail; 2, partial hind limb paralysis; 3, full hind limb paralysis; 4, full hind limb paralysis, partial front limb paralysis; 5, moribund or death.

2.6 Cell staining, flow cytometry, and purification

Single cell suspensions were stained with antibodies for CD4 (GK1.5, BioLegend), CD8a (53-6.7, BioLegend), TCRβ (H57-597, eBioscience), c-casp3 (Asp175, Cell Signaling Technologies, CST), CD45.2 (104, BioLegend), Foxp3 (FJK-16s, eBioscience), Ki67 (B56, BD Biosciences), TNFα (MP6-XT22, BioLegend), IFNγ (XMG1.2, BioLegend) DR5 (MD5-1, BioLegend), LAP-TGFβ (TW7-16B4, BioLegend), IL-10 (JES5-16E3, BioLegend), CTLA-4 (UC10-4B9, BioLegend), CD73 (TY/11.8, BioLegend), CD39 (24DM51, BioLegend), CD11c (N418, BioLegend), CD19 (ID3, BD Biosciences), F4/80 (BM8, Biolegend), NK1.1 (PK136, eBioscience), CD49b (DX5, Biolegend) and Insulin (R&D, 182410). Surface staining was performed on ice for 15 min. Dead cells were discriminated by staining with Ghost Viability Dye (Tonbo Biosciecnes) in phosphate-buffered saline (PBS) prior to surface staining. For cytokine expression analysis, cells were activated with 100 ng/mL PMA (Sigma) and 500 ng/mL Ionomycin (Sigma) in complete RPMI containing 10% FBS and Monensin (eBioscience) for 4 hr. For

intracellular staining of cytokines and transcription factors, cells were stained with surface markers, fixed in Fix/Perm buffer (eBioscience) for 45 minutes, washed twice in permeabilization buffer (eBioscience) and stained in permeabilization buffer for 30min on ice. Immunostaining for Ki67 was performed using the BD Cytofix/Cytoperm kit. Samples were acquired on a Fortessa (BD Biosciences) and analyzed by FlowJo (Treestar, Inc.) or sorted on an Aria II (BD Biosciences). Identification of various immune cell populations was first sub-gated on live CD45.2$^+$ cells. From this gate, the following strategy for each population was used: TCRβ^+CD4$^+$Foxp3$^-$ [herein referred to as CD4$^+$], TCRβ^+CD4$^+$Foxp3$^+$ [Treg], TCRβ^+CD8$^+$ [CD8$^+$], TCRβ^-CD49b$^+$ or TCRβ^- NK1.1$^+$ [NK$^+$], TCRβ^- CD11c$^+$ [CD11c$^+$], TCRβ^- F4/80$^+$ [F4/80$^+$] and all other TCRβ^- cells. Gating for sorting these populations remains the same except for the CD4$^+$ Foxp3$^-$ and Treg populations. CD4$^+$ Foxp3$^-$ and Treg populations used the following strategy, respectively: TCRβ^+CD4$^+$Foxp3(YFP)$^-$ (C57BL/6) or TCRβ^+CD4$^+$CD25$^-$(BALB/c) [CD4], and TCRβ^+CD4$^+$Foxp3(YFP)$^+$ (C57BL/6) or TCRβ^+CD4$^+$CD25$^+$ CD127$^-$ (BALB/c) [Treg]. NOD Tregs were isolated as TCRβ^+CD4$^+$Foxp3(GFP)$^+$ and CD4s were isolated as TCRβ^+CD4$^+$Foxp3 (GFP)$^-$.

2.7 Tumor models

The B16.F10 were obtained from M.J. Turk (Dartmouth College, New Hampshire) [233]. The MC38 colon adenocarcinoma cells were obtained from J.P. Allison (M.D. Anderson Cancer Center, Texas) [234]. The CT26 cells were obtained from R. Binder

(University of Pittsburgh, Pennsylvania) [235]. These cells were cultured as previously described [236]. C57BL/6 mice were injected with $1.25x10^5$ B16 melanoma cells (intradermally, i.d.) or $2.5x10^5$ (time-course), or $5.0x10^5$ (anti-PD-1 experiments) MC38 colon carcinoma cells (subcutaneously, s.c.). Mice injected with MC38 were treated with 100 μg isotype (Rat IgG2a, Leinco) or anti-PD1 (Leinco) (intraperitoneally, i.p.) as previously described [77]. Tumors were measured every 3 days with a digital caliper in two dimensions (width and length) and presented as tumor size (mm^2; defined as *w* x *l*). BALB/c were injected with $1.25x10^5$ CT26 colorectal carcinoma s.c. and measured every 3 days for tumor growth. Tumors were prepared for single cell suspension with an enzymatic digestion of Collagenase IV (200 U/mL) and Dispase (1 U/mL) in cRPMI or Liberase (50 μg/mL, Sigma Aldrich) and mechanical disruption. Tumors for ATAC-sequencing were processed with negative selection for $CD105^-$ cells by incubation of cells with Biotin CD105 (MJ7/18, ThermoFisher) for 15-20 mins, wash with sort buffer, incubation with Pierce Magnetic Streptavidin beads for 30 minutes and isolation of cells on a magnet.

Individual tumors were measured every 3 days with a digital caliper in two dimensions (width and length) and presented as tumor size (mm^2; defined as *w* x *l*). Individual tumors that were >$50mm^2$ at Day 13 post injection and continued to grow were classified as non-responders, tumors that were greater than $50mm^2$ at Day 13 but decreased by Day 15 were classified as late responders, and tumors that were less than $50mm^2$ by Day 13 and continued to decrease were classified as early responders. Early and late responders were grouped together and labeled as responders for downstream

analysis. Tumors from the anti-PD1 cohort were isolated on Day 16 after MC38 inoculation.

2.8 ATAC sequencing library preparation

5,000 Tregs ($CD4^+Foxp3(YFP)^+$), and 5,000 CD4 effectors, the latter herein referred to as CD4 (($CD4^+Foxp3(YFP)^-$) were isolated from the tumor and non-draining lymph node (NDLN, or LN) and were double sorted directly into lysis buffer (10 mM Tris-HCl, pH 7.4, 10 mM NaCl, 3 mM MgCl2, 0.1 % IGEPAL CA-630); purity was confirmed to be >95%. Treg and CD4 lysates were then resuspended a transposition reaction mix from the Illumina Tn5 Tagmentation Kit (Illumina FC-121-1030) for 45 mins at 37°C. DNA was purified by Qiagen Reaction MiniElute Kit (#28204). Library amplification was performed using PCR Primers from the Nextera DNA Library Preparation Kit (Illumina) and NEBNext High-Fidelity 2X PCR Master Mix. Qiagen PCR Cleanup Kit was used to isolate the purified library. DNA was then pooled and sequenced with Paired-End 75bp cycle Illumina NextSeq or NovaSeq system.

2.9 RNAseq library preparation

Bulk RNAseq was performed as previously described by Chang (Gracie) Liu and Hiroshi Yano [20]. Briefly, 500 Tregs and CD4 effectors were double sorted from tumor and LN of isotype or anti-PD1 treated animals. Cells were sorted directly into lysis buffer and

cDNA synthesis was performed using the Clontech SMART-Seq v4 kit. Libraries were prepared using the Nextera DNA Library Preparation Kit (Illumina). DNA was then pooled and sequenced with Paired-End 75bp cycle Illumina NextSeq system.

2.10 ATAC sequencing analysis

The ATAC-seq data analysis was performed by Dhivyaa Rajasundaram. Data was quality controlled, trimmed, and aligned to the mouse reference genome (mm10) using BWA-MEM. Peak calling was performed using MACS2 version 2.1.2 with the options -B, -q 0.01, – nomodel, -f BAM, -g mm. Peaks that overlapped blacklisted regions were removed. Read numbers, and feature distribution plots were obtained using the ataqv package in R. Count tables were generated using the Rsubread featureCounts version 1.28.1 on the filtered BAM alignments. Sample similarities were assessed by Principal Component Analysis (PCA), and hierarchical clustering. Differentially accessible chromatin regions were assessed using DESeq2. Gene Ontology and KEGG Pathway analyses were performed on annotated peaks using the clusterProfiler package.

2.11 RNA sequencing analysis

RNA sequencing analysis was performed by Dhivyaa Rajasundaram. First, quality controlled FASTQ files were aligned to the Ensembl Mus musculus genome (GRCm38) using STAR aligner (version 2.5.1) [237]. HTSeq-count was used to generate counts of

reads uniquely mapped to annotated genes using the GRCm38 annotation gtf file [238]. Differential gene expression analysis between the different conditions was performed by DESeq2 using a model based on the negative binomial distribution [239]. The resulting P-values were adjusted using the Benjamini and Hochberg approach for controlling the false discovery rate, and differentially expressed genes were determined at the 5% threshold [240]. Gene set enrichment analysis was used to assess the statistical enrichment of gene ontologies, and pathways [241].

2.12 Single Cell analysis

Two Female NOD.*Tnfsf10*$^{L/L}$ and three NOD.*Tnfsf10*$^{L/L}$ E8I$^{Cre\text{-}GFP}$ mice were sacrificed and islet cells were isolated as highlighted previously. The islet sample from each mouse was labeled with a unique hashing antibody (TotalSeq C, Biolegend) for 30 mins on ice. Islet cells were then divided into two groups; the first group was taken directly for library preparation (no cell sorting) while the other was stained for Ghost Viability Dye (Tonbo Biosciences) in phosphate-buffered saline (PBS) and taken for sorting. Live cells were sorted from each sample and then pooled at equal numbers and then prepared for cDNA via the Chromium Single Cell 5' Reagent Kit (10X Genomics). Libraries were sequenced on NovaSeq at the UPMC Genome Center.

To analyze the raw sequencing data, Anthony Cillo first utilized CellRanger's mkfastq function to create FASTQ files. Next, Jian Cui and I used Cellranger count to align the demultiplexed reads to reference genome mm10 and create gene barcode

matrices. Finally, Jian Cui and I used CITESeqCount to unhash the samples. The data were visualized via t-distributed stochastic neighbor embedding (t-SNE) by Jian Cui.

Single cell for cytotoxic molecule analysis was performed by downloading GSE141786 and analyzing intra-islet $CD8^+$ cells for *Perforin*, *FasL*, *Tnfsf10*, and *Granzyme B* across time points.

2.13 Treg TCRseq and data analysis

TCR library preparation was performed as previously published [20]. Briefly, Tregs from *Foxp3*$^{Cre\text{-}YFP}$ individual mice were isolated day 16 post B16 tumor inoculation. DNA was purified with the QIAmp DNA Micro Kit (Qiagen), and TCRbeta-enriched library was generated with TCRbeta ImmunoSeq (Adaptive Biotechnologies), following the manufacturer's protocol. Sequencing was performed on Illumina MiSeq.

2.14 Treg microsuppression assays

Treg microsuppression assays were performed as previously described [77,242]. Briefly, Treg cells were isolated from the spleen of naïve mice or ndLN and tumor-infiltrating lymphocytes (TIL) of mice 12 or 18 days after injection with B16 or CT26. Isolated Tregs were co-cultured with CellTrace Violet (Life Technologies)-labeled $CD4^+Foxp3^-$ responder T cells in the presence of mitomycin-C-treated TCRβ-depleted splenocytes and anti-CD3ε (1 μg/mL) for 72 hrs at 37°C.

2.15 Adoptive transfer

7-8 week old NOD.Thy1.1 and NOD.*Tnfsf10*$^{L/L}$ E8I$^{Cre\text{-}GFP}$ mice were harvested for lymph nodes (LNs) and splenocytes. Negative selection for CD8^{+} T cells was performed on these samples (method is previously described in section 2.7) with addition of Ter119 (TER-119, Biolegend), CD4 (RM4-5, Biolegend), CD11b (M1/70, Biolegend), CD11c (N418, Biolegend), CD19 (6D5), Ly6G (1A8, Biolegend), CD45R/B220 (RA3-6B2, Biolegend), TCRγ/δ (eBioGL3, eBioscience), CD49b (DX5, eBioscience), CD16/32 (93, eBioscience) biotinylated antibodies. Negative selection to acquire CD4^{+} cells was performed on WT 7-8 week old NOD with similar method above, substituting CD4 for CD8. 1x10^{6} WT Thy1.1 CD8^{+}, 1x10^{6} *Tnfsf10*$^{L/L}$ E8I$^{Cre\text{-}GFP}$ CD8^{+}, and 2x10^{6} CD4^{+} T cells in PBS, were injected intravenously (i.v.) into 7-8 week old NOD-SCID females. Islet, NDLN, and pancreatic draining lymph node (PLN) were isolated at 3, 5, and 7 weeks post injection and analyzed for percentages of cells transferred via flow cytometry.

2.16 mRNA isolation, cDNA synthesis, and quantitative PCR

Cell populations were isolated from naïve *Foxp3*$^{Cre\text{-}YFP}$.B6 or *Foxp3*^{Cre}.BALB/c mice or from the NDLN and tumor-infiltrating lymphocytes (TIL) of B16 bearing *Foxp3*$^{Cre\text{-}YFP}$.B6 and *Tnfsf10*$^{L/L}$ *Foxp3*$^{Cre\text{-}YFP}$.B6 mice. Cells were isolated from spleen, NDLN, PLN, and islet from 10 week old female Foxp3$^{Cre\text{-}GFP}$.NOD and 12 week old female E8I$^{Cre\text{-}GFP/Cre\text{-}GFP}$.NOD. RNA was extracted using the RNAeasy Micro Plus Kit (Qiagen). cDNA was produced using the High-Capacity cDNA Reverse Transcription Kit (Thermo) following

the manufacturer's instructions. EvaGreen based qPCR was performed using the following primers: *Tnfsf10* forward, 5' TCTGTGGCTGTGACTTACATG 3', reverse, 5' AAGCAGGGTCTGTTCAAGATC 3' and *HPRT* forward, 5' TCAGTCAACGGGGGACATAAA 3', reverse, 5' GGGGCTGTACTGCTTAACCAG 3'. Relative quantification was determined via the delta CT method.

2.17 Quantification and Statistical Analysis

Statistics were performed with Prism v8.0.0. Student t tests were used when only two experimental groups were involved. Tumor growth and EAE curves were analyzed using Two-way ANOVA with multiple comparisons correction with sequential time point measurements. The Log-Rank (Mantel-Cox) test was utilized for diabetes incidence statistical analysis. "n" represents number of mice used in the experiment, with number of individual experiments listed in legend. All *p*-values were two-sided, and statistical significance assessed at or below 0.05.

3.0 Epigenetic Regulation of the Treg phenotype in the TME

3.1 Introduction

Regulatory T cells (Tregs) are a unique subset of $CD4^+$ T cells characterized by the expression of transcription factor, *Foxp3*. Unlike their more traditionally pro-inflammatory conventional $CD4^+Foxp3^-$ (Tconv) counterparts, Tregs are distinct in their ability to suppress activated T cells which is key for regulation of aberrant immune responses. Depletion of these cells can lead to systemic immune activation and lethal autoimmunity [74-77]. The majority of Tregs are derived from the thymus, reside in lymphoid tissues, and are categorized as naïve or central Tregs (cTregs). Tregs that reside in non-lymphoid tissues can be categorized as effector Tregs (eTregs) [243,244]. eTregs, adopt unique transcriptional signatures in various tissues that enable them to function and maintain their suppressive phenotype in different inflammatory environments [245]. For example, Tregs can infiltrate into the tumor microenvironment (TME) to suppress activated T cells. Increased proportion of Tregs compared to $CD8^+$ T cells in the TME is an indication of worse prognosis in multiple cancer types [71,246-249] .Treg depletion in mouse models leads to tumor clearance; however, these mice will eventually succumb to lethal autoimmunity [76,77]. Tregs that are in the tumor tissue may adopt a Treg effector-like phenotype to persist in the TME despite a harsh, evolving environment. Tregs must withstand hypoxia, high lactate, and low glucose in the TME [250,251]. Tregs rapidly acquire transcriptional changes that enable them to adapt to this environment and maintain their

suppressive phenotype limit conversion to a pro-inflammatory ex-Treg [245,252]. However, the regulation of this transcriptional change is unclear.

Transcription is regulated by various epigenetic mechanisms; one important example being chromatin accessibility [253,254]. Opening of tightly packed chromatin over areas of promoters and enhancers can aid in recruitment of transcription factors and the polymerase complex to aid in activation of gene transcription while closing chromatin can dampen transcription [253]. Chromatin accessibility signatures are different among cell types and can be altered during cellular differentiation and activation [255,256]. Moreover, chromatin accessibility can dynamically change over time which may indicate how the cell is responding to environmental cues [257].

Therefore, I hypothesized that Tregs in the TME might acquire a distinct chromatin accessibility signature which might regulate their unique transcriptional signature, and effector Treg phenotype in the TME. I also considered murine response to anti-PD1 therapy may influence Treg chromatin accessibility.

In this study I had three distinct goals: (1) determine chromatin accessibility changes of Tregs in the TME compared to periphery that might influence their distinct transcriptional signature (2) examine if Tregs change their chromatin accessibility over time in a developing tumor (3) examine if chromatin accessibility changes depending on response to immunotherapy.

3.2 Results

3.2.1 Tregs have distinct chromatin accessibility in the TME compared to LN but do not alter accessibility across the course of disease

To examine the chromatin accessibility profiles of Tregs in the TME, I performed the low-input assay for transposase-accessible chromatin using sequencing (ATAC-seq) [258] (Table 1). Insert size distribution demonstrated the typical peaks around <100, 200, 400, etc, corresponding to open chromatin, mono-nucleosomes, di-nucleosomes, etc, respectively (Fig 4A) [259]. I performed a time course experiment on Tregs and $CD4^+$ $Foxp3^-$ (Tconv) cells from *Foxp3*$^{Cre\text{-}YFP}$ mice that were injected with B16 melanoma or MC38 colon adenocarcinoma (Fig 5A). Not surprisingly, the majority of accessible peaks in Tregs from the LN and B16 and MC38 tumors were identified in promoters of genes, most likely indicative of gene transcription regulation (Fig 4B).

I found that Tregs in the TME altered their chromatin accessibility compared to the LN (Fig 5B-C). Interestingly, when the time points were compared, the majority of variance was from location rather than time point (Fig 5B-E). This was in contrast to previous literature that suggests chromatin accessibility in various cell types can change over time in various environments [257]. Moreover, pairwise comparisons between time points showed few peaks that were greater than log2fold change (fc) greater than or less than 1.5 and statistically significant ($p<0.05$) (Fig 4C-D). Future analysis will also determine if Tconv cells also had no change in chromatin accessibility over time.

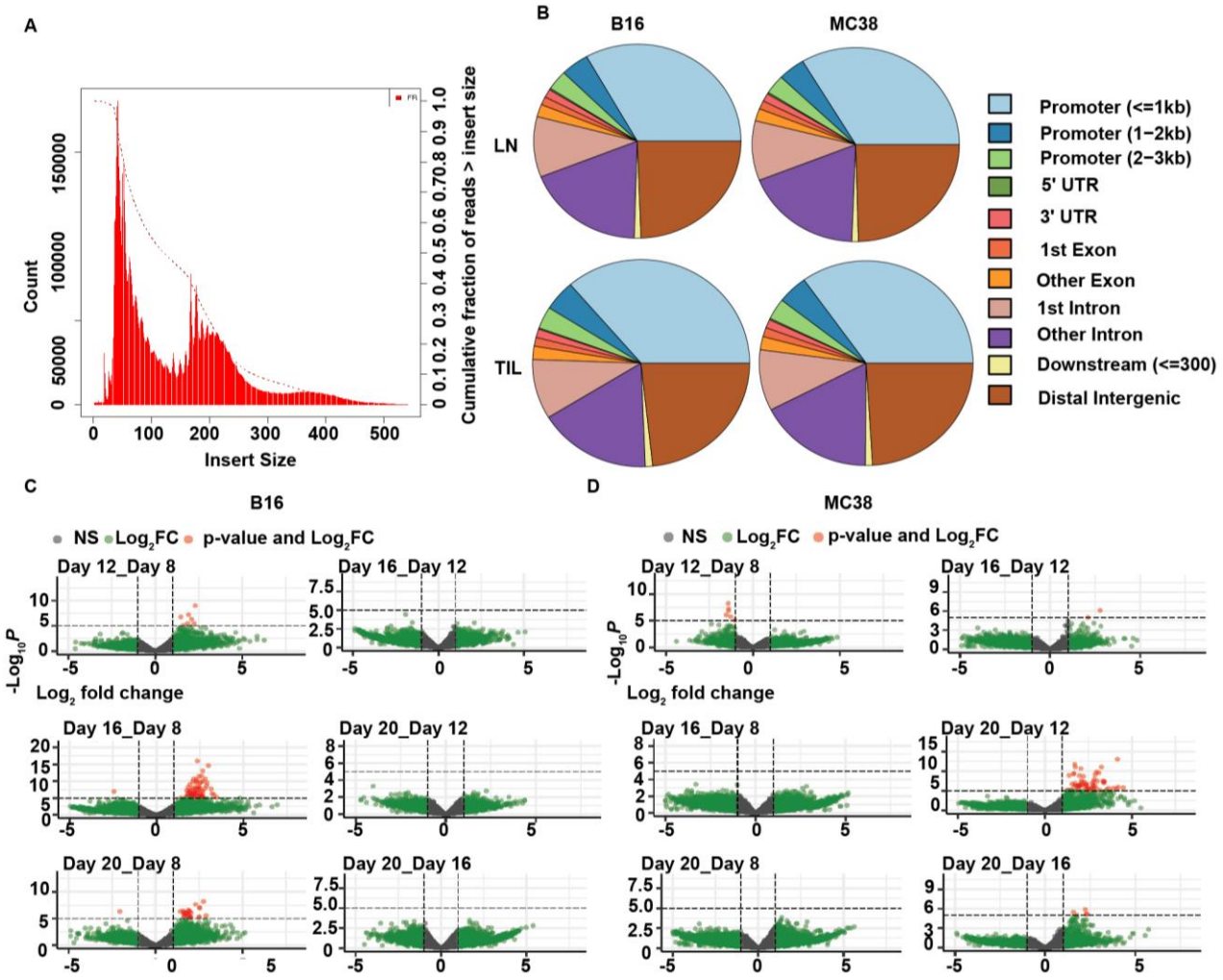

Figure 4 ATAC-seq library and individual time point comparisons

(A) Representative insert size plot **(B)** Pie chart indicating location of genomic accessible peaks for Tregs in NDLN (LN) and TIL in B16 and MC38 **(C)** Pairwise comparisons of individual time points for Tregs in B16 and **(D)** MC38.

Table 1 ATACseq quality control and mapping statistics

Mapping statistics for ATACseq samples including percentage of total reads mapped to the murine genome (mapped reads %), and Transcription Start Site enrichment (TSS enrichment).

Cell Type	Tumor	Sample ID	Sample Name	Total Unique non-mitochondrial reads	Mapped Reads (%)	TSS Enrichment
Treg	B16	BD03	Treg LN Day 8_1	55,529,723	90.596	9.041
		BD07	Treg LN Day 8_2	15,099,531	90.98	10.505
		BD08	Treg LN Day 12_1	18,116,437	90.876	11.688
		BD16	Treg LN Day 12_2	49,651,361	88.092	8.937
		BD08	Treg LN Day 16_1	19,852,196	88.217	7.181
		BD16	Treg LN Day 16_2	16,569,601	88.088	8.572
		BD11	Treg LN Day 20_1	30,820,774	91.544	9.406
		BD15	Treg LN Day 20_2	34,503,152	85.025	7.597
		BD04	Treg TIL Day 8_1	56,177,911	91.202	8.722
		BD08	Treg TIL Day 8_2	18,429,309	90.19	10.592
		BD06	Treg TIL Day 12_1	24,483,837	89.002	6.953
		BD14	Treg TIL Day 12_2	54,881,402	83.078	0
		BD06	Treg TIL Day 16_1	35,442,752	86.374	7.038
		BD14	Treg TIL Day 16_2	21,637,688	87.408	8.524
		BD12	Treg TIL Day 20_1	44,797,794	89.996	8.973
		BD16	Treg TIL Day 20_2	46,504,620	88.103	0
	MC38	BD27	Treg LN Day 8_1	23,296,686	88.979	8.963
		BD31	Treg LN Day 8_2	18,381,449	88.732	8.599
		BD43	Treg LN Day 12_1	35,088,198	88.976	10.151
		BD47	Treg LN Day 12_2	45,364,354	87.783	10.76
		BD35	Treg LN Day 16_1	32,067,488	88.74	10.071
		BD39	Treg LN Day 16_2	27,285,807	87.212	9.612
		BD19	Treg LN Day 20_1	17,649,270	88.381	8.785
		BD23	Treg LN Day 20_2	47,757,867	81.172	2.46
		BD28	Treg TIL Day 8_1	18,477,927	88.504	8.108
		BD32	Treg TIL Day 8_2	17,267,030	89.137	8.136
		BD44	Treg TIL Day 12_1	52,290,742	90.048	9.701
		BD48	Treg TIL Day 12_2	36,446,646	87.851	9.303
		BD36	Treg TIL Day 16_1	46,852,116	86.427	8.371
		BD40	Treg TIL Day 16_2	24,435,827	88.121	9.961
		BD20	Treg TIL Day 20_1	21,288,587	87.663	7.231
		BD24	Treg TIL Day 20_2	46,332,049	86.543	6.024
CD4	B16	BD01	CD4 LN Day 8_1	45,855,000	89.647	9.618
		BD05	CD4 LN Day 8_2	29,306,126	88.384	10.301
		BD07	CD4 LN Day 12_1	14,918,001	86.721	5.676
		BD15	CD4 LN Day 12_2	43,969,271	87.374	8.188
		BD07	CD4 LN Day 16_1	22,172,402	89.054	7.389
		BD13	CD4 LN Day 16_2	21,077,289	86.857	8.466
		BD09	CD4 LN Day 20_1	51,660,892	83.373	7.903
		BD13	CD4 LN Day 20_2	49,076,215	85.595	8.393
		BD02	CD4 TIL Day 8_1	54,626,960	90.969	8.834
		BD06	CD4 TIL Day 8_2	44,503,150	87.698	9.076
		BD05	CD4 TIL Day 12_1	16,940,458	89.296	6.419
		BD05	CD4 TIL Day 16_1	25,378,622	87.713	6.821
		BD15	CD4 TIL Day 16_2	18,605,410	86.86	7.892
		BD10	CD4 TIL Day 20_1	34,744,080	87.85	8.848
		BD14	CD4 TIL Day 20_2	58,153,785	84.291	7.661
	MC38	BD27	CD4 LN Day 8_1	16,217,130	88.282	8.866
		BD31	CD4 LN Day 8_2	35,239,487	85.977	7.156
		BD43	CD4 LN Day 12_1	42,601,404	86.687	9.86
		BD47	CD4 LN Day 12_2	42,070,847	88.081	10.406
		BD35	CD4 LN Day 16_1	26,312,492	86.867	9.124
		BD39	CD4 LN Day 16_2	29,577,063	89.243	10.12
		BD19	CD4 LN Day 20_1	17,034,058	88.658	8.986
		BD23	CD4 LN Day 20_2	11,633,971	87.329	8.327
		BD28	CD4 TIL Day 8_1	21,848,973	87.474	8.051
		BD32	CD4 TIL Day 8_2	21,654,444	86.878	9.012
		BD44	CD4 TIL Day 12_1	84,988,827	84.499	6.567
		BD48	CD4 TIL Day 12_2	40,490,722	86.77	8.683
		BD36	CD4 TIL Day 16_1	45,810,019	85.618	7.843
		BD40	CD4 TIL Day 16_2	25,653,475	88.845	9.962
		BD20	CD4 TIL Day 20_1	22,438,858	90.357	7.858
		BD24	CD4 TIL Day 20_2	35,092,761	82.24	5.536

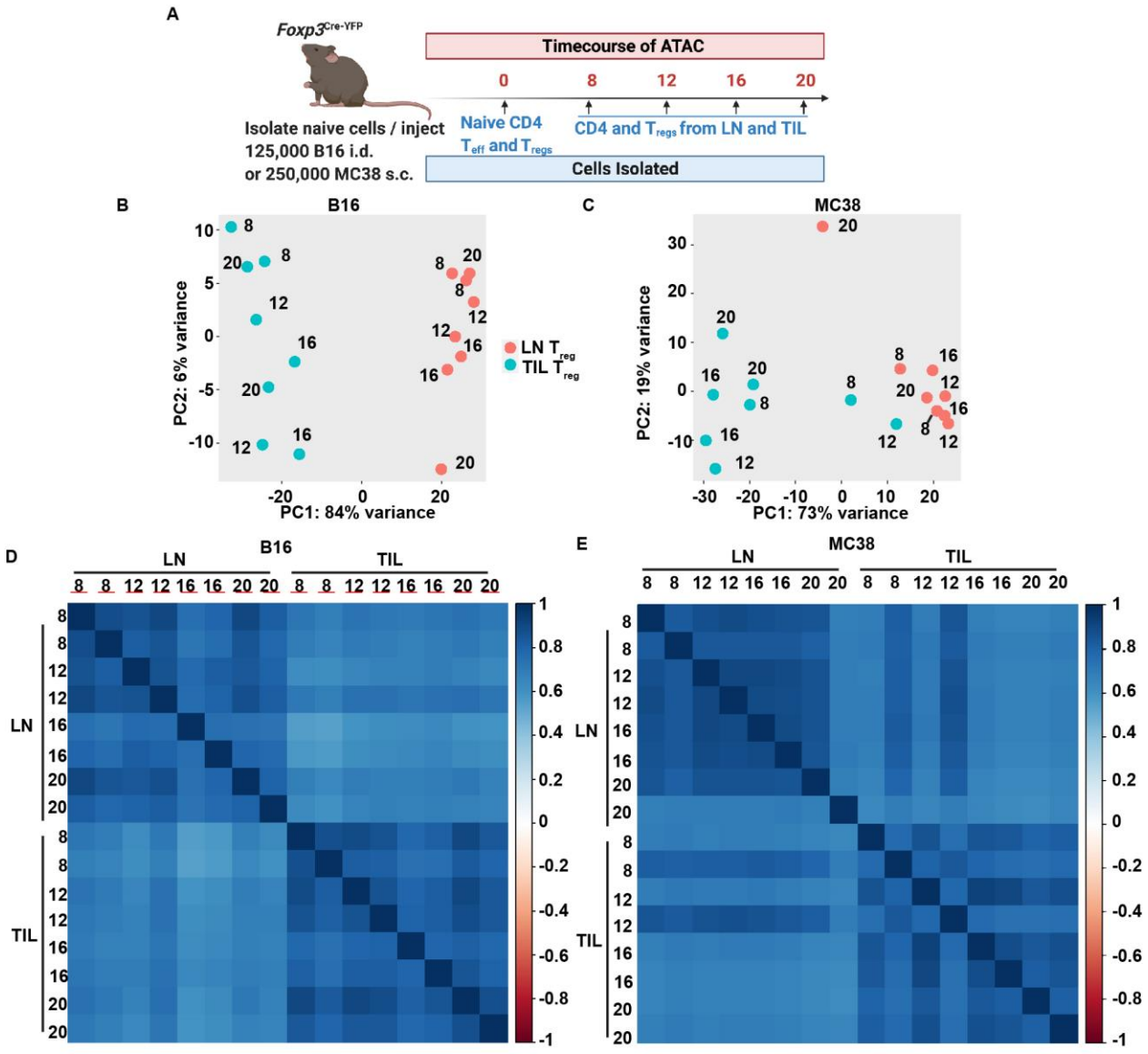

Figure 5 The TME drives changes in chromatin accessibility in Tregs but independent of time

(A) ATAC seq schematic **(B-C)** PCA analysis of LN and TIL Tregs from B16 **(B)** PCA analysis of LN and TIL Tregs from MC38 **(C)**. Day post tumor inoculation is indicated alongside each data point **(D-E)** Correlation plots comparing LN and TIL Tregs from B16 **(D)** and MC38 **(E)**.

3.2.2 Treg Epigenetic Signature in LN vs tumor-infiltrating lymphocytes (TIL)

Since there was not a time-dependent change in chromatin accessibility of TIL Tregs, the time points were pooled and then I focused on further examining differences between LN and TIL Tregs. I hypothesized these differences may be due to Treg activation and function in the TME, as T cell activation can induce chromatin remodeling [6,252,260].

Utilizing the same cutoffs in the previous analysis, 7,232 differentially open regions and 17,664 differentially closed regions were identified in Tregs in the tumor compared to the LN of B16 (Fig 6A). In addition, 7,417 differentially open regions and 12,512 differentially closed regions in Tregs in MC38 tumors compared to the LN were identified (Fig 6A). The peaks that were differentially open and closed in Tregs from either B16 or MC38 were well dispersed throughout promoters, exons, intergenic regions, etc. (Fig 6B). KEGG pathway enrichment identified activation of various pathways involved in metabolism of Tregs such as fatty acid elongation, phenylalanine metabolism, and butanoate metabolism, which have been documented to aid in the expansion and differentiation of T cells and Tregs [261-263] (Fig 7A-B).

Next, C7 pathway analysis, which examines immunologic signatures, was examined between LN and TIL Tregs in both B16 and MC38 tumors. This analysis identified enrichment for pathways involving “induced” or pTregs (Fig 8A). I considered that Tregs in the TME could be induced from a Tconv $CD4^{+}Foxp3^{-}$ precursor and the chromatin accessibility changes were representative of this conversion. However, TCRβ repertoire analysis showed little similarity of TCR sequences between Tregs and Tconv $CD4^{+}Foxp3^{-}$ in the TME (Fig 8B). These data indicate that Tregs in the TME are most

likely thymically derived and the peaks involved in the “induced” pathways may also be involved in tTregs in the TME.

In addition, there was enrichment of pathways in both B16 and MC38-derived Tregs involved in the Treg vs Tconv comparison (Fig 6C). Tregs may be controlling chromatin accessibility at loci that are important for Treg function and ensuring they maintain a suppressive phenotype rather than convert to a more pro-inflammatory Tconv in the TME. Moreover, previous studies have demonstrated that during T cell activation, Foxp3 can repress chromatin accessibility at various Foxp3 targets, potentially to retain their suppressive phenotype and limit an effector transition in a harsh inflammatory environment [252]. To address this question, the peaks in the LN vs TIL Treg data set were extrapolated to the nearest gene and then compared to the published “Treg transcriptional signature” [10]. This established signature describes transcriptional changes that are increased and decreased in Tregs compared to Tconv cells. These changes are critical to Treg identity and function. When the Treg transcriptional signature was compared to the list of chromatin accessibility of Tregs from the LN vs TIL Tregs, TIL Tregs were found to have differentially regulated peaks associated with the Treg transcriptional signature genes in the TME (Fig 5D-E).Genes such as *Satb1*, *Tgfbr3, Gramd3,* and *Klrd1* that are traditionally transcriptionally dampened in Treg vs Tconv are also not accessible in tumor-infiltrating Tregs (Fig 6D-E). For example, repression of *Satb1* expression has been shown to be important for Treg suppressive function and elimination of this repression leads to a transition to a Tconv effector phenotype. Moreover, this negative regulation of *Satb1* gene expression is regulated by Foxp3 [264,265]. Furthermore TβRIII (regulated by *Tgfbr3*) is downregulated in Tregs compared to Tconv, and is regulated by Foxp3

expression[10,266]. Therefore, I argue that Tregs in the TIL are reinforcing their suppressive phenotype through regulation of chromatin accessibility at loci important for Tconv conversion and function.

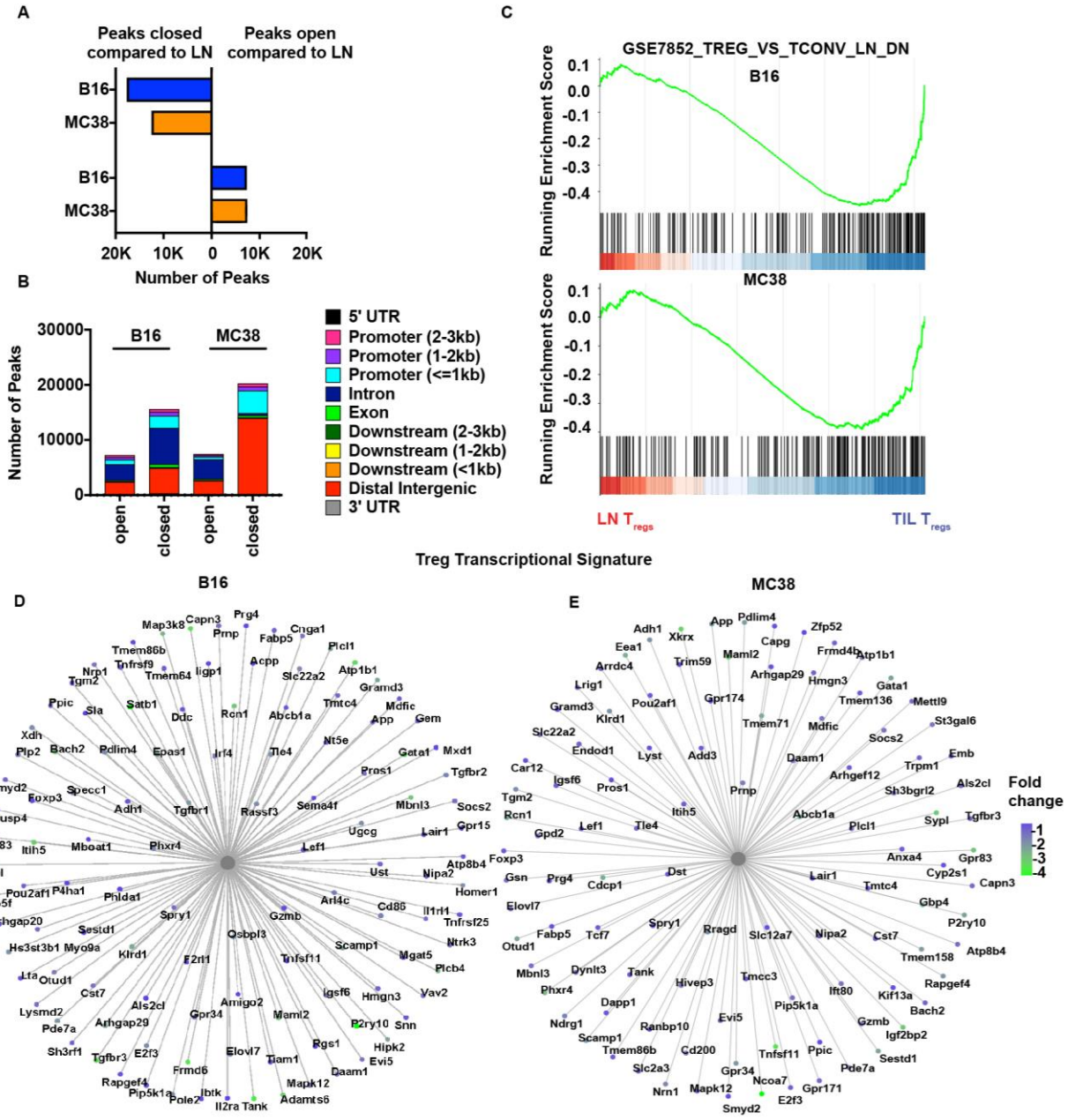

Figure 6 TIL Tregs regulate chromatin accessibility at Tconv signature genes

(A) Differentially accessible peaks that are open or closed in TIL Tregs compared to LN Tregs for the indicated tumor type. **(B)** Genomic location of differentially accessible genes that are open or closed in TIL Tregs vs LN for indicated tumor type **(C)** GSEA enrichment analysis for TIL Tregs vs LN Tregs **(D-E)** GSEA enrichment analysis of Treg transcriptional signature for TIL Tregs vs LN Tregs in B16 **(D)** and MC38 **(E)**

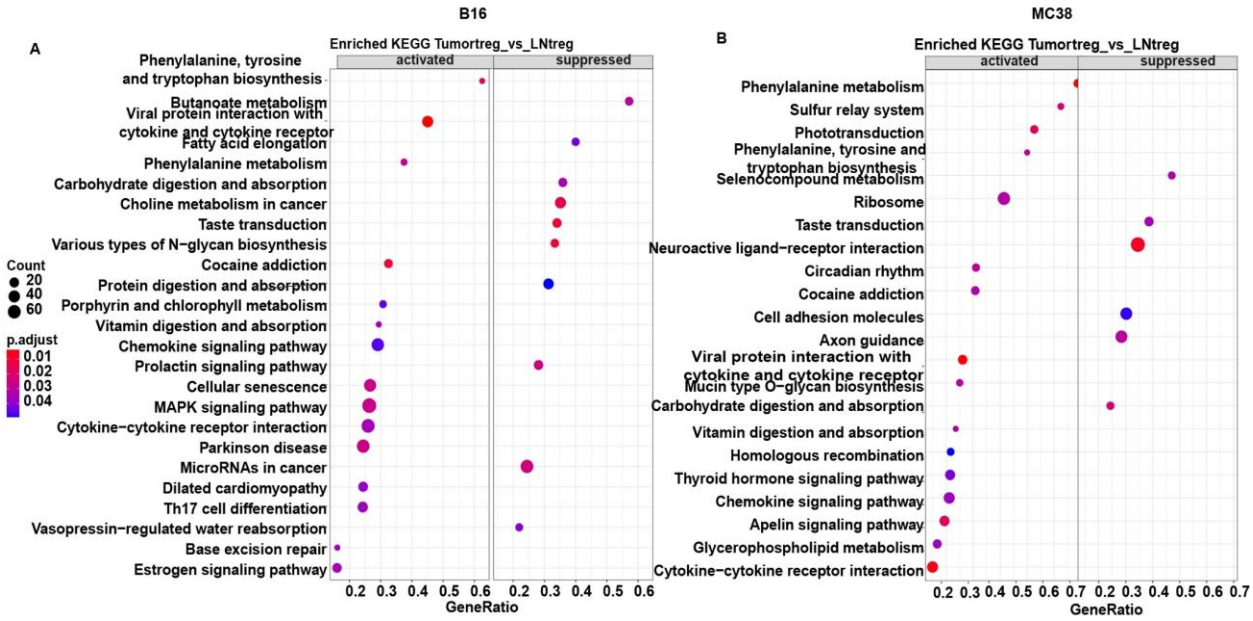

Figure 7 KEGG enrichment analysis for LN Treg vs TIL Treg ATAC peaks

(A-B) KEGG enrichment analysis for LN vs TIL Tregs in B16 (A) and MC38 (B).

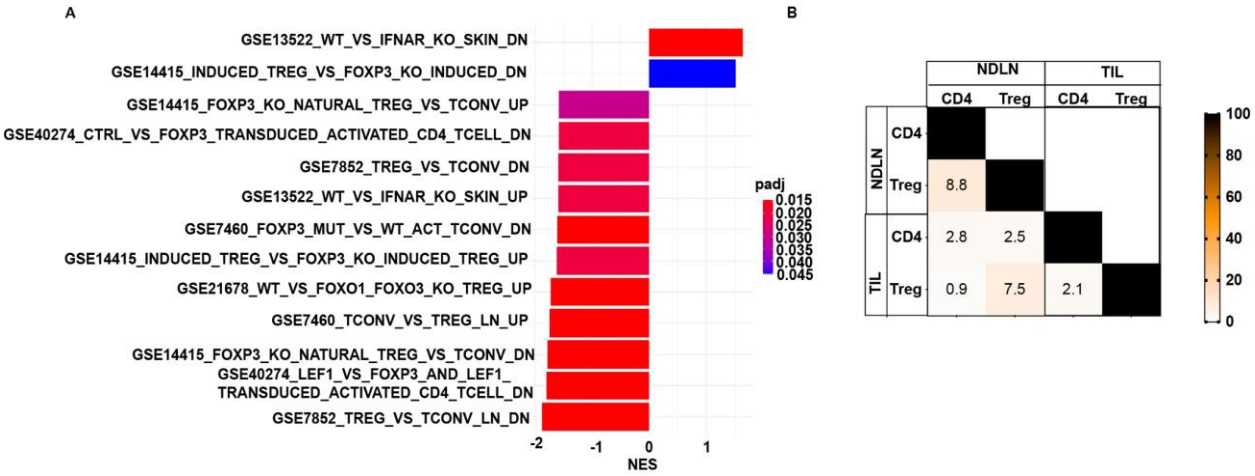

Figure 8 GSEA analysis reveals enrichment for pathways involved in pTreg vs tTreg in TIL vs LN Tregs

(A) Normalized enrichment score (NES) GSEA plots for TIL vs LN Tregs in B16 **(B)** *Foxp3*$^{Cre\text{-}YFP}$ mice were injected with 125,000 B16 cells i.d. and Tconv and Tregs were isolated at Day 16 from NDLN and TIL. Cells were subjected to TCR-sequencing. Morisita Horn Similarity Index was applied to determine sequence similarity between indicated populations.

3.2.3 Immunotherapy does not impact chromatin accessibility of TIL Tregs

Anti-PD1 treatment can significantly reduce tumor burden in a percentage of mice and patients [126-130]. Previous reports have demonstrated that treatment of mice with immunotherapy can impact Tregs; therefore, I questioned if the chromatin accessibility of the Treg genome would be changed in a mouse responding to anti-PD1 compared to a non-responder [77,267,268]. Therefore, I performed ATAC-seq on mice injected with the anti-PD1 sensitive tumor line, MC38. I stratified groups into responders and non-responders (NR) and isolated Tregs and Tconv from tumor and LN. Mice that were treated with anti-PD1 and decreased tumor growth after Day 13 or Day 15 were determined as responders while all mice with no decrease in tumor growth were categorized as non-responders.

Mice treated with isotype antibody were included as a control. PCA analysis found initial clustering was mainly dependent on cell type and tissue location (Fig 9A). Moreover, Tregs from anti-PD1 treated mice did not have specific clustering, indicating there is no change in chromatin accessibility dependent on response to therapy (Fig 9B). Similar results were found with transcriptional status indicating that anti-PD1 does not have an impact on transcription and chromatin accessibility of Tregs from the tumor (data not shown). Future studies will further examine if this trend is similar in $CD4^+$ $Foxp3^-$ Tconv cells.

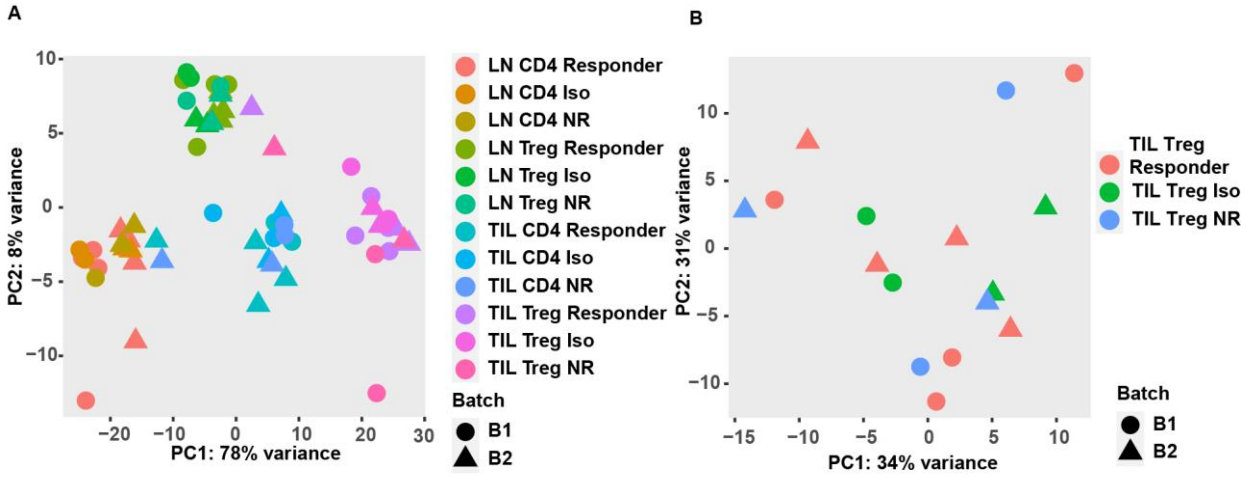

Figure 9 Response to anti-PD1 does not affect Treg chromatin accessibility

(A) PCA analysis of LN CD4, LN Treg, TIL CD4, and TIL Treg from mice treated with anti-PD1 or isotype (Iso) and stratified based on response to anti-PD1. NR, non-responder. Batch of sequencing run is indicated by shape **(B)** PCA analysis of TIL Tregs from mice treated with anti-PD1 or Iso and stratified based on response to anti-PD1.

3.3 Summary

I report three main findings from my study. First, TIL Tregs are altered in their genomic chromatin accessibility profile compared to LN Tregs. I hypothesized that activation of Tregs in the TME would trigger enhanced chromatin accessibility throughout the genome. Indeed, previous studies comparing naïve to in vitro activated $CD4^+$ $CD25^-$ T cells, demonstrated stimulated cells had increased accessibility at 11,386 loci and only 3,674 loci with decreased accessibility [255]. However, I found TIL Tregs closed more peaks than they opened when comparing to the LN Tregs. These changes are most likely indicative of an effort to limit conversion to a Tconv effector-like phenotype and ultimately allow Tregs to maintain a suppressive phenotype.

Second, although there were significant changes between TIL Tregs and LN Tregs, the TIL Tregs do not change their genomic chromatin accessibility over time. The TME is a dynamic environment with influx of a variety of immune cells and active immunoediting [50]. Therefore, I was surprised to find that TIL Tregs in B16 and MC38 do not change chromatin accessibility over time in the tumor. Previous studies have indicated that cells can change chromatin accessibility over time due to changes in environmental cues; however, we did not find that observation in our time course data [257]. Moreover, it would be of interest to examine if $CD4^+$ $Foxp3^-$ T cells also have minimal changes in chromatin accessibility over time.

Third, Tregs present in mice responding to anti-PD1 immunotherapy did not change their chromatin accessibility or transcriptional profile. Treatment of MC38 tumor bearing mice with anti-PD1 can yield response in a percentage of animals. While a main target of anti-PD1 is $CD8^+$ T cells, anti-PD1 could have direct and indirect effects on

Tregs. Anti-PD1 may directly bind to Tregs. PD-1 expression on Tregs may have an important role in their function and blocking may limit this function in the TME. In a murine model, T cell ligation of PD-1 to PD-L1 induces Foxp3 expression in $CD4^+$ $Foxp3^-$ T cells as well as increases the level of suppressive capability [269-274]. Moreover, Tregs require PD-1 expression to suppress activated $CD8^+$ T cells in mice infected with chronic lymphocytic choriomeningitis virus (LCMV) clone 13 [275,276]. Moreover, anti-PD1 has been shown to directly regulate Treg number in the TME, potentially due to ADCC [268]. Therefore, blocking of PD-1 may decrease suppressive capacity of Tregs or alter Treg number. However, these studies are further complicated by in vitro studies showing anti-PD-1 blockade enhances Treg suppression and proliferation [277].

Anti-PD1 therapy may also have indirect effects on Tregs. For example, anti-PD1 may re-invigorate $CD8^+$ T cells to produce higher amounts of proinflammatory molecules such as IFNγ [278]. Our lab has shown that IFNγ produced in the TME induces a less functional, fragile Treg, and Treg response to IFNγ was required for response to anti-PD1 [77,267]. Therefore, it was interesting we did not find a difference in Treg chromatin accessibility regardless of treatment with anti-PD1 or response to the therapy. This indicates that anti-PD1 may be impacting signaling pathways or protein function rather than chromatin accessibility.

3.4 Author Contributions

D.A.A.V conceived, directed and obtained funding along with R.E.D. for the project; R.E.D., C.J.W and D.A.A.V. conceptualized, designed, and performed the experiments. R.E.D., C.J.W and D.A.A.V. wrote the manuscript; R.E.D, H.Y., and G.C.L. performed all experiments. D.R. contributed to all bioinformatics analysis.

4.0 Regulatory T Cell-Derived TRAIL is Not Required for Peripheral Tolerance

Data within this chapter were taken from my previous publication **Dadey, R.E**., Grebinoski, S., Zhang, Q., Brunazzi, E.A., Burton, A., Workman, C.J., Vignali, D.A.A. "Regulatory T Cell-Derived TRAIL Is Not Required for Peripheral Tolerance" Immunohorizons. 2021:Jan22;5(1):48-58. doi: 10.4049/immunohorizons.2000098 under our own Copyright (open access).

4.1 Introduction

Tregs are one component of the immune system that can maintain the checks and balances through suppression of T cell activation. For example, Tregs are critical for limiting multiple models of autoimmunity such as the Non-Obese Diabetic (NOD) mouse, a spontaneous model of autoimmune diabetes, and the Myelin Oligodendrocyte Glycoprotein (MOG) C57BL/6 model of Experimental Autoimmune Encephalomyelitis (EAE). Treg depletion in these models rapidly results in overt diabetes and exacerbated EAE disease severity, respectively [169,170,279]. Despite this important role, Tregs can also suppress the anti-tumor response and therefore are an effective barrier to limiting tumor growth [1,2]. Tregs have multiple mechanisms of suppression and can utilize these mechanisms in the TME and autoimmune environment. Tregs can suppress through production of inhibitory cytokines, targeting of dendritic cell function, metabolic disruption

and direct cytolysis [31,34,35]. My lab has shown that Tregs from IL10 and IL35 deficient C57BL/6 mice upregulated cell cytotoxic molecule, TRAIL, in order to suppress responding T cells and that Tregs from BALB/c mice express higher levels of TRAIL than Tregs from C57BL/6 mice [280]. In addition, Tregs can produce TRAIL in an allogenic skin graft model to suppress activated T cells [281]. Taken together, these observations suggest that Tregs can utilize TRAIL to suppress immune cells in various disease environments.

In this study, I had two specific goals: (1) investigate TRAIL function in an inducible, cell-type specific manner by generating *Tnfsf10*$^{L/L}$ mice on C57BL/6, BALB/c, and NOD backgrounds, as studies thus far have only utilized blocking antibodies or constitutive *Tnfsf10* knock-out mice, (2) assess if Tregs require and/or are dependent on TRAIL as a mechanism of suppression within the tumor or autoimmune microenvironment by utilization of *Tnfsf10*$^{L/L}$*Foxp3*^{Cre} mice.

4.2 Results

4.2.1 TRAIL is expressed on Tregs in the TME

I hypothesized that Tregs utilize TRAIL to suppress the anti-tumor response. Therefore, I initially assessed TRAIL expression in multiple cell populations isolated from the TME of B16 tumor bearing mice, and I found substantial upregulation of *Tnfsf10* transcript in the tumor infiltrating lymphocytes (TIL) compared to the non-draining lymph node (NDLN) (Fig 10A). Interestingly, Tregs and CD4^{+}Foxp3^{-} were trending to have higher *Tnfsf10* levels in the TME compared to other cells in the TME. It is important to

note that TRAIL protein expression was difficult to discern, as previously reported, which may be due to its low level of expression [282].

4.2.2 Generation of a *Tnfsf10*$^{L/L}$ mouse

To directly access the importance of TRAIL expression in distinct cell types in the TME, in particular in Tregs, Amanda Burton generated a novel *Tnfsf10*$^{L/L}$ mouse. LoxP sites were inserted in the intron between exon 1 and 2 and following exon 5 along with an artificial exon containing a truncated non-functional version of the human nerve growth factor receptor (hNGFR). (Fig 10B-C). The hNGFR was intended to serve as a reporter for Cre mediated deletion of *Tnfsf10.* However, upon validation of the strain, it was found that expression of hNGFR was minimal following Cre-mediated deletion, likely due to the weak transcription strength of the *Tnfsf10* promoter consistent with challenges experienced in detected TRAIL expression (data not shown). This may also have been due to inefficient splicing into the artificial exon. In order to assess the role of TRAIL in Tregs, I crossed the *Tnfsf10*$^{L/L}$ mice with *Foxp3*$^{Cre\text{-}YFP}$.B6 mice and fidelity of Treg specific deletion was verified by cell specific genotyping (Fig 10D-E). Taken together, Amanda Burton has successfully generated a *Tnfsf10*$^{L/L}$ murine model, thus enabling me to specifically examine the role of TRAIL in Tregs.

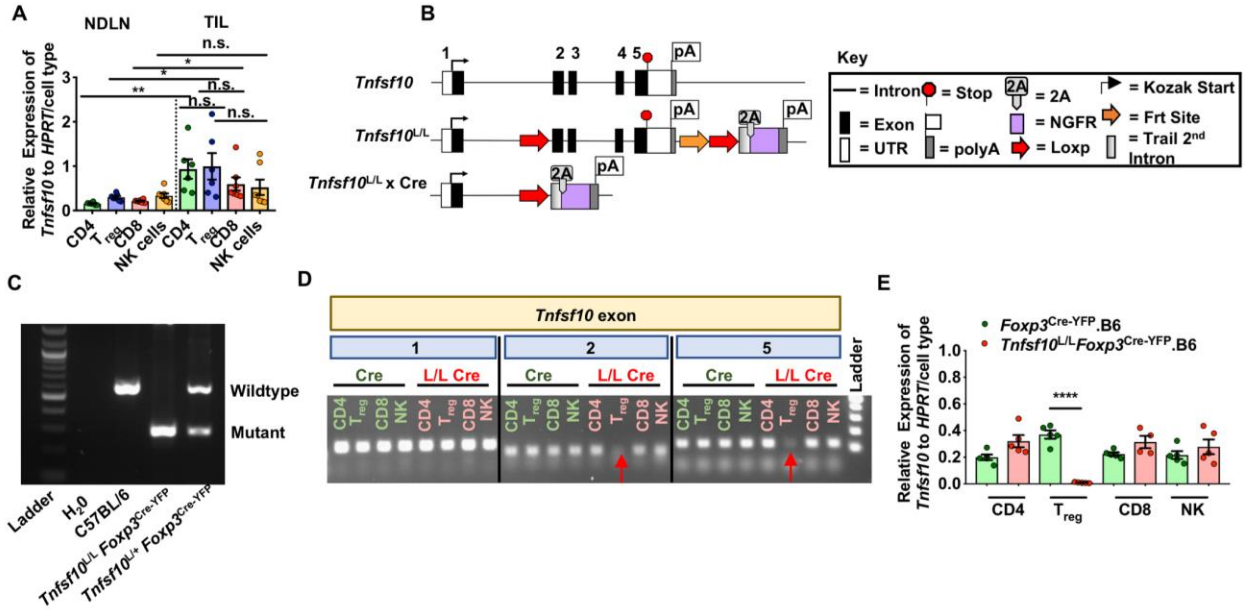

Figure 10 TRAIL is expressed on Tregs in the TME and generation of a *Tnfsf10*L/L mouse

(A) C57BL/6 *Foxp3*$^{Cre\text{-}YFP}$ mice were injected with 125,000 B16 cells i.d. and sacrificed 12 days post inoculation. Cells were sorted and qPCR was performed for *Tnfsf10* and *HPRT*. **(B)** Schematic of the *Tnfsf10*$^{L/L}$ mouse. **(C)** Genotyping PCR of genomic tail DNA of *Tnfsf10*$^{L/L}$ targeted mice . **(D)** Cells were sorted from *Foxp3*$^{Cre\text{-}YFP}$.B6 and *Tnfsf10*$^{L/L}$ *Foxp3*$^{Cre\text{-}YFP}$.B6 mice, genomic DNA isolated and PCR performed using primers specific for exons 1, 2 and 5 of *Tnfsf10*. **(E)** Cells were sorted from *Foxp3*$^{Cre\text{-}YFP}$.B6 and *Tnfsf10*$^{L/L}$ *Foxp3*$^{Cre\text{-}YFP}$.B6 mice and qPCR performed for *Tnfsf10* and *HPRT.* Data in **(A)** is representative of 1 experiment with 4-5 mice/group. Data in **(C-D)** is representative of 1 experiment with 1 mouse/group. **(E)** is representative of 2 experiments with 1-5 mice/group. Statistical analysis was determined by Student's unpaired *t* test (n.s., not significant, *p < 0.05, **p < 0.01, ****p < 0.0001).

4.2.3 Treg-restricted deletion of *Tnfsf10* does not affect tumor growth or suppression in C57BL/6 mice

Previous reports have shown that Tregs from C57BL/6 mice can utilize TRAIL to suppress the immune response [280,281]. To assess this, I first examined the suppressive capacity of Tregs from naïve *Tnfsf10*$^{L/L}$*Foxp3*$^{Cre\text{-}YFP}$.B6 mice. Surprisingly, the suppressive capacity of *Tnfsf10*-deficient Tregs was equivalent to wild-type (WT) Tregs (Fig 11A). Next, in order to assess if Tregs primarily depend on TRAIL to suppress the anti-tumor response, I injected *Foxp3*$^{Cre\text{-}YFP}$.B6 and *Tnfsf10*$^{L/L}$*Foxp3*$^{Cre\text{-}YFP}$.B6 mice with B16 melanoma. I chose this model due to studies describing the important role of Treg suppression in B16 tumor growth [76,77]. However, I found no difference in B16 tumor growth in *Tnfsf10*$^{L/L}$*Foxp3*$^{Cre\text{-}YFP}$.B6 mice (Fig 11B).

Furthermore, Tregs from the NDLN or TIL of *Tnfsf10*$^{L/L}$*Foxp3*$^{Cre\text{-}YFP}$.B6 mice with B16 bearing tumors were fully capable of suppressing in vitro (Fig 11C). Moreover, the suppressive activity of Tregs from *Tnfsf10*$^{L/L}$*Foxp3*$^{Cre\text{-}YFP}$.B6 mice did not change if Tregs were isolated at a later time point (Fig 12A). I also examined an additional tumor model, MC38 colon adenocarcinoma, which has been shown to be sensitive to TRAIL-induced cytotoxicity but found no differences in tumor growth between *Foxp3*$^{Cre\text{-}YFP}$.B6 and *Tnfsf10*$^{L/L}$*Foxp3*$^{Cre\text{-}YFP}$.B6 mice (Fig 11D) [283]. In an effort to understand if Treg-restricted deletion of *Tnfsf10* would impact tumor growth in a model of an active immune response that justifies a strong involvement of Treg-mediated negative feedback, I treated *Tnfsf10*$^{L/L}$*Foxp3*$^{Cre\text{-}YFP}$.B6 mice with anti-programmed cell death (PD-1) therapy and found no change in response to the immunotherapy (Fig 11D).

Tregs utilize TRAIL to suppress through induction of cell death in $CD4^+$ $Foxp3^-$ T cells [280,281]. However, in *Tnfsf10*$^{L/L}$*Foxp3*$^{Cre\text{-}YFP}$.B6 mice, I did not find a difference in activation/cleavage of the main downstream executioner caspase 3 in $CD4^+$ $Foxp3^-$ nor $CD8^+$ T cells when compared to *Foxp3*$^{Cre\text{-}YFP}$.B6 mice (Fig 11E-F). I also assessed other immune and non-immune populations, including tumor cells, but did not find differences in cell death (Fig 12B-E). This indicated that loss of TRAIL in Tregs did not affect cell death in immune and non-immune populations in the TME. Interestingly, the low expression of the murine TRAIL agonistic cell death receptor, DR5, may explain the lack of effect of Treg-mediated deletion of TRAIL (Fig 12F).

TRAIL can also suppress responding cells by inhibiting proliferation and T cell activation/function rather than cytotoxicity [284-287]. However, the proliferation of $CD4^+$ $Foxp3^-$ and $CD8^+$ T cells, measured by Ki67 expression, was not affected (Fig 11G-H). I also analyzed the functional status of $CD4^+$ $Foxp3^-$ and $CD8^+$ T cells and found no changes in production of pro-inflammatory cytokines TNFα and IFNγ (Fig 11I-L). I conclude that Treg-restricted deletion of *Tnfsf10* does not affect Treg suppression, tumor growth, cell death, nor proliferation and function of T cells.

Next, I hypothesized that Treg-restricted deletion of TRAIL may not lead to a change in tumor growth since *Tnfsf10*$^{L/L}$*Foxp3*$^{Cre\text{-}YFP}$.B6 Tregs still retain other mechanisms of suppression. Thus, I examined the expression of suppressive molecules IL-10, LAP-TGFβ, CTLA4, CD39, CD73 and indeed, expression was equivalent between WT Tregs and TRAIL deficient Tregs. (Fig 12G-K). Moreover, expression of the proliferation marker, Ki67, and markers of activation/exhaustion, PD-1 and LAG3,

remained unchanged in the Tregs in tumors of *Tnfsf10*$^{L/L}$ *Foxp3*$^{Cre\text{-}YFP}$ mice (Fig 12L-P). These results further indicate that the suppressive phenotype of *Tnfsf10*-deficient Tregs is unaffected.

I also found no change in the proportion of Tregs nor proportion of total immune cells in the tumor at day 12 (Fig 12Q-R) or day 18 (Fig 12S). Finally, while others have argued that TRAIL plays a role in Treg apoptosis, I found no change in Treg cell death in the TME (Fig 12T) [288]. Taken together these data suggest that Tregs are not primarily dependent upon TRAIL to suppress in the TME via cell death, inhibition of cell proliferation or function. This may be due to minimal expression of DR5 and/or the utilization of other suppressive molecules.

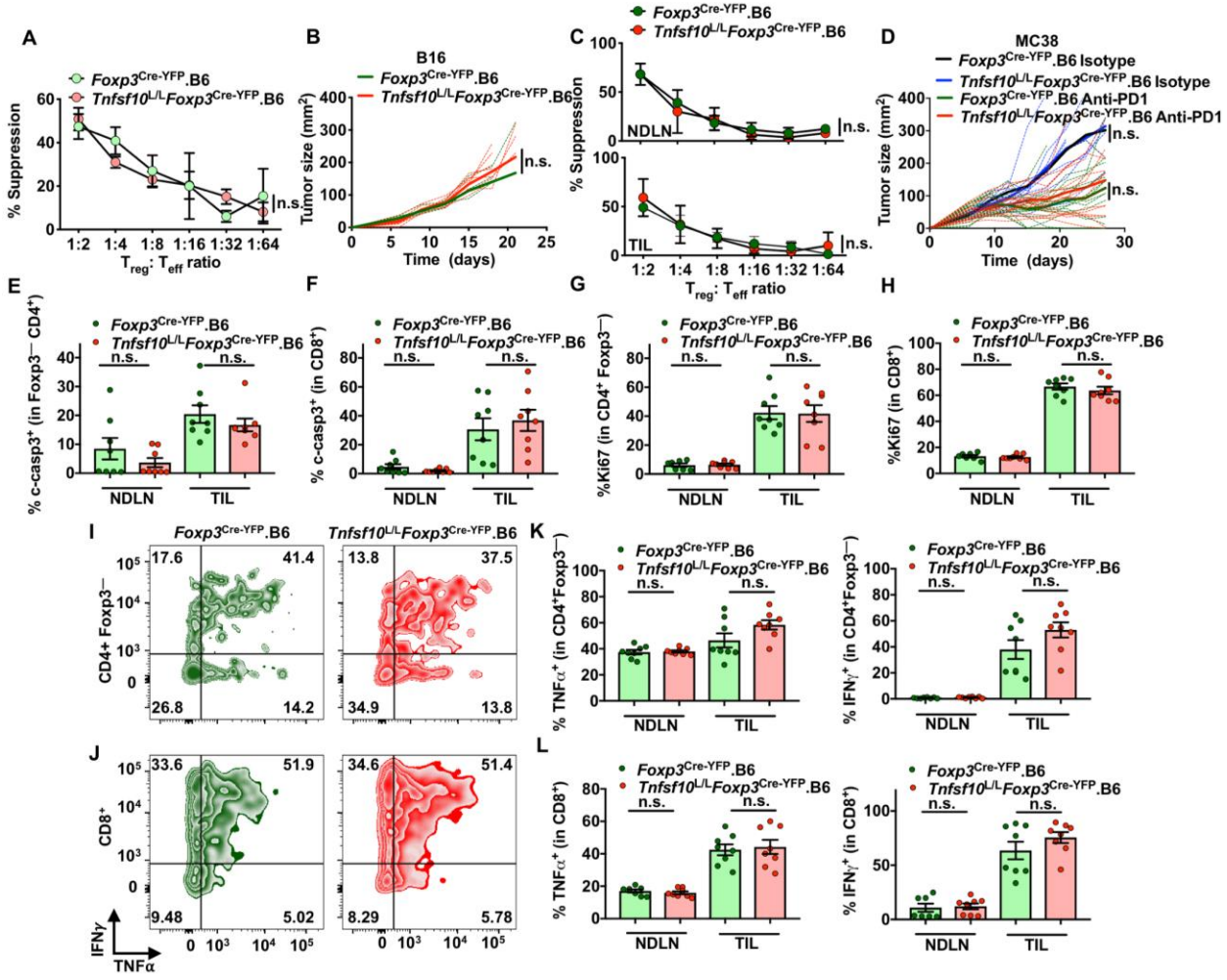

Figure 11 Treg-restricted deletion of *Tnfsf10* does not affect tumor growth nor suppression in C57Bl/6 mice

(A) Tregs were isolated from *Foxp3*$^{Cre\text{-}YFP}$.B6 and *Tnfsf10*$^{L/L}$ *Foxp3*$^{Cre\text{-}YFP}$.B6 naïve mice and cultured with effector CD4^{+} T cells, APCs and anti-CD3 antibody (Ab) for 72 h in a classical microsuppression assay. **(B)** Mice were injected with 125,000 B16 i.d. and tumor size was measured. **(C)** Mice were injected with 125,000 B16 i.d. and sacrificed at Day 12 post tumor inoculation. Microsuppression as previously described in (A) was performed. **(D)** *Foxp3*$^{Cre\text{-}YFP}$.B6 and *Tnfsf10*$^{L/L}$ *Foxp3*$^{Cre\text{-}YFP}$.B6 mice were injected with 500,000 MC38 s.c. and treated with isotype or anti-PD1 on Days 6, 9, and 12 and measured for tumor growth. **(E-F)** CD4^{+} Foxp3^{-} **(E)** and CD8^{+} T cells **(F)** were examined for percent expression of c-casp3 **(G-H)** CD4^{+} Foxp3^{-} and **(G)** CD8^{+} T cells **(H)** were examined for percent expression of Ki67. **(I-J)** CD4^{+} Foxp3^{-} and **(I)** CD8^{+} T cells **(J)** from the TIL were gated for IFNγ and TNFα after 4 hour stimulation. Representative plots shown.

(K-L) Tabulated data for IFNγ and TNFα from $CD4^+$ $Foxp3^-$ and $CD8^+$ T cells. Data in **(A)** is representative of 1 experiment with 3-4 mice/group. Data in **(B-L)** is representative of 2 experiments with 6-9 mice/group. Statistics were determined using 2-way ANOVA **(A-D)** and Student unpaired t test **(E-H, K-L)** (ns, not significant). Expression and functional data in **(A,C, E-L)** was determined by flow cytometry.

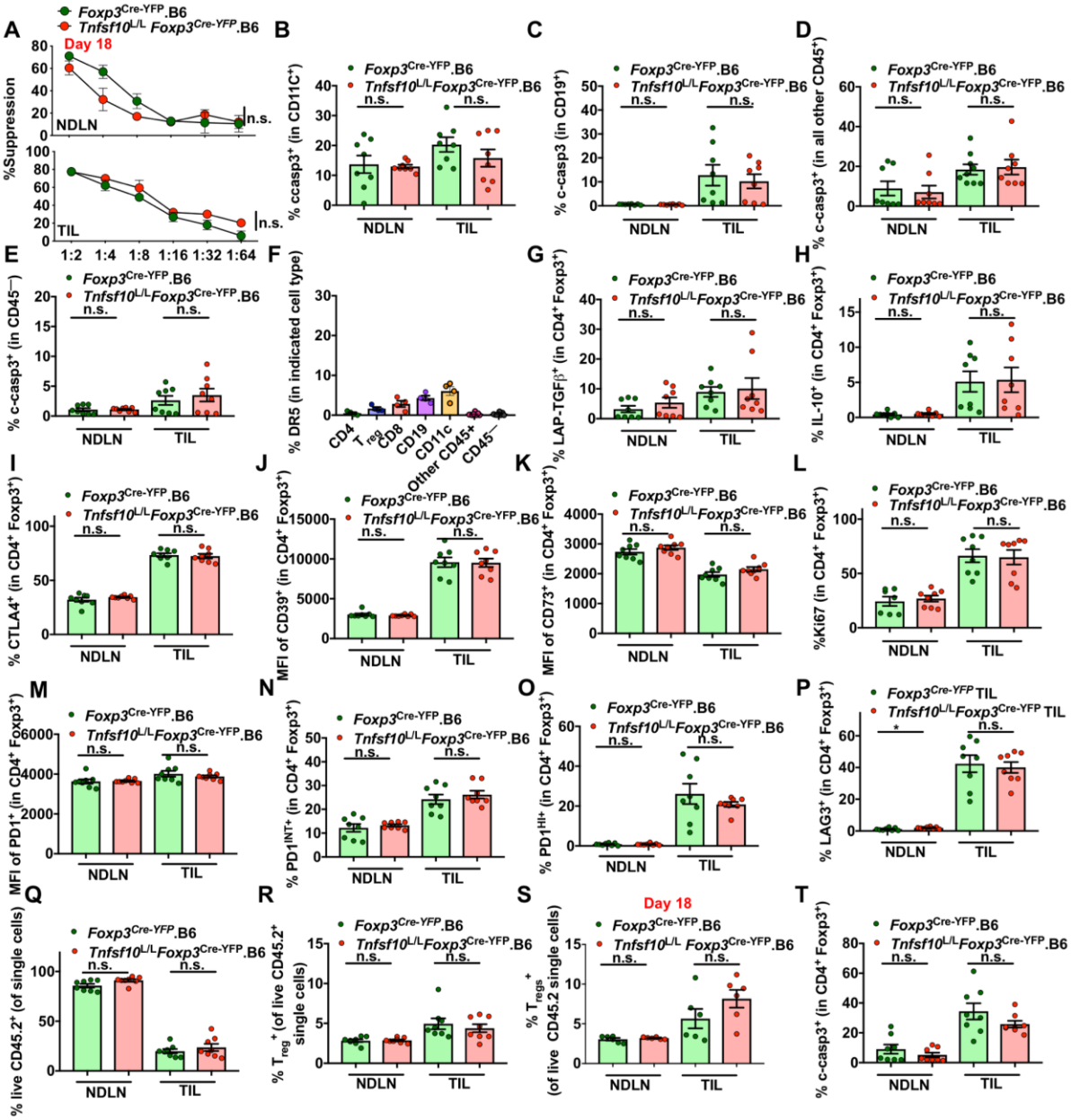

Figure 12 No change in cell death in other populations and maintenance of other Treg suppressive molecules in C57BL/6 mice

(A) *Foxp3*$^{Cre\text{-}YFP}$.B6 and *Tnfsf10*$^{L/L}$ *Foxp3*$^{Cre\text{-}YFP}$.B6 mice were injected with 125,000 B16 i.d. and Tregs were isolated on Day 18 from NDLN and TIL to perform a classical microsuppression assay. **(B)** *Foxp3*$^{Cre\text{-}YFP}$.B6 and *Tnfsf10*$^{L/L}$ *Foxp3*$^{Cre\text{-}YFP}$.B6 mice were injected with 125,000 B16 i.d. and TCRβ^{-}CD11c^{+} cells were stained for percent expression of c-casp3. **(C-E)** TCRβ^{-}CD19^{+} **(C)** CD45^{+}TCRβ^{-}CD19^{-}CD11c^{-} cells **(D)** and CD45^{-} cells **(E)** were stained for percent expression of c-casp3. **(F)** % positive surface DR5 expression was determined by flow cytometry. **(G)** Tabulated LAP-TGFβ and **(H) %** IL-10 expression on Tregs **(I)**

%CTLA4 expression on gated Tregs. **(J)** Gated MFI (MFI of gated positive cells) of $CD39^+$ Tregs **(K)** Gated MFI of CD73 on Tregs **(L)** % Ki67 on Tregs **(M)** MFI of PD-1 in $PD\text{-}1^+$ Tregs. **(N)** %PD-1 intermediate in Tregs **(O)** %PD-1 high in Tregs **(P)** %LAG3 on Tregs **(Q)** % live $CD45.2^+$ on gated single cells **(R-S)** $\%CD4^+$ $Foxp3^+$ Tregs in live $CD45.2^+$ single cells at Day 12 **(R)** and Day 18 **(S)**. **(T)** $\%CD4^+$ $Foxp3^+$ Tregs were gated for percent positive expression of c-casp3. Data in **(A-E) and (G-T)** are representative of 2 experiments with 6-8 mice/group. **(F)** is representative of 1 experiment with 4 mice/group. 2-way ANOVA **(A)** was used. Student unpaired t test **(B-E, G-T)** was used. (ns, not significant). Expression and functional data in **(A-T)** determined by flow cytometry.

4.2.4 Treg-restricted deletion of *Tnfsf10* does not affect tumor growth or suppression in BALB/c mice

While I did not observe a primary role for TRAIL in Tregs in C57BL/6 mice, I hypothesized I may see differences in BALB/c mice given the previous studies in which TRAIL had a more predominant role in BALB/c Tregs compared with Tregs from C57BL/6 mice [280]. Moreover, other studies have revealed TRAIL can play a part in regulating the Th1/Th2 balance [289-292]. Therefore, the *Tnfsf10*$^{L/L}$ mice were backcrossed to the Th2-prone BALB/c background and then crossed it to the BALB/c *Foxp3*^{Cre} mouse [106]. Initially, I assessed the function of naïve TRAIL-deficient Tregs in a standard in vitro suppression assay and interestingly, the level of suppression was equivalent to WT Tregs (Fig 13A). Next, I assessed tumor growth in *Foxp3*$^{Cre\text{-}YFP}$.BALB/c, *Tnfsf10*$^{L/L}$.BALB/c, and *Tnfsf10*$^{L/L}$*Foxp3*$^{Cre\text{-}YFP}$.BALB/c mice, using the BALB/c CT26 colon carcinoma model, in which Tregs suppress the anti-tumor response [293,294]. While I did not observe a difference in tumor growth (Fig 13B), I did see a small decrease in suppression in TRAIL-deficient Tregs isolated from CT26 tumors compared to WT Tregs (Fig 13C). However, this was

not the case at a later time point (Fig 14A). Next, I determined that cleaved caspase levels in $CD4^+$ $Foxp3^-$, $CD8^+$ T cells, tumor cells, and other cell populations were equivalent (Fig 13D-E*)* (Fig 14B-E) suggesting that Tregs were not dependent upon TRAIL mediated cytotoxicity in the TME of BALB/c mice, possibly due to low DR5 expression in the TME (Fig 14F).

Furthermore, I did not see any changes in Ki67, TNFα, and IFNγ in T cells suggesting that Tregs do not suppress by limiting proliferation nor function of responding T cells (Fig 13F-K). I also observed that TRAIL deficient Tregs in the TME still retained other suppressive molecules indicating that other molecules may aid in suppression in the TME despite loss of TRAIL (Fig 14G-K). Furthermore, I did not see any differences in expression of Ki67, PD-1, LAG3, and c-casp3 on Tregs (Fig 14L-Q). The proportion of immune cells and Tregs remained unchanged on both day 12 and 18 (Fig 14R-T). Taken together, these data suggest that despite the reported higher levels of TRAIL expression in BALB/c Tregs, they are not primarily dependent upon TRAIL as a means of suppression in the TME [280].

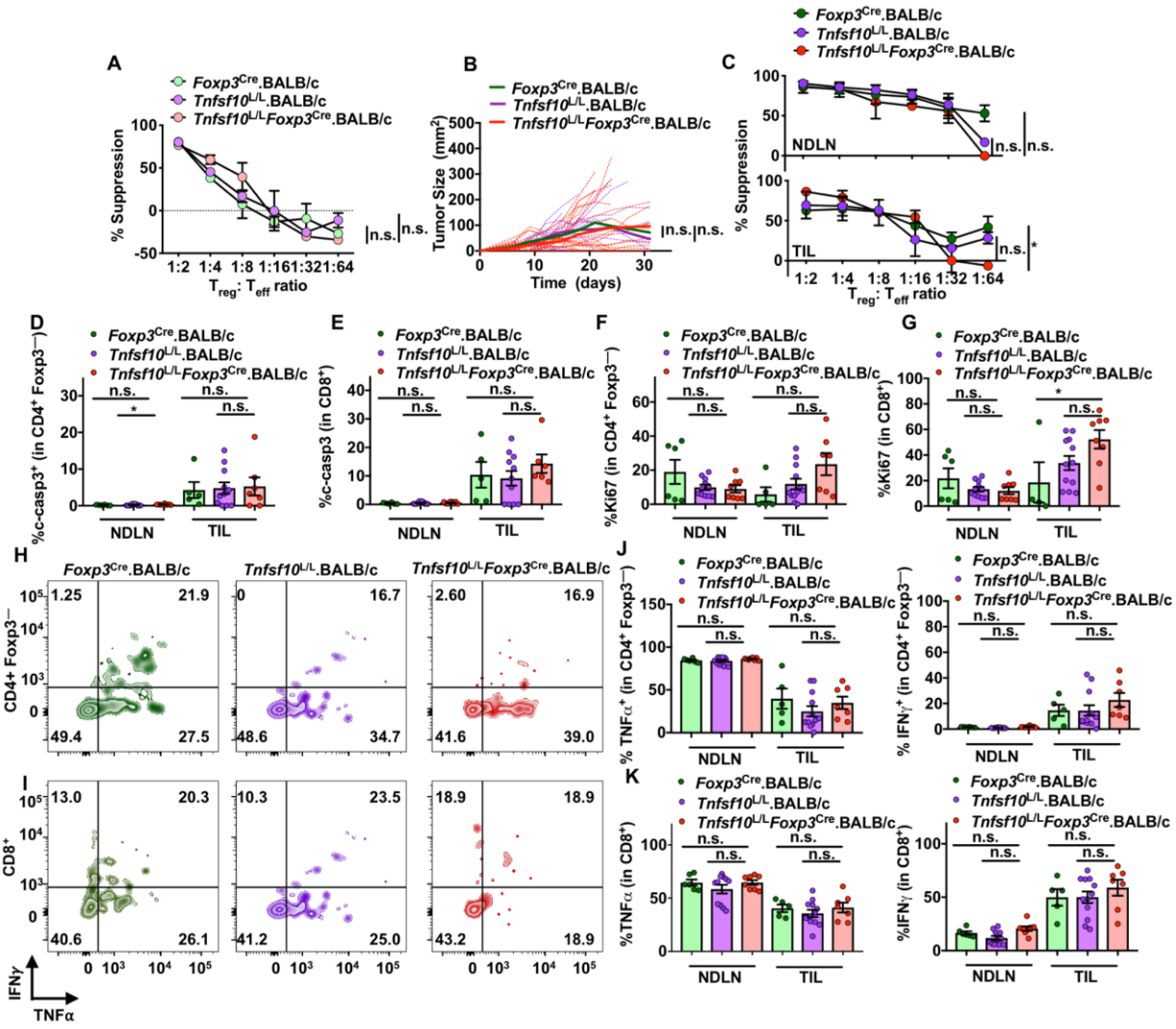

Figure 13 Treg-restricted deletion of *Tnfsf10* does not affect tumor growth nor suppression in BALB/c mice

(A) Tregs (TCRβ$^+$CD4$^+$CD25$^+$CD127$^-$) were sorted from *Foxp3*^{Cre}.BALB/c, Tnfsf10$^{L/L}$.BALB/c, *Tnfsf10*$^{L/L}$ *Foxp3*^{Cre}.BALB/c naive mice and cultured with effector T cells, APCs, and anti-CD3 Ab for 72 h in a classical microsuppression assay. **(B)** Mice were injected with 125,000 CT26 s.c. and tumor size was measured. **(C)** Mice were injected with 125,000 CT26 s.c. and sacrificed at Day 12 post tumor inoculation. Microsuppression as previously described in **(A)** was performed. **(D)** CD4$^+$ Foxp3$^-$ and **(E)** CD8$^+$ T cells from were examined for percent expression of c-casp3 **(F)** CD4$^+$ Foxp3$^-$ and **(G)** CD8$^+$ T cells were examined for percent expression of Ki67. **(H)** CD4$^+$ Foxp3$^-$ and **(I)** CD8$^+$ T cells from the TIL were gated for IFNγ and TNFα after 4 hr stimulation, representative plots shown. **(J,K)** Tabulated data for IFNγ and

TNFα from $CD4^+$ $Foxp3^-$ and $CD8^+$ T cells. Data in **(A)** are representative of 1 experiment with 2-3 mice/group. Data in **(B)** are representative of 4 experiments with 14-25 mice/group. Data in **(C-K)** are representative of 2 experiments with 3-12 mice/group. Statistics were determined using 2-way ANOVA **(A-C)** and Student unpaired t test **(D-G, J-K)** (ns, not significant, *$p < 0.05$). Expression and functional data in (**A, C-K)** was determined by flow cytometry.

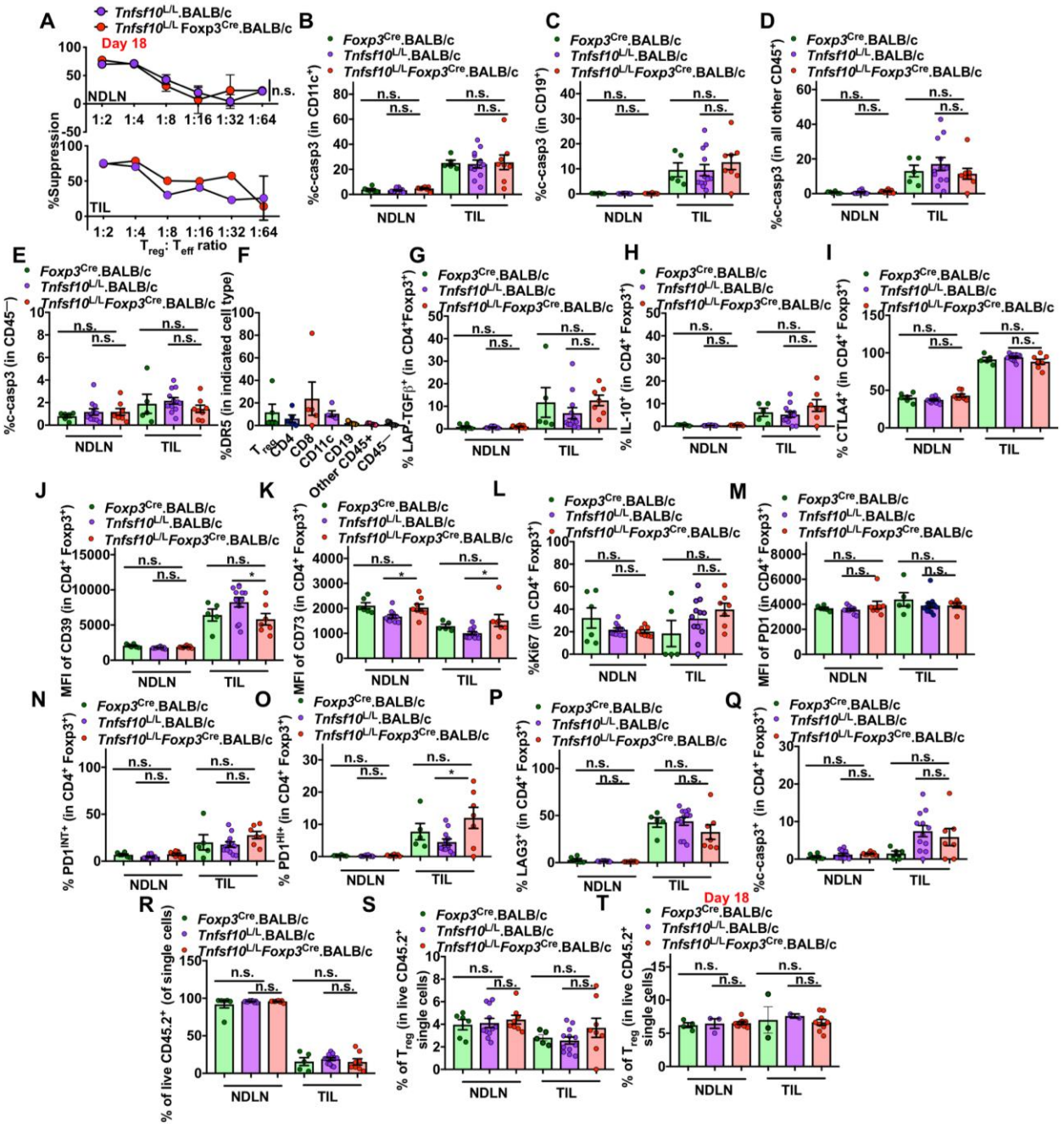

Figure 14 No change in cell death in other populations and maintenance of other Treg suppressive molecules in BALB/c mice

(A) *Tnfsf10*$^{L/L}$.BALB/c and *Tnfsf10*$^{L/L}$ *Foxp3*^{Cre}.BALB/c mice were injected with 125,000 CT26 s.c. and Tregs were isolated on Day 18 from NDLN and TIL to perform a classical microsuppression assay. **(B)** *Foxp3*^{Cre}.BALB/c, Tnfsf10$^{L/L}$.BALB/c, *Tnfsf10*$^{L/L}$ *Foxp3*^{Cre}.BALB/c mice were injected with 125,000 CT26 s.c. and TCRβ^{-}CD11c^{+} cells were stained for percent expression of cleaved-caspase3 (c-casp3). **(C)** TCRβ^{-}

$CD19^+$, **(D)** $CD45^+TCR\beta^-CD19^-CD11c^-$ cells and **(E)** $CD45^-$ cells were stained for percent expression of c-casp3. **(F)** Cell populations were stained for % positive DR5 expression. **(G)** Tabulated LAP-TGFβ and **(H)** IL-10 % expression on Tregs **(I)** %CTLA4 expression on gated Tregs. **(J)** Gated MFI of CD39 on Tregs **(K)** Gated MFI of CD73 on Tregs. **(L)** %Ki67 on Tregs **(M)** MFI of PD-1 in $PD\text{-}1^+$ Tregs **(N)** %PD-1 intermediate in Tregs **(O)** %PD-1 high in Tregs **(P)** %LAG3 on Tregs **(Q)** $\%CD4^+$ $Foxp3^+$ Tregs were gated for percent positive expression of c-casp3. **(R)** % live $CD45.2^+$ on gated single cells **(S)** $\%CD4^+$ $Foxp3^+$ Tregs in live $CD45.2^+$ single cells at Day 12 **(T)** $\%CD4^+$ $Foxp3^+$ Tregs in live $CD45.2^+$ single cells at Day 18. Data in **(A)** is representative of 1 experiment with 2-3 mice/group pooled. **(B-E, G-S)** is representative of 2 experiments with 6-12 mice/group. Data in **(F, T)** is representative of 1 experiment with 2-9 mice/group. 2-way ANOVA **(A)** was used. Student unpaired t test **(B-E, G-T)** was used. (ns, not significant, $*p < 0.05$). Expression and functional data in **(A-T)** was determined by flow cytometry.

4.2.5 Treg-restricted deletion of Tnfsf10 does not affect autoimmune diabetes

Since Tregs are also critical in limiting autoimmunity, I hypothesized that Tregs may utilize TRAIL to suppress in the autoimmune microenvironment. Also, it has been reported that TRAIL can regulate cell death of diabetogenic T cells in the pancreatic islet of Non-Obese Diabetic (NOD) mice [295]. While it was proposed that this was mediated by TRAIL expressing pancreatic beta cells, I hypothesized that Tregs may also utilize TRAIL to suppress T cells in this environment [295]. Indeed, T cells express the highest levels of *Tnfsf10* in the islet (Fig 15A). I hypothesized that Treg-restricted deletion of *Tnfsf10* would limit suppression of diabetogenic T cells and lead to exacerbated autoimmune diabetes.

Interestingly, I found that deletion of *Tnfsf10* in Tregs did not significantly alter diabetes incidence nor insulitis in female (Fig 15B-D) or male (Fig 16A) mice, although there was a slight trend towards reduced diabetes incidence. Moreover, I did not find any

changes in cell death in $CD4^{+}Foxp3^{-}$ and $CD8^{+}$ T cells in the islet (Fig 15E-F). As seen with the tumor data, I found that the levels of proliferation and cytokine production in the diabetogenic T cells of the islet were similar in both WT and *Tnfsf10*$^{L/L}$Foxp3$^{Cre\text{-}GFP}$.NOD mice (Fig 15G-L). This would indicate that Tregs do not require TRAIL to suppress diabetogenic T cells in the pancreatic islet of NOD mice.

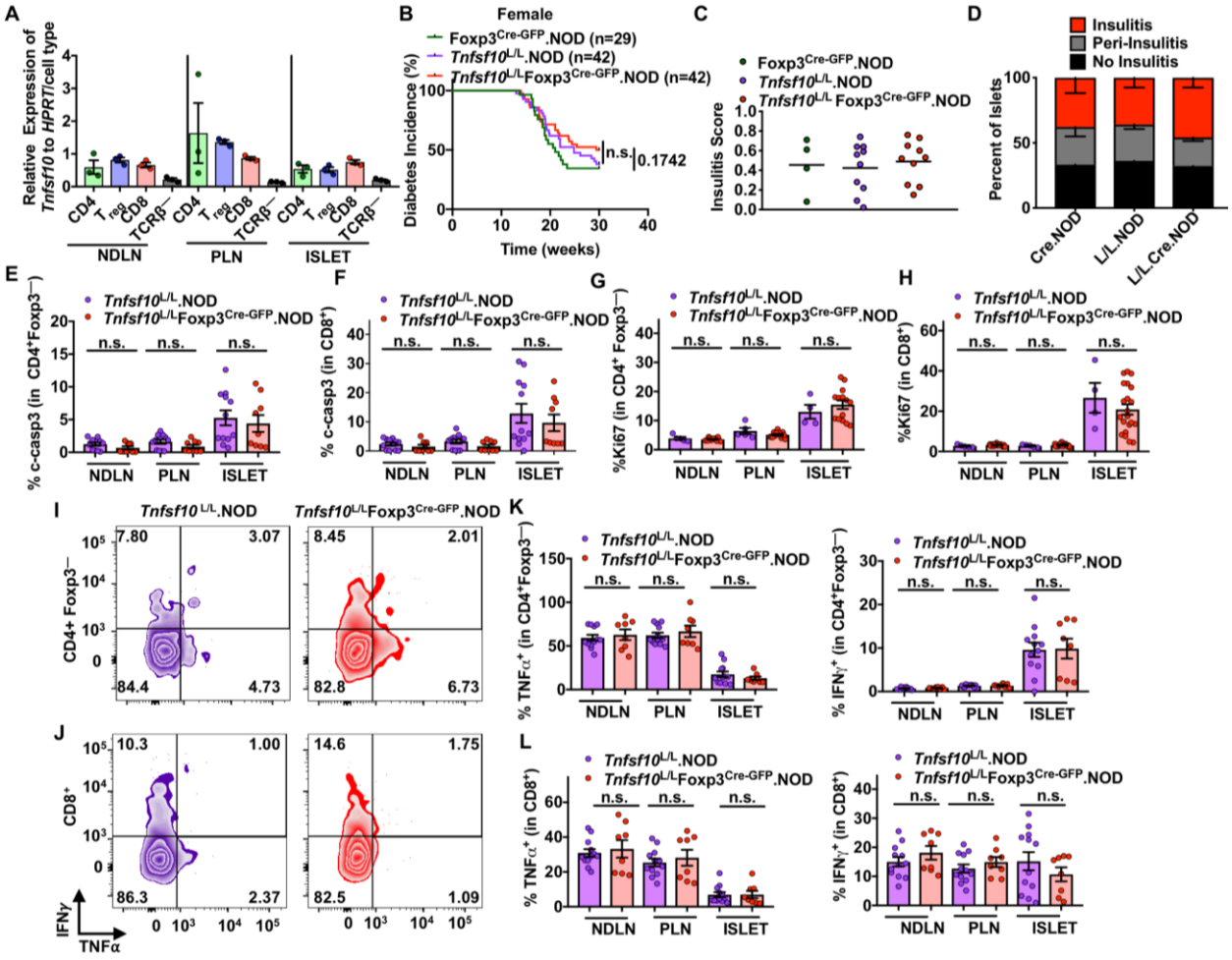

Figure 15 Treg-restricted deletion of *Tnfsf10* does not affect diabetes incidence, insulitis nor suppression in NOD mice

(A) 12 week old female NOD Foxp3$^{Cre\text{-}GFP}$ mice were sacrificed. Cells were sorted and qPCR was performed for *Tnfsf10* and *HPRT*. **(B)** Diabetes onset monitored in *Tnfsf10*$^{L/L}$Foxp3$^{Cre\text{-}GFP}$.NOD females and co-caged controls. **(C-D)** Histological assessment of insulitis performed in female *Tnfsf10*$^{L/L}$Foxp3$^{Cre\text{-}GFP}$.NOD and co-caged controls at 12 weeks of age. **(E)** CD4^{+} Foxp3$^{—}$ and **(F)** CD8^{+} T cells were examined for percent expression of cleaved-caspase3 (c-casp3). **(G)** CD4^{+} Foxp3$^{—}$ and **(H)** CD8^{+} T cells were examined for percent expression of Ki67. **(I)** CD4^{+} Foxp3$^{—}$ and **(J)** CD8^{+} T cells from the TIL were gated for IFNγ and TNFα after 4 hour stimulation, representative plots shown. **(K,L)** Tabulated data for IFNγ and TNFα from CD4^{+} Foxp3$^{—}$ and CD8^{+} T cells. Data in **(A)** are representative of 1 experiment with 3 mice/group. Data in **(B)** are representative of >3 experiments with 29-42 mice/group. Data in **(C-D)** are representative of 1

experiment with 4-10 mice/group. Data in **(E-L)** are representative of 2 experiments with 4-21 mice/group. Statistics were determined using Log-rank (Mantel Cox) test **(B)** and Student unpaired t test **(E-H, K-L)** (ns, not significant). Expression data in (**E-L)** was determined by flow cytometry.

I also examined DR5 expression on immune and non-immune cells in the islet and found minimal expression of DR5 on immune cells but higher expression on Insulin^{+} beta (β) cells (Fig 16B). Reports of direct TRAIL-mediated beta cell killing have been inconsistent [296-300]. However, upon examination of Insulin positive cells, I found no change in cell death (Fig 16C). Interestingly, I did see a reduction in cell death in the CD11c^{+} population (Fig 16D). TRAIL can have an effect on dendritic cells; however, it is unclear what impact this may play in this system as I did not see a consequence of altered disease [301]. Future studies may elucidate what other impact this has in autoimmune diabetes.

I found that *Tnfsf10*-deficient Tregs isolated from the TME retained their suppressive phenotype. I questioned if this remained true for *Tnfsf10*-deficient Tregs isolated from the islet. I found Tregs still expressed functional markers such as LAP-TGFβ, IL-10, and CD39 (Fig 16E-G) and even had an increase in CD73 expression (Fig 16H). This further indicates that *Tnfsf10*-deficient Tregs retain their suppressive phenotype in the islet. As seen in the tumor, I found no change in Treg proliferation (Fig 16I), as measured by Ki67, and no change in activation/exhaustion markers PD-1 and LAG3 (Fig 16J-M). These data indicate that TRAIL did not have an effect on Treg cell death nor the proportion of immune cells and Tregs in the TME. Interestingly, while I did not observe a difference in total immune cell proportions within the islet (Fig 16N), I did see an increased proportion of intra-islet Tregs in *Tnfsf10*$^{L/L}$Foxp3$^{Cre\text{-}GFP}$.NOD mice (Fig

16O). Interestingly, reduced Treg cell death was only observed in 10 week old mice (Fig 16P) as there was no difference in 12 week old mice (Fig 16Q). Therefore, I conclude that Tregs are not dependent on TRAIL to suppress in the islet.

Finally, I examined if Treg-derived TRAIL had a role in the MOG model of Experimental Autoimmune Encephalomyelitis (EAE) using the *Tnfsf10*$^{L/L}$*Foxp3*$^{Cre\text{-}YFP}$.B6 mice. As seen with the tumor and NOD models, I did not observe a difference in EAE score and initiation of the disease between WT and *Tnfsf10*$^{L/L}$*Foxp3*$^{Cre\text{-}YFP}$.B6 mice (Fig 8R). Therefore, I conclude that Tregs do not require nor are dependent on TRAIL as a means of suppression in autoimmune microenvironments.

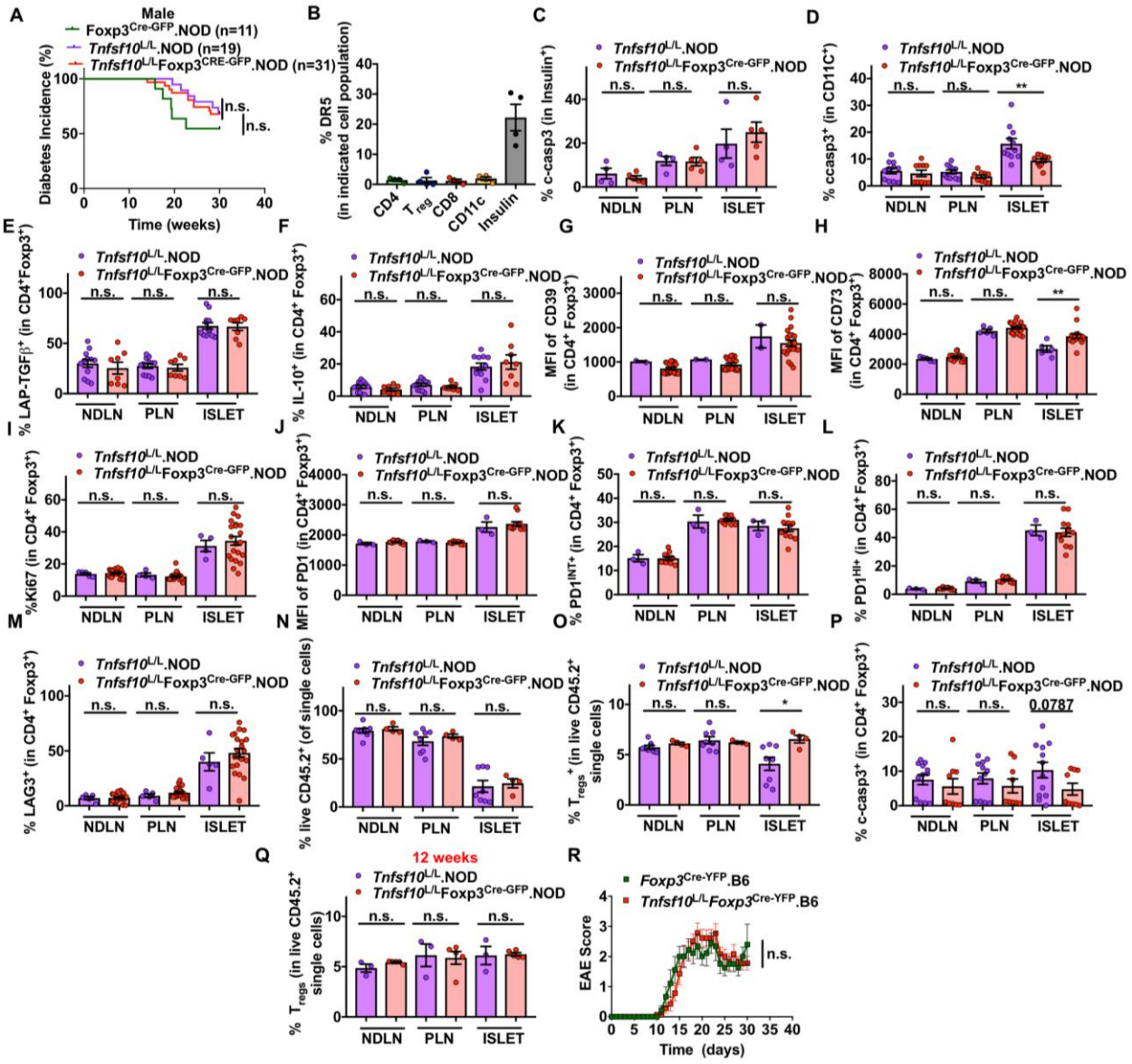

Figure 16 Treg-restricted deletion of *Tnfsf10* effects cell death of CD11c^{+} and Tregs in the diabetic islet

(A) Diabetes onset monitored in *Tnfsf10*$^{L/L}$Foxp3$^{Cre\text{-}GFP}$.NOD males and co-caged controls. **(B)** Islets from 10 week old female *Foxp3*$^{Cre\text{-}GFP}$.NOD mice were stained for surface DR5 on indicated cell populations. **(C)** Insulin^{+} cells isolated from *Tnfsf10*$^{L/L}$.NOD and *Tnfsf10*$^{L/L}$ *Foxp3*$^{Cre\text{-}GFP}$.NOD female mice were stained for percent expression of cleaved-caspase3 (c-casp3). **(D)** TCRβ^{-}CD11c^{+} cells were stained for percent expression of c-casp3. **(E)** Tabulated LAP-TGFβ and **(F)** %IL-10 expression on Tregs **(G)** gated MFI of CD39 on Tregs **(H)** gated MFI of CD73 on Tregs. **(I)** %Ki67 on Tregs **(J)** MFI of PD-1 in PD-1^{+} Tregs **(K)**

%PD-1 intermediate in Tregs **(L)** %PD-1 high in Tregs **(M)** %LAG3 on Tregs **(N)** % live CD45.2^{+} on gated single cells **(O)** %CD4^{+} Foxp3^{+} Tregs in live CD45.2^{+} single cells at 10 weeks **(P)** %CD4^{+} Foxp3^{+} Tregs were gated for % positive expression of c-casp3. **(Q)** %CD4^{+} Foxp3^{+} Tregs in live CD45.2^{+} single cells at 12 weeks. **(R)** EAE scoring in *Tnfsf10*$^{L/L}$Foxp3$^{Cre\text{-}YFP}$.B6 mice and co-caged controls.

Data in **(A)** are representative of >3 experiments with 11-31 mice/group. **(B)** is representative of 1 experiment with 4 mice/group. **(C-P)** is representative of 2 experiments with 4-19 mice/group. Data in **(Q)** are representative of 1 experiment with 3-5 mice/group. Data in **(R)** are representative of 3 experiments with 9-14 mice/group. Statistics were determined using Log-rank (Mantel Cox) test **(A)** and Student unpaired t test **(C-Q)** and 2-way ANOVA **(R)**. (ns, not significant, *p < 0.05, **p < 0.01, ***p < 0.001, ****p < 0.0001). Expression and functional data in **(B-Q)** was determined by flow cytometry.

4.3 Summary

I report four key developments from my studies. First, my lab created the first conditional *Tnfsf10*$^{L/L}$ knockout mouse, which allows for cell type-specific deletion of TRAIL. While I focused my efforts on understanding TRAIL biology in Tregs, this novel resource could be used to examine the role of TRAIL in other cell populations.

Second, I utilized the *Tnfsf10*$^{L/L}$ mice and determined that Tregs are not primarily dependent upon TRAIL as a means of suppression within the TME. I was surprised by the lack of change in suppression in the TME due to previous reports which indicated that Tregs use TRAIL as a means of suppressing activated Tconv in vitro and in vivo [281]. The authors of the study confirming a functional role of TRAIL in Tregs utilized a DR5 blocking antibody to limit Treg-derived TRAIL binding to DR5 on Tconv cells and subsequent

induction of cell death. However, my studies determined no change in Treg suppression of Tconv proliferation or cell death in the *Tnfsf10*$^{L/L}$*Foxp3*$^{Cre\text{-}YFP}$ mice at steady state or in the TME. I propose these differences may be due to the distinct models and stimulation conditions. I support this statement in three examples.

First, anti-DR5 blocking may have impacts on other immune cells rather than specifically limiting Treg-derived TRAIL induced apoptosis of Tconv cells. For example, TRAIL binding to DR5 on Tregs can promote Treg number and proliferation [290] . Therefore, anti-DR5 blocking in vitro or in vivo may alter Treg proliferation and number which would reduce suppressive capacity of Tregs towards activated Tconv.

Second, the in vivo murine models of disease were distinct. While the in vitro assays demonstrated Tregs did not use TRAIL to suppress, it is possible that Tregs differentially utilize TRAIL in different disease models in vivo. The DR5 blocking study examined TRAIL suppression in the context of adoptive transfer and allogenic skin graft models, while I studied the TME and autoimmune diabetes. Therefore, future studies could examine adoptive transfer or an allogeneic skin graft in the *Tnfsf10*$^{L/L}$*Foxp3*$^{Cre\text{-}YFP}$ mice to determine if Tregs utilize TRAIL to suppress Tconv in these models.

Third, the stimulating conditions for in vivo and in vitro suppression assays are distinct between my study and the anti-DR5 blocking studies [281]. These differences in stimulation conditions may differentially regulate TRAIL on Tregs. Future studies may determine if adjusting stimulation conditions may alter TRAIL suppression via Tregs.

My third development from my study is that I found that Tregs from autoimmune diabetes and Experimental Autoimmune Encephalomyelitis (EAE) environments are not

primarily dependent upon TRAIL as a means of suppression. Previous reports have indicated an important role for TRAIL in prevention of autoimmune disease [299,302-304]. For instance, TRAIL blockade exacerbated EAE disease score and degree of inflammation in the central nervous system (CNS) [302]. Moreover, TRAIL$^{-/-}$ mice or TRAIL blockade also aggravated disease in NOD mice [303]. Consequently, it was interesting when I found no change in EAE nor autoimmune diabetes disease initiation or severity in the *Tnfsf10*$^{L/L}$*Foxp3*$^{Cre\text{-}YFP}$ and NOD. *Tnfsf10*$^{L/L}$Foxp3$^{Cre\text{-}GFP}$ mice, respectively.

Fourth, these data, along with previously published work in which multiple mechanisms of Treg suppression were deleted, suggests that Tregs are capable of utilizing multiple mechanisms of suppression and are able to overcome or compensate when a mechanism is compromised or blocked [280].

While we did not determine a primary role of TRAIL in T_{regs} within the TME, it will be important in the future to assess different models in which DR5 is more highly expressed. It will also be important to examine the role of TRAIL in other cell types and other disease models such as infectious disease and autoimmune models; this is elaborated on in the discussion.

4.4 Author Contributions

D.A.A.V conceived, directed and obtained funding along with R.E.D. for the project; R.E.D., C.J.W and D.A.A.V. conceptualized, designed, analyzed the experiments. R.E.D., C.J.W and D.A.A.V. wrote the manuscript; R.E.D and S.G. performed all experiments.

Q.Z. and E.A.B. aided in diabetic mouse colony maintenance, breeding, and diabetes incidence. C.J.W. and A.B. contributed to experimental design, analysis, and developing mouse strains.

5.0 CD8-restricted deletion of TRAIL prevents autoimmune diabetes

5.1 Introduction

Type 1 diabetes (T1D) is a polygenic autoimmune disease that is characterized by immune-mediated destruction of insulin-producing pancreatic beta (β) cells[149,305]. Depletion of these cells by the immune system can cause hyperglycemia which leads to dangerous complications such as increased risk for cardiovascular disease/events, ketoacidosis, and death. Exogeneous insulin can control excessive glucose and limit disease, but cannot prevent nor cure the disease. Efforts to prevent the development of T1D have been limited as patients are typically diagnosed with T1D after a majority of the beta cells have been destroyed.

Therefore, efforts to understand how β cells are destroyed and how to prevent β cell death could be key in unlocking a preventative treatment for T1D. Current studies suggest that autoreactive $CD8^+$ T cells are a key member in destruction of β cells. In the autoimmune diabetes mouse non-obese diabetic (NOD) model, autoreactive cytotoxic $CD8^+$ T cells are considered to recognize class I major histocompatibility complex (MHC class-I) on islet antigen presenting β cells and cause destruction of these cells[186]. $CD8^+$ T cell production of Perforin, Granzyme, pro-inflammatory cytokines, and expression of Fas-L are thought to activate cell death cascades which trigger activation and cleavage of cell death executioner casp-3[186,306]. Caspase-3 will catalyze cleavage of cellular substrates leading to cell death[307]. However, mechanisms such as Perforin, Granzyme, and Fas-L, do not lead to complete β cell death in vivo and the signals necessary for beta

cell death remains unclear [186]. Therefore, more studies are still required to understand what molecules may trigger this cell death.

Tumor necrosis factor-related apoptosis-inducing ligand (TRAIL/Apo2L, *Tnfsf10*) is a type II transmembrane protein that can activate cellular apoptosis [198]. TRAIL is regulated by cell activation and Type 1 (IFNα, IFNβ) and Type 2 interferons (IFNγ); it is expressed in many activated cells such as T cells, NK cells, and dendritic cells. TRAIL is implicated in many disease settings such as cancer, viral infection, and autoimmunity[308]. In autoimmune diabetes, the role of TRAIL is multifaceted and relies on the cell type. For example, TRAIL production by β cells is thought to play a protective role in the islet of NOD mice as TRAIL knock out mice or TRAIL blocking experiments lead to exacerbated autoimmune diabetes [292,295,309,310]. Others have identified that $CD8^+$ T cells can use TRAIL as a mechanism to trigger beta cell death; however, it is unknown if this mechanism occurs in vivo and is responsible for complete β cell death [296]. Therefore, the purpose of my study was to understand if deletion of TRAIL (*Tnfsf10*) from $CD8^+$ T cells would limit β cell death and lessen disease [311].

5.2 Results

5.2.1 $CD8^+$ restricted deletion of *Tnfsf10* promotes protection to autoimmune diabetes

I first questioned the level of expression of cytotoxic molecules expressed by intra-islet $CD8^+$ T cells that could contribute to β cell death. To address this, we analyzed a

published single cell RNA-sequencing data set of immune cells from female NOD islets isolated at 4, 8, and 15 weeks of age [312]. Jian Cui bioinformatically isolated the $CD8^+$ T cells and analyzed levels of cytotoxic molecules, Perforin (*Prf1*), FasL (*FasL*), Granzyme B (*Gzmb*), and TRAIL (*Tnfsf10*) (Fig 17A). From the molecules investigated, *Gzmb* and *Tnfsf10* had the highest expression. Due to the previously documented role for *Gzmb* in β cell death, I decided to focus my efforts on studying on the lesser studied *Tnfsf10* [186].

To address if $CD8^+$ T cells utilize TRAIL to target β cells, I generated a $CD8^+$ T cell-specific deletion of *Tnfsf10* by crossing the NOD.*Tnfsf10*$^{L/L}$ mouse model to the NOD.E8I$^{Cre\text{-}GFP}$ mouse. I confirmed deletion of *Tnfsf10* in $CD8^+$ T cells by cell-specific genotyping (Figure 18A). Importantly, loss of *Tnfsf10* resulted in almost 100% protection of diabetes in female and male NOD.*Tnfsf10*$^{L/L}$ E8I$^{Cre\text{-}GFP}$ mice (Fig 17B, 18B) with significantly reduced insulitis scoring (Fig 17C-D).

I hypothesized that deletion of *Tnfsf10* may result in reduced disease in other models. Therefore, I utilized B6.*Tnfsf10*$^{L/L}$ *E8I*$^{Cre\text{-}GFP}$ mice and challenged these mice with B16 melanoma. I found no change in B16 tumor growth in B6.*Tnfsf10*$^{L/L}$ E8I$^{Cre\text{-}GFP}$ mice compared with controls, indicating that $CD8^+$-restricted deletion may not have an impact on all disease models (Fig 18C).

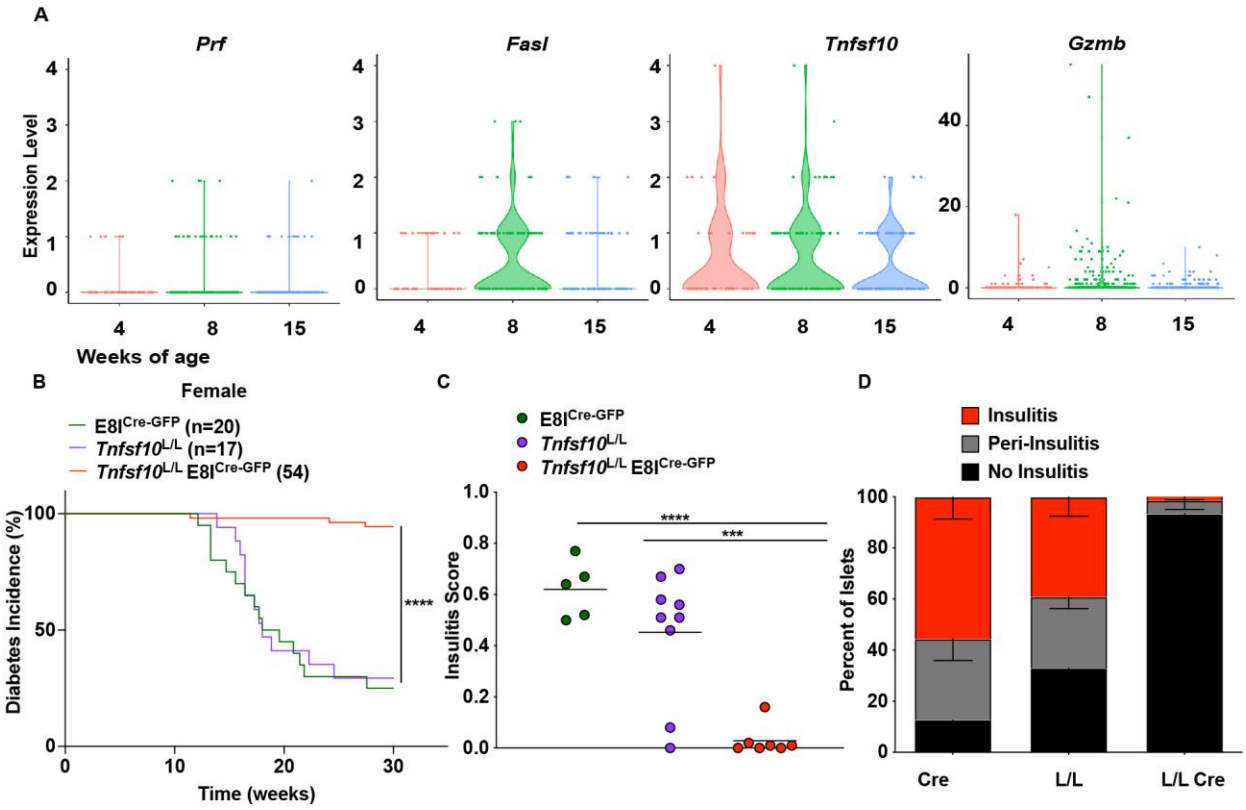

Figure 17 *Tnfsf10* is expressed in intra-islet CD8⁺ T cells and *Tnfsf10* deletion protects NOD mice from diabetes

(A) Expression of *Perforin*, *Fas-ligand*, *Granzyme B*, and *Tnfsf10* on intra-islet CD8⁺ T cells from 4, 8, and 15 week old NOD females. **(B)** Diabetes onset monitored in *Tnfsf10*$^{L/L}$E8I$^{Cre-GFP}$.NOD females and co-caged controls. (**C)** Histological assessment of insulitis performed in female *Tnfsf10*$^{L/L}$E8I$^{Cre-GFP}$.NOD and co-caged controls at 12 weeks of age. Data in **(B)** are representative of more than 5 experiments with >17 mice per group. Data in **(C)** is representative of 2 experiments with 5-9 mice/ group. Statistics were determined through 2-way ANOVA **(B)** and student unpaired t-test **(A)** (***p < 0.001, ****p < 0.0001).

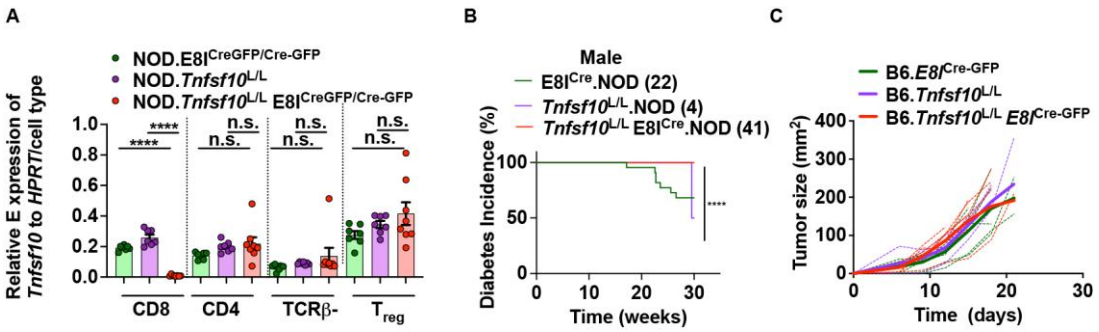

Figure 18 Validation of *Tnfsf10* deletion in CD8⁺ T cells and evaluation of the impact of *Tnfsf10* deletion from CD8⁺ T cells on diabetes incidence and tumor growth

(A) Cells were sorted from *Foxp3*$^{Cre\text{-}YFP}$.B6 and *Tnfsf10*$^{L/L}$ *Foxp3*$^{Cre\text{-}YFP}$.B6 mice and qPCR performed for *Tnfsf10* and *Hprt.* **(B)** Diabetes onset monitored in *Tnfsf10*$^{L/L}$E8I$^{Cre\text{-}GFP}$.NOD males and co-caged controls. **(C)** Mice were injected with 125,000 B16 i.d. and tumor size was measured. Data in **(A)** is representative of 2 experiments with 7-8 mice per group. Data in **(B)** is representative of >3 experiments with 4-41 mice per group. Data in **(C)** is representative of 2 experiments with 4-8 mice per group. Statistics were performed with a student unpaired t-test **(A)** and 2-way ANOVA **(B)** (n.s. not significant, ***p < 0.001, ****p < 0.0001).

5.2.2 Reduced immune cell infiltration in the diabetic islet in *Tnfsf10*$^{L/L}$ E8I$^{Cre\text{-}GFP}$ mice is not due to migration deficiencies

To confirm my findings of reduced immune infiltration in the islets of *Tnfsf10*$^{L/L}$ E8I$^{Cre\text{-}GFP}$ mice, I examined levels of immune cells by flow cytometry. There was a statistically significant reduction of immune cell number and percentage in the diabetic islet in the *Tnfsf10*$^{L/L}$ E8I$^{Cre\text{-}GFP}$ mice but no change in immune cell number and percentage in the peripheral lymph nodes (Fig 19A-C). There was also a reduction in CD8⁺ T cells in the islets of *Tnfsf10*$^{L/L}$ E8I$^{Cre\text{-}GFP}$ compared to E8I$^{Cre\text{-}GFP}$ controls, confirming the insulitis results (Fig 19D-E).

Due to the reduction in immune cells in the islet of *Tnfsf10*$^{L/L}$ E8I$^{Cre\text{-}GFP}$ mice, I hypothesized that deletion of *Tnfsf10* on CD8^{+} T cells may render these cells unable to migrate into the islet. To access this, I reconstituted NOD-SCID females with an equal ratio of congenically mismatched WT CD8^{+} and *Tnfsf10*-deficient CD8^{+} T cells along with bulk CD4^{+} T cells (Fig 19F). Immune infiltration of these cells in the NDLN, PLN, and islet were accessed at 3, 5, and 7 weeks post transfer. At 3 weeks post transfer, I found no differences in the ratio of transferred cells, indicating these cells may not have inherent deficiencies in ability to migrate to the islet (Fig 19G-H). However, I did see a reduction in numbers of *Tnfsf10*-deficient CD8^{+} T cells at 5 and 7 weeks after transfer (Fig 19G-H).

To determine why there is a reduction in percentage of *Tnfsf10*-deficient CD8^{+} T cells at 5 and 7 weeks after transfer, I analyzed the phenotype of transferred cells to examine differences in cell death, survival, and proliferation signals. Interestingly, I found no difference in intra-islet CD8^{+} T cell expression of survival marker BCL-2, but did see a small but statistically significant decrease in BCL-2^{+} expression in peripheral *Tnfsf10* $^{-/-}$ CD8^{+} T cells (Fig 20A). I found no difference in cell death between *Tnfsf10*$^{+/+}$ and *Tnfsf10* $^{-/-}$ CD8^{+} T cells but I did find a statistically significant reduction in cell proliferation marker, Ki67 in *Tnfsf10* $^{-/-}$ CD8^{+} T cells at 5 weeks post transfer (Fig 20B-C). This could indicate that deletion of TRAIL could alter proliferative ability of these cells.

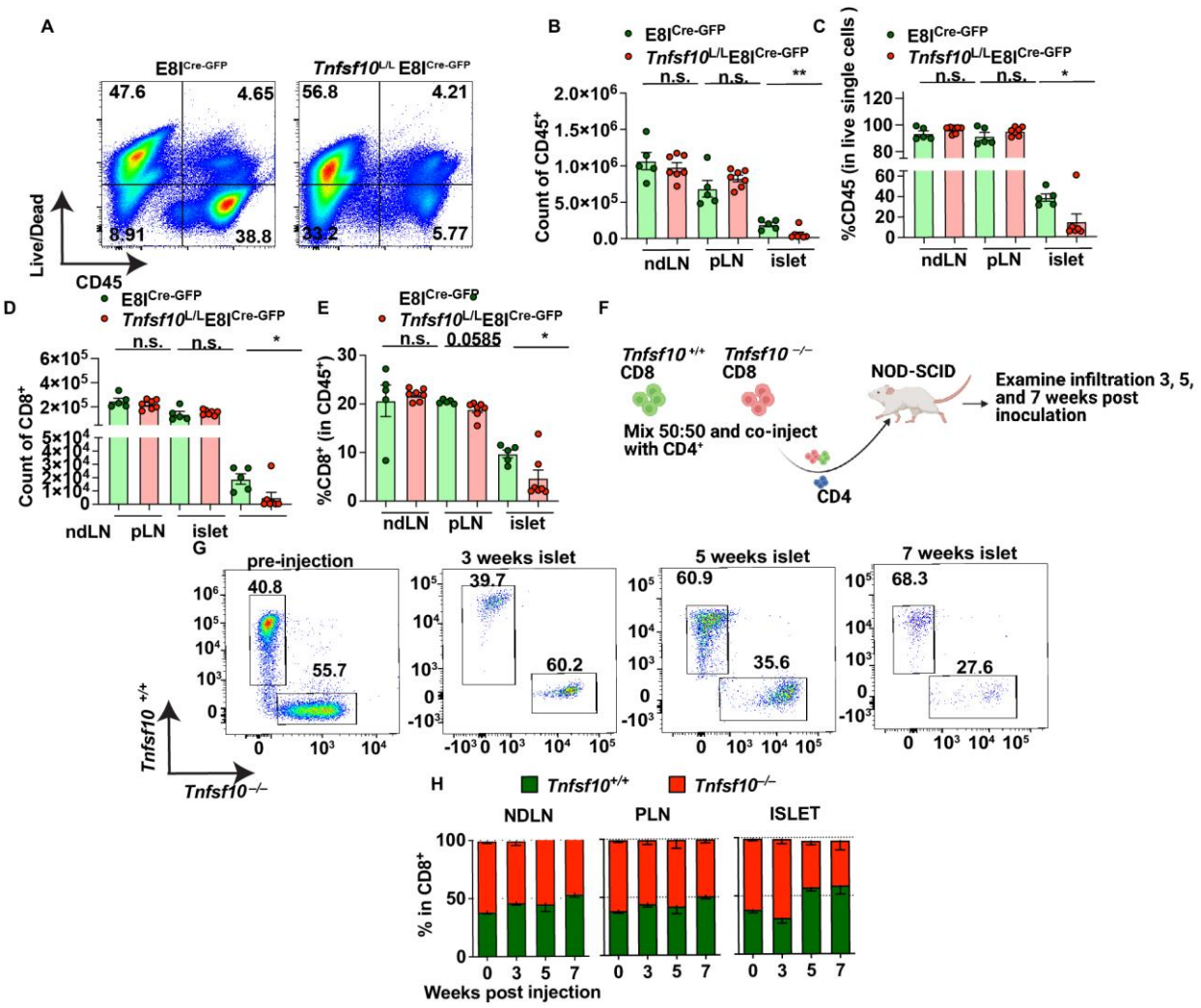

Figure 19 Limited immune infiltration in the islets of *Tnfsf10*$^{L/L}$ E8I$^{Cre\text{-}GFP}$ mice is not due to migration defects

(A) Representative plots of live immune infiltration in islets from 12 week old E8I$^{Cre\text{-}GFP}$ and *Tnfsf10*$^{L/L}$E8I$^{Cre\text{-}GFP}$ female mice. **(B)** count of live CD45.1^{+} on gated single cells **(C)** %CD45.1^{+} on gated live single cells **(D)** count of CD8^{+} T cells gated on live TCRβ^{+} single cells **(E)** % of CD8^{+} T cells gated on live TCRβ^{+} single cells out of CD45.1^{+} cells **(F)** Adoptive transfer schematic **(G)** Representative plots of adoptive transfer pre-injection, 3, 5, and 7 weeks post injection. **(H)** Ratios of wild-type to mutant CD8^{+} T cells over time in corresponding tissues Data in **(A-E)** is representative of two experiments with 5-6 mice per group. Data in

(G-H) are representative of two experiments, 2 mice per time point. Statistics were performed with a student unpaired t-test **(B-E)** (n.s. not significant, * $p<0.05$, ** $p<0.01$).

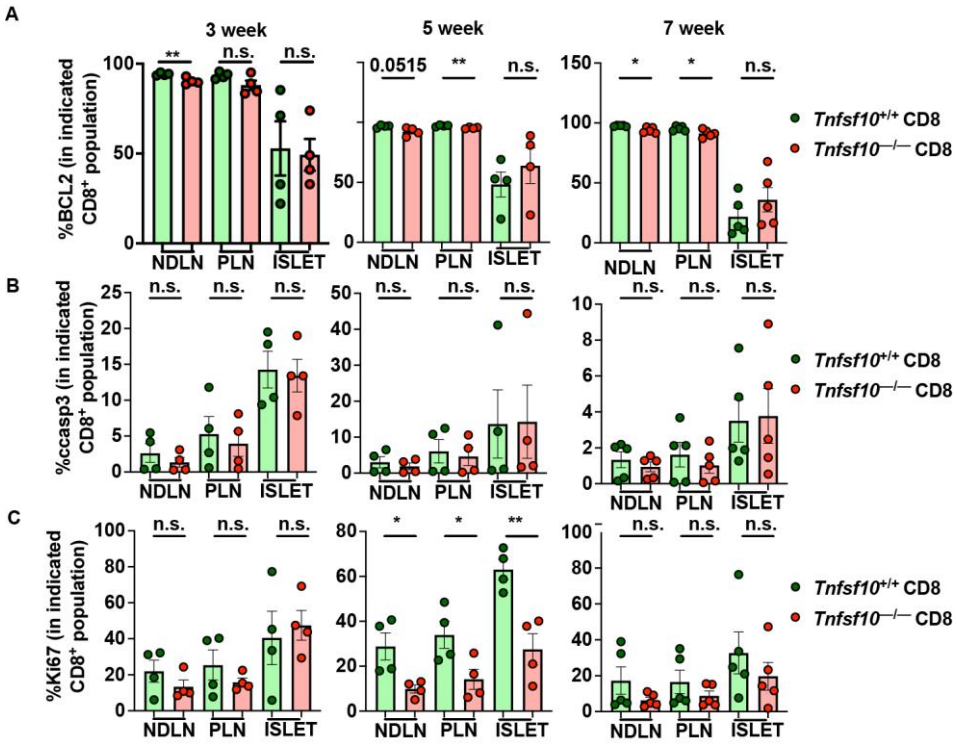

Figure 20 Phenotype of adoptively transferred CD8⁺ T cells

(A) %BCL2⁺ in indicated CD8⁺ T cell populations at 3, 5, and 7 weeks post transfer **(B)** %c-casp3⁺ in indicated CD8⁺ T cell populations at 3, 5, and 7 weeks post transfer **(C)** %Ki67⁺ in indicated CD8⁺ T cell populations at 3, 5, and 7 weeks post transfer. Data in **(A-C)** is representative of two experiments with 2 mice per time point. Statistics were performed with a student unpaired t-test **(A-C)** (n.s. not significant, * $p<0.05$, ** $p<0.01$).

5.2.3 Single cell transcriptional analysis reveals differences in islet makeup of *Tnfsf10*$^{L/L}$ E8I$^{Cre-GFP}$ and *Tnfsf10*$^{L/L}$ mice

To identify what other impact CD8^{+} T cell-restricted deletion of *Tnfsf10* may have on the islet microenvironment, my lab performed single cell RNA sequencing on bulk islets from *Tnfsf10*$^{L/L}$E8I$^{Cre-GFP}$ and *Tnfsf10*$^{L/L}$ mice. Single cell analysis confirmed the previous observations that islets from *Tnfsf10*$^{L/L}$E8I$^{Cre-GFP}$ had limited immune cell infiltration (Fig 21A). Further analysis revealed percentages of endocrine cells such as α and β cells were altered in islets *Tnfsf10*$^{L/L}$ E8I$^{Cre-GFP}$ mice (Fig 21B). Future analysis will further interrogate this data set for changes in the transcriptome of these cells. The single cell analysis reveals that CD8^{+} T cell-derived TRAIL may have some role in regulation of endocrine cell number in the islet.

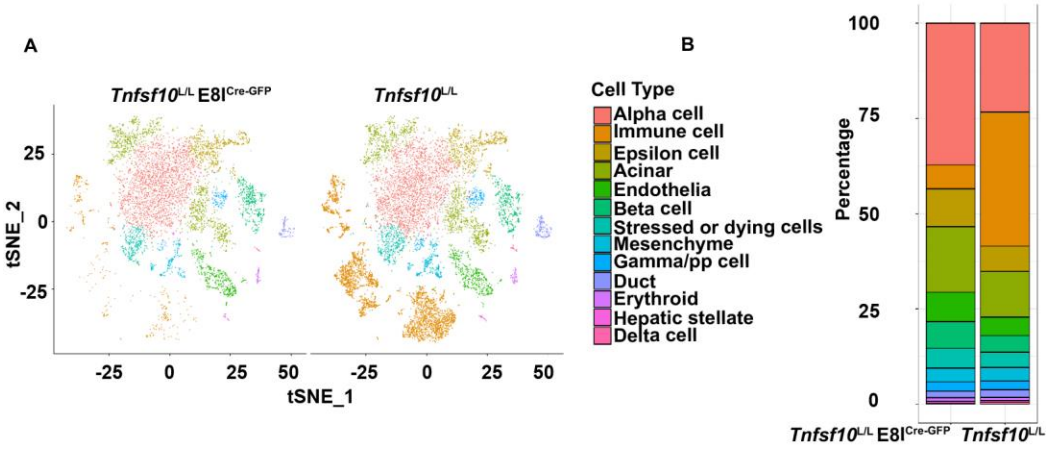

Figure 21 Transcriptional differences in islets from *Tnfsf10*$^{L/L}$E8I$^{Cre-GFP}$ and *Tnfsf10*$^{L/L}$ mice

(A) Single cell RNA sequencing tSNE clustering of bulk and single cells from bulk islets from *Tnfsf10*$^{L/L}$ E8I$^{Cre-GFP}$ and *Tnfsf10*$^{L/L}$ mice. **(B)** Stacked-bar graph of percent cellular makeup of islets for indicated genotype.

5.2.4 β cells may be targets of CD8$^+$ T cell-derived TRAIL

The transcriptional analysis identified changes in percentages of endocrine cells in the islet of *Tnfsf10*$^{L/L}$E8I$^{Cre\text{-}GFP}$ mice. Therefore, I sought to understand which cell population expresses the murine agonistic TRAIL receptor, DR5. I hypothesized that β cells may express DR5 due to previous reports that demonstrate TRAIL can induce apoptosis of β cells [296]. To access this, immunohistochemistry (IHC) was performed on 12 week old pancreas from *Tnfsf10*$^{L/L}$E8I$^{Cre\text{-}GFP}$ and E8I$^{Cre\text{-}GFP}$ mice. Preliminary data suggest intra-islet insulin staining may overlap DR5 staining (Fig 22A). Therefore, β cells may be the target of CD8$^+$ T cell-derived TRAIL.

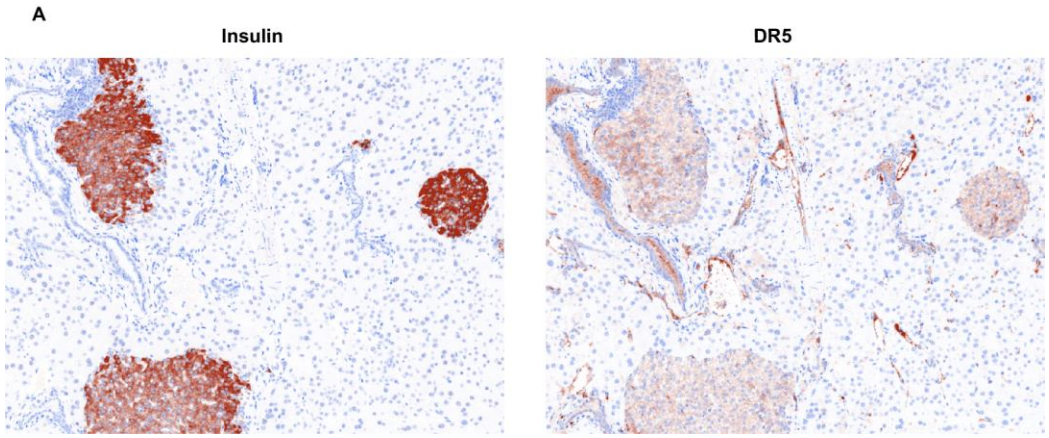

Figure 22 β cells may be targets of CD8$^+$ T cell-derived TRAIL

(A) IHC path view of Insulin and DR5 staining in 12 week old E8I$^{Cre\text{-}GFP}$ female mouse pancreas

5.2.5 IFNα may regulate TRAIL expression on intra-islet CD8$^+$ T cells

Given that β cells could be the target of CD8$^+$ T cell derived TRAIL, I questioned what may be regulating TRAIL expression on CD8$^+$ T cells in islets. Previous studies have

demonstrated a role for IFNα in upregulation of TRAIL on various cell types [208,313]. Moreover, there is a link for IFNα in initiation and development of autoimmune diabetes/T1D[160-163,314]. Therefore, I hypothesized that IFNα produced in the diabetic islet may upregulate TRAIL on $CD8^+$ T cells and contribute to β cell death. To test this, I cultured islet-derived $CD8^+$ T cells ex vivo with IFNα with or without TCR stimulation and examined TRAIL expression by flow cytometry. TRAIL was upregulated in intra-islet $CD8^+$ with IFNα regardless of stimulation conditions (Fig 23A). However, there was no increase in NDLN $CD8^+$ T cells, potentially indicating this upregulation is only limited to antigen-specific $CD8^+$ T cells. Therefore, I conclude that IFNα may cause upregulation of TRAIL on $CD8^+$ T cells to cause direct β cell death.

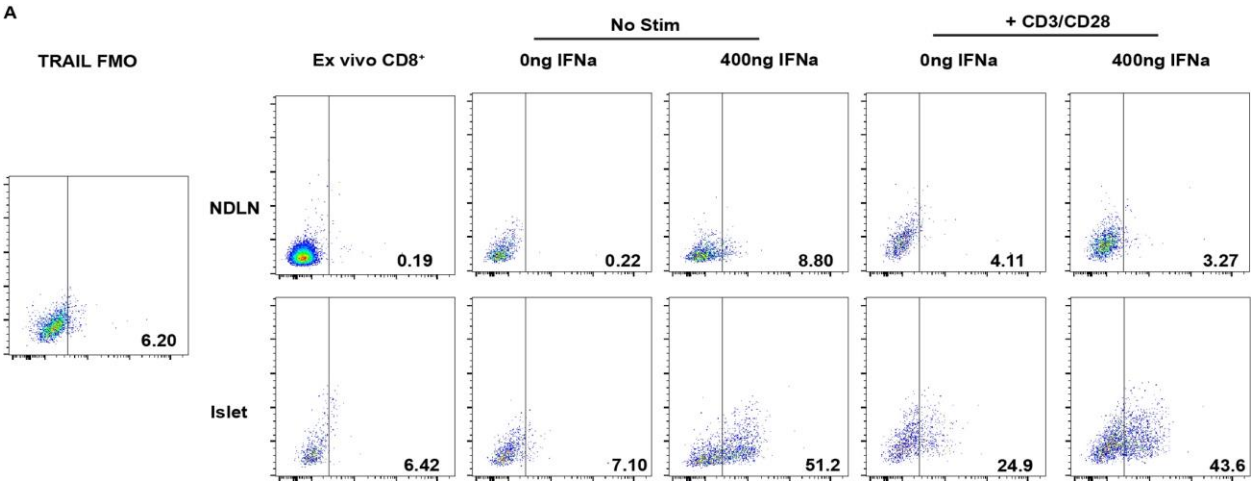

Figure 23 IFNα induces TRAIL expression in intra-islet $CD8^+$ T cells

(A) $CD8^+$ T cells were isolated from the NDLN or islet and cultured with or without 10ug/mL anti-CD3 and anti-CD28 and 400 ng IFNα. Cells were cultured overnight and analyzed for TRAIL (x-axis) versus forward scatter (y-axis) via flow cytometry

5.3 Summary

I report four main findings from my study. First, I found that *Tnfsf10* was one of highest expressed cytotoxic molecules in $CD8^+$ T cells in the NOD islet and its deletion on $CD8^+$ T cells yielded almost 100% protection of male and female NOD mice from diabetes. These data directly contrast the previously published protective role for TRAIL in autoimmune diabetes which indicate that TRAIL blockade or *Tnfsf10*$^{-/-}$ mice have exacerbates diabetes [303,304]. However, these studies argued that TRAIL production by β cells targeted diabetogenic T cells for cell death; blockade or deletion of *Tnfsf10* decreased diabetogenic T cell death and enhanced disease [295]. In addition, other studies have identified a role for TRAIL in upregulation of decoy receptor 1 and tissue inhibitor of metalloproteinase-1 (TIMP-1) to reduce and resist against β cell apoptosis [299,309]. Accordingly, TRAIL plays many different roles in the islet, depending on cellular source.

Second, I found that *Tnfsf10*$^{L/L}$ E8I$^{Cre\text{-}GFP}$ mice had almost no immune infiltration in the islets. I considered that deletion of *Tnfsf10* may limit $CD8^+$ T cell ability to migrate to the islet which could lead to less β cell destruction, reduced inflammation, and reduced recruitment of additional immune cells to exacerbate disease. Indeed, TRAIL ligation to DR5 can affect migration of cells [315,316]. However, $CD8^+$ T cells from *Tnfsf10*$^{L/L}$E8I$^{Cre\text{-}GFP}$ did not have impaired migration. There were reduced $CD8^+$ T cells from *Tnfsf10*$^{L/L}$E8I$^{Cre\text{-}GFP}$ mice at a later timepoint post adoptive transfer, possibly due to reduced proliferation. Interestingly, TRAIL does have a known non-canonical role in maintaining proliferation of cells (discussed in section 1.5.2); TRAIL on $CD8^+$ T cells data may act in an autocrine mechanism to support $CD8^+$ T cell proliferation.

Third, $CD8^+$ T cell TRAIL could be directly targeting β cell death. However, evidence to support this finding is unclear. My preliminary analysis has identified $Insulin^+$ cells may be the highest DR5 expressing population in the islet. Previous reports have suggested antigen specific $CD8^+$ T cells can express and utilize TRAIL as a means of β cell killing [296]. Furthermore, children with acute-onset of T1D exhibited expression of TRAIL in their islets compared to no expression in non-diabetic patients [317]. Conversely, others have shown that TRAIL does not induce apoptosis of β cell lines or freshly isolated islets in vitro [295]. Therefore, future studies to further examine this role are required.

Finally, IFNα may regulate this induction of TRAIL expression on intra-islet $CD8^+$ T cells. Indeed IFNα has important roles in regulating TRAIL expression and initiation of T1D and autoimmune diabetes [220,292,313,318,319]. Therefore, future studies should examine the role of IFNα and its regulation of TRAIL on $CD8^+$ T cells.

5.4 Author Contributions

D.A.A.V conceived, directed and obtained funding along with R.E.D. for the project; R.E.D., C.J.W and D.A.A.V. conceptualized, designed, analyzed the experiments. R.E.D., C.J.W and D.A.A.V. wrote the manuscript; R.E.D and S.G. performed all experiments. Q.Z. and E.A.B. aided in diabetic mouse colony maintenance, breeding, and diabetes incidence. R.E.D. and J.C. contributed to bioinformatics analysis.

6.0 Discussion

Portions of this chapter (6.1.2, 6.1.3) were taken from my previous publication **Dadey, R.E.,** Workman, C.J., Vignali, D.A.A. “Regulatory T cells in the Tumor Microenvironment” Adv Exp Med Biol. 2020;1273:105-134. doi: 10.1007/978-3-030-49270-0_6, under copyright permission of Springer Nature (license number 4992560654498).

T cells are critical components of the immune system that regulate disease and maintain homeostasis. Tregs can utilize many functions to suppress activation of the immune response and limit autoimmunity, while cytotoxic $CD8^+$ T cells can limit infection and tumor development. However, Tregs and $CD8^+$ T cells play deleterious roles in various disease models. Here I provide a summary of my findings on Treg and $CD8^+$ T cell function in the TME and autoimmune diabetes and discuss the implications of these studies for future research. For each study, I will highlight my main findings, identify any limitations and implications for these studies, and future questions and directions.

6.1 Epigenetic Regulation of the Treg phenotype in the TME

In Chapter 3, I studied chromatin accessibility changes of Tregs in the TME and how this may be impacted with immunotherapy. Here I discuss my results and future directions.

6.1.1 TIL Tregs have drastically altered genomic chromatin accessibility compared to LN Tregs

My studies highlight that TIL Tregs have drastically altered chromatin accessibility across the genome compared to peripheral Tregs. I showed TIL Tregs close more peaks compared to LN Tregs than they open. Due to this trend of decreased genome accessibility in TIL Tregs compared to LN Tregs, I primarily focused on peaks that were less accessible in TIL Tregs compared to LN Tregs; however, future studies may investigate the peaks that are more accessible in TIL Tregs compared to LN Tregs. Investigation of these peaks may provide clues on Treg function and phenotype in the TME.

Treg stability is critical for maintenance of tolerance and resolution of inflammation. Loss of Treg stability can lead to limited immune suppression and multisystem lymphoproliferative disease [320-323]. Therefore, it is key that Tregs are able to adapt in inflammatory environments to maintain their suppressive phenotype, rather than convert to a pro-inflammatory Tconv phenotype. I found that Tregs in the TME may adapt to the harsh TME through regulation of chromatin accessibility loci that are important for a Tconv phenotype. It would be of interest to examine if Tregs regulate similar loci in other inflammatory environments, such as infection or autoimmune disease, or if different inflammatory environments require regulation of different loci important for Treg phenotype and function.

I considered that TIL Tregs reduced chromatin accessibility at loci important for conversion to a Tconv phenotype in two ways. First, chromatin accessibility of these loci directly limits transcription of genes involved in a Tconv phenotype. This is evidenced by

decreased chromatin accessibility in the gene encoding TβRIII, which is downregulated in Tregs compared to Tconv and may have roles in regulating Treg number and differentiation[266,324]. Second, Tregs regulate chromatin accessibility at the loci of regulators of transcriptional activity. For example, Satb1 is a transcriptional regulator that can control activation of many Tconv effector genes. Previous studies have shown overexpression of *Satb1* leads to reduced Treg function and transition to Tconv effector phenotype[264]. I found TIL Tregs reduce chromatin accessibility at the *Satb1* locus which may reduce transcription of the gene and ultimately limit Treg transition to Tconv phenotype in the harsh TME.

The mechanism of the Treg chromatin accessibility changes in the TME remains unclear. Treg activation and inflammation may activate chromatin remodelers that can regulate accessibility at various loci. For example, in inflammatory conditions, Foxp3 can bind to various loci and recruit the chromatin remodeler polycomb repressive complex 2 (PRC2) [252]. PRC2, aids in deposition of H3K27me3 (marker of gene repression) histone modifications which induce heterochromatin and downregulation of gene transcription. Indeed, I found a few molecules that are less accessible in TIL Tregs are targets of Foxp3 such as *Satb1*, *Tgfbr3*, and others. I can perform low-input ChIP-sequencing assays such as CUT&RUN or ChIP-qPCR to examine if TIL Tregs have higher H3K27me3 at loci such as *Satb1*, *Tgfbr3*, and others [325].

I observed many differences in Tregs from the LN and Tregs from the TIL; however, I have not accounted for differences in tissue location. B16 and MC38 tumors are grown in the dermis and subcutaneous skin, respectively. Comparison of TIL Tregs may be better compared to Tregs from the skin. Indeed, previous analysis has shown that

many transcripts identified in TIL Tregs were also identified in nonlymphoid tissue Tregs [294,326]. To better identify peaks that are specific to tumor Tregs, I am currently investigating ATAC sequencing of Tregs from naïve murine skin.

In addition, I focused the study on enrichment pathways such as Tconv vs. Treg, and the Treg transcriptional signature, but future studies will examine other enriched pathways to ascertain information about TIL Treg chromatin accessibility changes compared to the periphery.

Finally, future studies coupling transcriptomic data, such as qPCR of particular genes or bulk RNA sequencing, with chromatin accessibility data will confirm the observations of Treg regulation of genes involved in maintenance of a suppressive phenotype. These results provide information on the mechanisms Tregs use to maintain their suppressive phenotype in the TME. Future studies should examine how targeting these molecules may be harnessed for the treatment of cancer.

6.1.2 TIL Tregs do not change accessibility over time

The lack of change over time of Treg chromatin accessibility in the TME indicates that upon early entry into the TME, Tregs are presented with signal(s) to reorganize loci that will be important for Treg suppression throughout the tumor growth time course. Tight regulation of these loci over time in the dynamic inflammatory TME could provide the Treg with stability despite destabilizing conditions.

The TME may provide unknown signals to Tregs in order to maintain their chromatin accessibility profile over time. It would be of interest to understand what signals provide these cues.

Some signals may include hypoxia and acidity. The tumor contains rapidly expanding malignant cells that outgrow oxygen availability and induce a hypoxic environment [327]. Further, the pH of the TME is acidic due to its mechanism of glucose metabolism. Non-malignant cells in the presence of oxygen use oxidative phosphorylation (OXPHOS) to metabolize glucose. [328]. Without oxygen, cells convert pyruvate to lactic acid, which is known as anaerobic glycolysis. However, tumor cells are unique in that they convert pyruvate to lactic acid even in the presence of oxygen, which is known as the Warburg effect or aerobic glycolysis [329]. The switch to production of lactic acid is thought to provide cancer cells with glucose as a building block for nucleotides, amino acids, and lipids [330]. Tumor cells can then use the end product, lactate, as an additional energy source and shuttle excess out into the microenvironment, substantially lowering pH of the TME [331-333].

Hypoxia, low glucose, and lactic acid limit effector T cell function, including decreasing IFNγ production [334]. However, Tregs are uniquely capable of living in the high lactate and low glucose TME through metabolic reprogramming to OXPHOS, which allows resistance to the harsh TME [333,335]. Others showed that Tregs in the TME may rely more on glycolysis, with higher levels of glucose transporters and glycolytic flux [336]. This may also aid in their competition for the limited glucose in the TME. In addition, hypoxia upregulates hypoxia inducible factor 1 subunit alpha (HIF1α), which promotes Foxp3 expression in $CD4^+$ $Foxp3^-$ cells, further increasing numbers of Tregs in the TME [337,338]. Tregs have developed these characteristics to withstand the harsh metabolic requirements of the TME and thus survive and persist.

It may be of interest to culture LN and/or skin Tregs in hypoxia, low glucose, and or lactic acid in vitro to determine if this changes their chromatin accessibility profile mores similar to the TIL Treg profile. Moreover, future studies could examine this in vivo by treatment of tumor bearing mice with a hypoxia reducing agent, such as metformin, and determine if this alters TIL Treg chromatin accessibility over a time course [339].

One limitation of the time course study is that I restricted the analysis to Tregs from B16 and MC38 transplantable models. These tumor models grow extremely rapidly in mice (mice typically succumb to the disease at 20-25 days post injection)[340]. This rapid tumor growth may not completely represent the dynamic interplay between immune response and tumor that can occur over the series of months to years. Moreover, tumor cell lines are typically homogenous in tumor mutations burden and may not accurately represent the heterogenous nature of naturally arising tumor cells [341,342]. Therefore, it is possible that Tregs could change their chromatin accessibility over time in a naturally forming tumor that is undergoing immune editing over a longer time period. Therefore, I could examine Treg chromatin accessibility over time in a genetically engineered mouse model such as the *Tyr*^{CreERT2}*Braf*$^{LSL\text{-}V600E/+}$*Pten*$^{L/L}$ mice or a chemically induced model such as injection of methylcholanthrene (MCA) [343-345].

Another limitation of the time course study is that it is unclear if the analysis is examining the same Treg cell population or de novo population of Tregs. It is possible that once Tregs infiltrate the tumor, they maintain an altered accessibility profile and persist in the tumor. Alternatively, Tregs may be actively recruited to the TME over the time course and then change chromatin accessibility in response to signals from the TME. To address this question, I could treat tumor bearing mice with a molecule that inhibits

lymphocyte egress such as Fingolimod (FTY720) or PBS control and repeat the time course ATAC sequencing experiment [346,347]. This will determine if chromatin accessibility profiles of Tregs indeed stay the same over time or if I am examining newly infiltrated Tregs.

Analysis on how Tregs may alter their chromatin accessibility and transcriptome over time may indicate how these cells are playing a role in the dynamic immune and tumor interface.

6.1.3 TIL Treg chromatin accessibility does not change with response to checkpoint blockade

Although TIL and peripheral Tregs may be impacted directly or indirectly by anti-PD1 therapy, I found no transcriptional or chromatin accessibility changes in Tregs that were derived from mice treated with isotype or anti-PD1, despite some mice clearing the tumor. Moreover, I found no differences in the transcriptome or chromatin accessibility among various responses to anti-PD1 (responder, non-responder, isotype). Lack of chromatin accessibility and transcriptional changes in response to anti-PD1, may indicate that the mechanism of action of anti-PD1 is not to alter accessibility or transcriptome but rather another mechanism. Indeed, previous reports have shown that $CD8^+$ cells derived from the TME or from chronic LCMV infection had little change in chromatin accessibility when mice were treated with anti-PD-L1 [348,349]. These studies argued that targeting PD-1 and PD-L1 affected signaling rather than changes to the chromatin accessibility and transcriptome [348]. Therefore, I suggest that although Tregs are a potential cellular target of anti-PD1 immunotherapy, the direct or indirect effects of anti-PD1 on Tregs do not alter

their chromatin accessibility and transcriptome. It would be of interest to contrast these results to $CD4^+$ $Foxp3^-$ and $CD8^+$ T cells to examine if these cells also have no change in chromatin accessibility despite response to anti-PD1 therapy.

A limitation of my study is the analysis of a single therapy, anti-PD1. It is possible that treatment of mice with another immunotherapeutic regime may alter Treg chromatin accessibility and transcriptome. To address this, I could treat mice with anti-LAG3 or a combination of anti-LAG3 and anti-PD1 and examine if this impacts chromatin accessibility [135]. Treatment of mice with anti-CTLA4 could also be performed, although due to its potential mechanism of Treg depletion, may not be as informative. Treatment of mice with a therapy that targets Treg function, such as anti-GITR, may alter chromatin accessibility [350-353].

Finally, although I focused on murine Treg chromatin accessibility in response to immunotherapy, I would also be interested in applying my findings to humans that are treated with anti-PD1 and other immunotherapies. Moreover, I could also examine these samples to determine if Tregs from TIL, compared to peripheral Tregs, alter chromatin accessibility in similar loci in humans, and if Tregs alter chromatin accessibility over time in patient samples.

These studies provide important information on how Tregs maintain their function in the destabilizing TME and reveal anti-PD1 does not affect Tregs at a transcriptional or chromatin accessibility level.

6.2 Regulatory T Cell-Derived TRAIL is Not Required for Peripheral Tolerance

In Chapter 4, I studied the role of Treg expression of TRAIL in suppression of the immune response in the TME and autoimmune diabetes. Here I discuss my results and future directions.

6.2.1 Treg-restricted deletion of *Tnfsf10* has no effect on tumor growth or Treg suppression

I found that TRAIL production by Tregs is not required for suppression of cells derived from naïve or tumor bearing mice and is not required for suppression of the anti-tumor response. Lack of a role for Treg-derived TRAIL in suppression in the TME may also be due to five main reasons. First, there is limited DR5 expression in all cells the TME. In my analysis, I found minimal expression of agonistic TRAIL receptor, DR5 in all immune and non-immune populations in the TME. Indeed, previous reports demonstrate that DR5 is only lowly expressed in the thymus, spleen, and kidney and no expression in other tissues [354]. Moreover, previous analysis of individual immune cells has revealed minimal expression, although various environments and stimulation conditions can increase expression [222]. Tumor cells have also reported to express DR5, but I did not see expression nor any changes in cell death in the $CD45^{-}$ population in the B16 and MC38 tumor models [355]. Due to my observation of limited expression of DR5 in all cells in the TME, it would be of interest to utilize a murine model in which DR5 is over expressed in various immune and non-immune populations. This could be performed by creation of a *Tnfrsf10b* (DR5) overexpression retroviral vector. I could transduce $CD4^{+}$ or $CD8^{+}$ T cells

with DR5 retrovirus and culture these cells with *Tnfsf10*$^{+/+}$ or *Tnfsf10*$^{-/-}$ TIL Tregs in a classical microsuppression assay. This would determine if Treg-derived TRAIL has a limited role in suppression of T cells in the TME due to lack of DR5 expression.

The second reason for lack of a role for Treg-derived TRAIL in the TME is the presence of decoy receptors on immune and non-immune cells in the TME. In mouse, there are two TRAIL decoy receptors, DcR1 (TRAIL-R3) and DcR2 (TRAIL-R4) [356]. DcR1 lacks transmembrane and death domain while DcR2 has a non-functional death domain [357]. These receptors are thought to act as "decoys" that sequester TRAIL in order to limit agonistic receptor binding [357]. Therefore, it is possible $CD4^+$ or $CD8^+$ T cells in the TME express high decoy receptors and therefore do not respond to Treg-derived TRAIL. In order to address this possibility, I can examine levels of DcR1 and DcR2 compared to expression levels of DR5 on all immune and non-immune populations by flow cytometry. If DcR1 and DcR2 are highly expressed, I could then perform experiments to perform CRISPR electroporation and knock-out of DcR1 and DcR2 in $CD4^+$ or $CD8^+$and determine if this alters susceptibility to Treg-derived TRAIL.

Third, while I limited the analysis to B16, MC38, and CT26 tumor models in *Tnfsf10*$^{L/L}$ *Foxp3*$^{Cre\text{-}YFP}$ mice; I acknowledge that Treg-derived TRAIL may have different effects in other tumor models. DR5 expression may be increased in the immune compartment of other tumor models and Treg-derived TRAIL may play a role in these models. Future studies could examine a variety of murine tumor cell lines in the *Tnfsf10*$^{L/L}$ *Foxp3*$^{Cre\text{-}YFP}$ mice to examine tumor growth and DR5 expression in the immune and non-immune compartment. I can also examine levels of decoy receptors in these models.

A fourth reason for no change in the tumor growth in *Tnfsf10*$^{L/L}$*Foxp3*$^{Cre\text{-}YFP}$ mice is that Tregs still express other mechanisms of suppression. I found that *Tnfsf10*-deficient Tregs still expressed other molecules of suppression such as CD39/CD73, IL-10, CTLA-4, and others. I argue that Tregs possess inherent plasticity that endows an ability to utilize other suppressive molecules in the absence of TRAIL. Moreover, this plasticity could be examined if I created a mouse that lacked IL10, IL35, and TRAIL. Examination of *Il10*$^{L/L}$ *Ebi3*$^{L/L}$ *Tnfsf10*$^{L/L}$ *Foxp3*$^{Cre\text{-}YFP}$ mice could determine if these cells lose function or upregulate a different molecule to compensate for loss of these suppressive molecules [280].

Finally, it is possible that Treg-derived TRAIL may have some other unknown role in the TME. Single cell RNA sequencing of cells in the TME from *Tnfsf10*$^{L/L}$*Foxp3*$^{Cre\text{-}YFP}$ and *Foxp3*$^{Cre\text{-}YFP}$ mice could identify any unique transcriptional differences that could indicate if Treg-derived TRAIL has a unique role in the TME.

My results have shown that Tregs do not require TRAIL in order to suppress the anti-tumor response. These findings suggest that targeting Treg-derived TRAIL may not be beneficial as an immunotherapy for cancer.

6.2.2 Treg-restricted deletion of *Tnfsf10* has no effect on EAE or autoimmune diabetes

I propose that Treg-restricted deletion of *Tnfsf10* does not have an effect in autoimmune disease due to similar reasons we described previously for the TME. I will briefly discuss the five reasons here. First we found limited DR5 expression on cells in

the islet except for higher levels of DR5 on β cells in the islet; however, upon further investigation, this cell population did not have any changes in cell death. Second, decoy receptor expression may block Treg-derived TRAIL cytotoxicity. Third, Tregs may utilize TRAIL in other autoimmune environments; future directions will include examination of *Tnfsf10*$^{L/L}$*Foxp3*$^{Cre\text{-}YFP}$ in other autoimmune models. Fourth, Tregs still express other mechanisms of suppression.

Lastly, Treg-derived TRAIL may have an unknown role in the diabetic islet. This is demonstrated by two examples. First, I recorded decreased cell death in the CD11c^{+} population. TRAIL can play a role in regulating CD11c^{+} cell function; so further analysis of CD11c^{+} dendritic cells and their function in NOD.*Tnfsf10*$^{L/L}$Foxp3$^{Cre\text{-}GFP}$ might provide insight into the role of Treg-derived TRAIL in NOD mice [301]. Analysis could include flow cytometry analysis of markers such as CD80/86 (activation), MHCI (cross presentation) and IL-12 (function) [358]. Second, I found an unexpected increase in percentages of Tregs in the islet of NOD.*Tnfsf10*$^{L/L}$Foxp3$^{Cre\text{-}GFP}$ mice. This is in direct contrast to reports demonstrating TRAIL promoting Treg number and proliferation [290]. Therefore, TRAIL may have an unexpected role in limiting Treg number in the islet. Single cell RNA sequencing analysis of all cells in the islet from NOD.*Tnfsf10*$^{L/L}$Foxp3$^{Cre\text{-}GFP}$ and NOD.Foxp3$^{Cre\text{-}GFP}$ mice could give clues on the role of Treg-derived TRAIL on Tregs and CD11c^{+} cells in the islet.

While I found a few differences in the islet of NOD.*Tnfsf10*$^{L/L}$Foxp3$^{Cre\text{-}GFP}$ mice, none of these changes ultimately affected the disease outcome. I conclude that Tregs do not require TRAIL in order to suppress the immune response in EAE and autoimmune diabetes.

6.3 CD8-restricted deletion of *Tnfsf10* prevents autoimmune diabetes

In Chapter 5, I studied if $CD8^+$ production of TRAIL has implications in autoimmune diabetes. Here I discuss the results and future directions.

6.3.1 $CD8^+$ T cell deletion of *Tnfsf10* leads to almost 100% protection of NOD mice from diabetes

My studies discovered that deletion of *Tnfsf10* on $CD8^+$ T cells yields almost 100% protection of NOD mice from diabetes. Therefore, there is substantial interest in targeting TRAIL on $CD8^+$ T cells as a therapy for T1D. However, previously published reports have indicated other cells, such as β cells, utilize TRAIL as a protective mechanism in autoimmune diabetes [292,299]. Therefore, efforts to target TRAIL to limit autoimmune diabetes must be strictly limited to $CD8^+$ T cell-derived TRAIL. Future studies for targeting $CD8^+$ T cell-derived TRAIL could examine when $CD8^+$ T cells express TRAIL over other non-immune and immune cells. For example, $CD8^+$ T cells could express TRAIL at a high level at early stage of life while other cells, including β cells, express low levels. Treatment of mice with TRAIL blocking antibodies at an early stage of life may reduce disease while limiting off target effects. To determine this, levels of TRAIL in immune and non-immune cells will be determined by qPCR and flow cytometry. I can then treat mice with anti-TRAIL at the identified time point to limit $CD8^+$ T cell TRAIL cytotoxicity and examine diabetes incidence and insulitis.

Due to the interesting observation that $CD8^+$-restricted deletion of *Tnfsf10* leads to reduced autoimmune diabetes, I questioned if deletion of *Tnfsf10* on $CD8^+$ T cells would

affect all disease models in which $CD8^+$ T cells had an important role. I found tumor growth in B6.*Tnfsf10*$^{L/L}$E8I$^{Cre\text{-}GFP}$ mice was not altered. However, these studies are limited due to three reasons. First, I did not include B6.*Tnfsf10*$^{L/L}$E8I$^{Cre\text{-}GFP}$ mice treated with anti-PD1. As previously mentioned, $CD8^+$ T cells in the TME undergo change to an exhausted, less functional state. This includes decreased production of pro-inflammatory cytokines such as IFNγ, TNFα, altered metabolism, and more [359]. $CD8^+$ production of TRAIL may also be limited in exhausted cells. Therefore, I can treat B6.*Tnfsf10*$^{L/L}$E8I$^{Cre\text{-}GFP}$ and B6.E8I$^{Cre\text{-}GFP}$ mice with anti-PD1 to re-invigorate $CD8^+$ T cells, and examine if $CD8^+$ T cell deletion of *Tnfsf10* impacts tumor growth.

The second limitation of my tumor study is the use of different mouse backgrounds. The unique observation of reduced diabetes incidence was studied in NOD mice and the tumor result was studied in C57BL/6 mice. $CD8^+$ T cells in NOD mice may possess inherent differences in TRAIL expression, regulation, etc. compared to C57BL/6 $CD8^+$ T cells. Therefore, I could utilize a NOD tumor model such as a transplantable MCA cell line and monitor *Tnfsf10*$^{L/L}$E8I$^{Cre\text{-}GFP}$ NOD and E8I$^{Cre\text{-}GFP}$ NOD mice for tumor growth [360,361].

A final limitation of my study of $CD8^+$ T cell derived TRAIL in other disease settings is that I have limited my analysis to the TME. Previous reports have demonstrated a role for $CD8^+$ TRAIL in viral infection such as Influenza, West Nile virus, and others [361-363]. To determine if $CD8^+$ T cell-derived TRAIL has a role in viral infection, I can utilize *Tnfsf10*$^{L/L}$E8I$^{Cre\text{-}GFP}$ and E8I$^{Cre\text{-}GFP}$ mice and infect with Influenza, LCMV, and others and monitor mice for disease [364,365]. Moreover, I can further examine the role for $CD8^+$ T cell in autoimmune disease by examining the pre-established EAE mouse model in *Tnfsf10*$^{L/L}$E8I$^{Cre\text{-}GFP}$ and E8I$^{Cre\text{-}GFP}$ mice.

Although my indicated limitations will need to be examined, I conclude that $CD8^+$ T cell-restricted deletion of TRAIL yields almost 100% protection from diabetes.

6.3.2 Reduced immune cell infiltration may be due to reduced β cell cytotoxicity

My analysis revealed minimal immune infiltration into the islets of *Tnfsf10*$^{L/L}$E8I$^{Cre\text{-}GFP}$ mice. I considered two possible explanations for this result.

First, TRAIL on $CD8^+$ T cells could limit $CD8^+$ T cell migration to the islet. To further address this hypothesis, I will continue to expand my current adoptive transfer experiments to examine levels of Ki67 at more time points. I will also include control mice that are singly injected with each genotype (i.e. WT $CD8^+$ T cells with $CD4^+$ bulk T cells, or mutant $CD8^+$ T cells with $CD4^+$ bulk T cells). This will further expand on if TRAIL has an autocrine effects on $CD8^+$ T cell proliferation. Additionally, I could perform a set of in vitro experiments in which $CD8^+$ T cells from WT or *Tnfsf10*$^{L/L}$E8I$^{Cre\text{-}GFP}$ mice are stimulated with or without DR5 blocking antibody and examine if Ki67 levels are altered.

A second explanation for reduced immune infiltration in islets of *Tnfsf10*$^{L/L}$E8I$^{Cre\text{-}GFP}$ mice is that $CD8^+$ T cell-restricted deletion of *Tnfsf10* may yield a less functional cytotoxic response. Reduced cytotoxicity would lead to less β cell destruction, reduced inflammation, and reduced recruitment of additional immune cells to exacerbate disease. $CD8^+$ T cell-derived TRAIL could target a cell that is important in regulation of the immune response or the pancreatic β cells directly. For example, TRAIL can induce apoptosis in DR5 expressing Tregs [288]. TRAIL-expressing $CD8^+$ T cells could target Tregs in the LN or islet to hinder them less suppressive towards diabetogenic T cells; therefore, *Tnfsf10*$^{-/-}$ $CD8^+$ T cells are unable to target Tregs and increased suppression limits islet infiltration

and β cell destruction. While I found no differences in T cell numbers in the NDLN and PLN of *Tnfsf10*$^{L/L}$E8I$^{Cre\text{-}GFP}$ mice, analysis of survival, cell death, and function of these cells could give insight onto the reduced immune infiltration into the islet.

TRAIL-expressing CD8$^+$ T cells may also directly target β cells. To clarify the role for CD8$^+$ T cell derived TRAIL in β cell death, I am currently working to culture a β cell line or freshly isolated islets from NOD mice with recombinant TRAIL and determining cell death in these cells. Moreover, I will also culture a β cell line or islets from NOD mice with CD8$^+$ T cells from mutant or WT mice and determine if *Tnfsf10*$^{-/-}$ CD8$^+$ T cells are less cytotoxic to β cells. I can also include a DR5 blocking antibody to ensure specific binding of TRAIL to DR5 on β cells.

To further determine if CD8$^+$ T cell-restricted deletion of *Tnfsf10* is due to targeting a regulatory population or β cells directly, I can utilize my single cell RNA sequencing analysis to examine the phenotype of T cells and β cells from islets of WT and mutant mice and identify which populations are expressing DR5.

Finally, it would also be of interest to examine a C57BL/6 or NOR/LtJ (NOD mouse crossed to C57BL/KsJ and are resistant to diabetes) mouse that does not develop diabetes for DR5 expression on β cells [366]. If C57BL/6 or NOR/LtJ β cells do not express DR5, this may indicate that they are resistant to CD8$^+$ T cell-derived TRAIL cytotoxicity, and therefore resistant to β cell death and diabetes.

6.3.3 IFNα may induce TRAIL expression on CD8$^+$ T cells

My analysis found that CD8$^+$ T cell-derived TRAIL is extremely important for disease progression. Therefore, I was curious what might regulate TRAIL expression on CD8$^+$ T cells. I previously discussed the important role for IFNα in initiation and development of T1D and autoimmune diabetes (Section 1.4.1.1). I found that IFNα upregulates TRAIL on intra-islet CD8$^+$ T cells in vitro but not CD8$^+$ T cells from the periphery. Therefore, I propose two future directions to determine if IFNα regulates TRAIL induction of CD8$^+$ T cells to confer disease. First, I will examine levels of IFNAR on CD8$^+$ T cells from the NDLN, PLN, and islet to determine if these cells are more sensitive to IFNα-mediated TRAIL upregulation. Second, I can utilize CRISPR-Cas9 editing to delete IFNAR expression on CD8$^+$ T cells. I will transfer these cells to NOD-SCID mice and monitor for diabetes incidence and insulitis scoring.

My study examining the IFNα will provide clues on how CD8$^+$ T cells upregulate TRAIL and how this may impact β cell death and disease.

6.4 Closing statements

My data has analyzed two potential mechanisms of T cell checks and balances. First, while Tregs are important in limiting autoimmunity such as autoimmune diabetes, they also are resilient contributors to tumor growth and disease. Tregs are able to suppress activated immune cells in the TME, despite harsh inflammatory conditions. I revealed this may be possible through Treg regulation of chromatin accessibility regions

that are important for conversion to the Tconv phenotype in the TME. In addition, I demonstrated that Treg-restricted deletion of *Tnfsf10* did not limit suppression in the TME nor diabetic islet due to presence of other suppressive molecules. Further analysis of these suppressive mechanisms, regulation of these mechanisms, and targeting multiple arms of Treg function, may decrease Treg suppression of the anti-tumor response and restore proper checks and balances of these cells in the immune system.

Second, although $CD8^+$ T cells can play a protective role against tumor cell growth, they can contribute to autoimmune diabetes. I demonstrated that $CD8^+$ T cells may trigger autoimmune disease through production of TRAIL. Further analysis and potential targeting of $CD8^+$ T cell-derived TRAIL may limit β cells death and restore checks on balances of these cells to limit disease.

Appendix A *Nrp1* deletion on Tregs leads to variance in tumor growth models

Neuropilin-1 (Nrp1) is a cell surface molecule that is highly expressed on murine Tregs[76,77]. My lab previously published that deletion of *Nrp1* on Tregs results in decreased tumor growth in the transplantable B16 melanoma, MC38 colon adenocarcinoma, and EL4 T cell lymphoma cell lines, although the reduction in tumor growth was varied among tumor models[76,77]. Deletion also leads to change in Treg phenotype to a more Tconv effector-like, IFNγ secreting phenotype. Therefore, I questioned if all tumor models have a similar level in reduction of tumor growth in *Nrp1*$^{L/L}$*Foxp3*$^{Cre\text{-}YFP}$ mice.

Appendix A.1 Materials and Methods

To perform this, I injected 4-6 week old female and male *Nrp1*$^{L/L}$ *Foxp3*$^{Cre\text{-}YFP}$and *Foxp3*$^{Cre\text{-}YFP}$ mice with various tumor types: 125,000 B16 were injected i.d. in the hindflank, 250,000 MC38 cells were injected s.c. in the hindflank, 125,000 EL4 cells were injected i.d. in the hindflank, 125,000 cells PTEN-BRAF cells were injected i.d. in the hindflank, high dose 1,000,000 MEER cells were injected s.c. in the back of the neck, low dose 250,000 MEER cells were injected, s.c. in the back of the neck, 100,000 E0771-LMB cells were injected in the 4th mammary fat pad, 125,000 LLC cells were injected s.c. in the hindflank, 125,000 Panc02 cells were injected s.c. in the hindflank, and 1,000,000 Panc02 cells were injected orthotopically into the pancreas of mice by Jennifer Miller. All tumor models excluding the pancreas Panc02 model was measured at Day 6 post tumor

inoculation and every 3 days following with digital calipers. Tumors were measured every 3 days with a digital caliper in two dimensions (width and length) and presented as tumor area (mm^2; defined as *w* x *l*). Panc02 tumors injected into the pancreas were isolated at least 60 days post tumor inoculation and weighed by digital scale. The B16.F10 were obtained from M.J. Turk (Dartmouth College, New Hampshire) [233]. The MC38 colon adenocarcinoma cells were obtained from J.P. Allison (M.D. Anderson Cancer Center, Texas) [234]. The EL4 cells were obtained from ATCC. The PTEN-BRAF cells were obtained from G. Delgoffe (University of Pittsburgh, Pennsylvania)[344,367,368]. The MEER cell were obtained from Robert Ferris (Univeristy of Pittsburgh, Pennsylvania)[369]. The LLC cell line was acquired from ATCC. The Panc02 cell line was acquired from Herb Zeh (University of Pittsburgh, Pennsylvania).

Appendix A.2 Results and Discussion

To access if Treg-restricted deletion of *Nrp1* has an effect on all tumor models, I injected *Nrp1*$^{L/L}$ *Foxp3*$^{Cre\text{-}YFP}$and *Foxp3*$^{Cre\text{-}YFP}$ mice with one of the following tumors: B16 melanoma, MC38 adenocarcinoma, EL4 T cell lymphoma, PTEN-Braf melanoma, MEER head and neck cell line, E0771-LMB breast cancer line, LLC Lewis Lung carcinoma, and Panc02 pancreatic cell line and monitored tumor growth.

I found that deletion of *Nrp1* from Tregs does not result in complete tumor clearance in all tumor models. As demonstrated in previous publications, I found *Nrp1* deletion on Tregs resulted in reduced tumor growth in B16, MC38, and EL4 (Appendix Fig 1A-C)[76,77]. In addition, all other tumor models have some reduction in tumor growth

(Appendix Fig 1D, F-I) or tumor burden (Appendix Fig 1J), except for the high dose of MEER head and neck (Appendix Fig 1E). The lack of response in the high dose of MEER may be due limited time for immune cells to infiltrate into the high tumor burden environment (Appendix Fig 1E). Moreover, a few other models such as LLC and Panc02 (both subcutaneous and orthotopic injection) had a less robust difference between mutant and wild-type tumor growth (Appendix Fig 1H-J).

These tumor models have differences in growth kinetics, their antigenicity, tumor mutational burden, and immune infiltrate[368,370-375]. However, since I saw some difference in most of the tumor models, I conclude that Nrp1 plays an important role in Tregs, regardless of tumor type.

However, I argue that future studies could examine tumor models with a less robust difference, such as LLC and Panc02, to see if *Nrp1*$^{-/-}$ Tregs in this environment may be less Tconv effector-like and produce less IFNγ production whereas tumor models such as B16 or PTEN-BRAF could have more Tconv effector-like Tregs and more production of IFNγ.

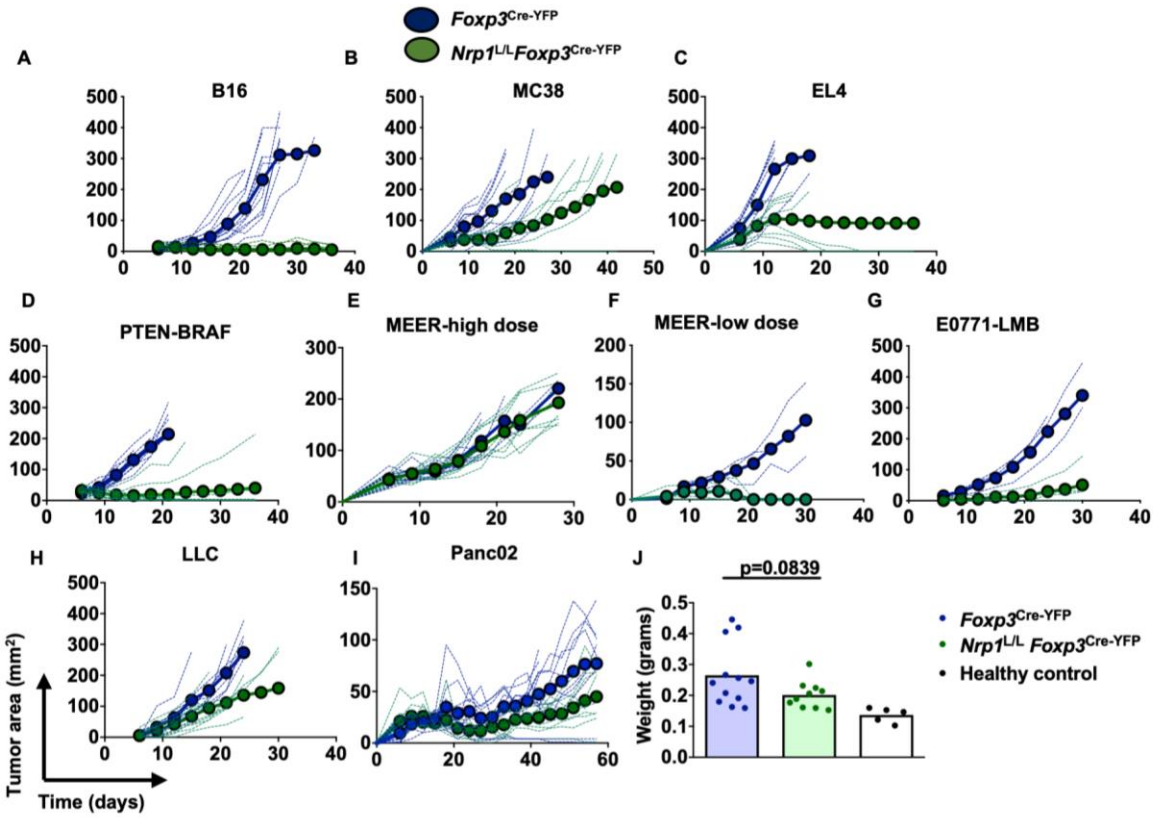

Appendix Figure 1 Tumor growth is varied in *Nrp1*$^{L/L}$ *Foxp3*$^{Cre\text{-}YFP}$ mice

(A) Indicated mice were injected with 125,000 B16 i.d. and monitored for tumor growth **(B)** Indicated mice were injected with 250,000 MC38 s.c. and monitored for tumor growth **(C)** Indicated mice were injected with 125,000 EL4 i.d. and monitored for tumor growth **(D)** Indicated mice were injected with 125,000 PTEN-BRAF i.d. and monitored for tumor growth **(E)** Indicated mice were injected with 1,000,000 MEER s.c. and monitored for tumor growth **(F)** Indicated mice were injected with 250,000 MEER s.c. and monitored for tumor growth **(G)** Indicated mice were injected with 100,000 E0771-LMB in the 4th mammary fat pad and monitored for tumor growth **(H)** Indicated mice were injected with 125,000 LLC s.c. and monitored for tumor growth **(I)** Indicated mice were injected with 125,000 Panc02 s.c. and monitored for tumor growth **(J)** Indicated mice were injected with 1,000,000 Panc02 orthotopically into the pancreas and sacrificed and analyzed for pancreas weight

Data in **(A)** are representative of 2 experiments with 11-12 mice/group. **(B)** is representative of 2 experiment with 9-11 mice/group. **(C)** is representative of 2 experiments with 8-9 mice/group. Data in **(D)** is

representative of 2 experiments with 10-11 mice/group. Data in **(E)** is representative of 2 experiments with 9-14 mice/group. Data in **(F)** is representative of 1 experiment with 3-6 mice/group. Data in **(G)** is representative of 1 experiment with 3-4 mice/group. Data in **(H)** is representative of 2 experiments with 10-11 mice/group. Data in **(I)** is representative of 2 experiments with 10-11 mice/group. Data in **(J)** is representative of 2 experiments with 10-12 mice/group. Statistics were determined using Student unpaired t test **(J)**

Appendix B Treg-derived Neuropilin-1 is not required for Fetal Maternal Tolerance (FMT)

Neuropilin-1 (Nrp1) has an important role on Tregs in the TME. However, the evolutionary relevance of Nrp1 on Tregs remains elusive. In pregnancy, the maternal immune system must adapt to tolerate the semi-allogeneic fetus, an immune barrier commonly known as fetal-maternal tolerance (FMT) [376]. While there are multiple mechanisms that contribute to this tolerance, Tregs have been shown to be instrumental in suppressing the maternal immune response to the fetus [377]. Therefore, I hypothesized that Tregs in placental animals evolved to express Nrp1 to protect the fetus from the maternal immune system.

Appendix B.1 Materials and Methods

To study fetal resorption, I performed timed mating with >4 week old BALB/c males and 4-6 week old female C57BL/6 *Nrp1*$^{L/L}$ *Foxp3*$^{Cre\text{-}YFP}$and C57BL/6 *Foxp3*$^{Cre\text{-}YFP}$ mice. Mice were monitored daily for plugs and were removed from the cage if a plug was detected. Females were analyzed for resorption 12 days post plug detection. Resorption was calculated for % of resorption per all embryos and resorption per pregnancy. Pup weight was also monitored after pups from timed mating were allowed to give birth. Pup weight was monitored at indicated time points post birth.

Appendix B.2 Results and Discussion

To examine if *Nrp1* deletion on Tregs increases fetal resorption, I crossed B6.*Nrp1*$^{L/L}$ *Foxp3*$^{Cre\text{-}YFP}$and B6.*Foxp3*$^{Cre\text{-}YFP}$ to allogenic BALB/c males and accessed fetal resorption 12 days post vaginal plug detection (Appendix Fig 2A). Interestingly I found no difference in the percentage of resorption in all embryos examined and embryos per mother (Appendix Fig 2B-C). Moreover, I found no differences in development or weight gain of these pups post-birth (data not shown, and Appendix Fig 2D). Therefore, I conclude that Treg-derived Nrp1 is not required for the FMT barrier and the evolutionary relevance of Nrp1 on Tregs remains unclear.

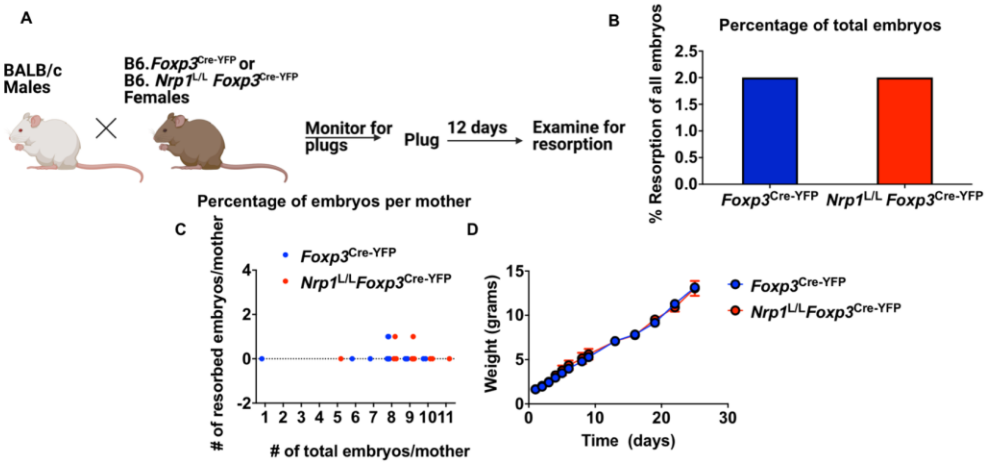

Appendix Figure 2 Nrp1 is not required for Treg-mediated Fetal Maternal Tolerance

(A) Breeding schematic **(B)** Indicated mice B6 females were bred to BALB/c females, monitored for vaginal plugs, and sacrificed and examined for fetal resorption. Percentage of total embryos across the study are displayed **(C)** Fetal resorption was monitored as described in (B). Percentage of resorbed embryos per female are displayed. **(D)** Pups from indicated pregnant females were monitored for weight gain in grams post birth.

Data in **(B)** are representative of >3 experiments with 8-10 mice/group. **(C)** is representative of 2 experiments with 8-10 mice/group. Data in **(D)** is representative of 3 experiments with 6-12 mice/group.

Appendix C Publications and Awards

Appendix C.1 Publications related to thesis study

Research articles

1.) **Dadey, R.E.,** Grebinoski, S., Zhang, Q., Brunazzi, E.A., Burton, A., Workman, C.J., Vignali, D.A.A. (2021) Regulatory T Cell-Derived TRAIL Is Not Required for Peripheral Tolerance. *Immunohorizons* 5(1):48-58.

Review Articles

1.) **Dadey R.E**, Workman CJ, Vignali DAA (2020) Chapter 6: Regulatory T cells in the Tumor Microenvironment. In: Birbrair A (ed) Tumor microenvironment. Springer, Cham

Appendix C.2 Publications from Collaborations

Research Articles

1.) Somasundaram A., Cillo, A.R., Lampenfeld, C., Oliveri, L., Velez, M.A., Joyce, S., Calderon, M.J. **Dadey, R.,** Rajasundaram, D., Normolle, D.P., Watkins, S.C., Herman, J.G., Kirkwood, J.M., Lipson, E.J., Ferris, R.L., Bruno, T.C., Vignali, D.A.A. (2020) Immune Dysfunction in Cancer Patients Driven by IL6 and IL8 induction of an inhibitory receptor module in peripheral $CD8^+$ T cells. *BioRxiv*. 2020.05.06.081471

2.) Overacre-Delgoffe, A.E., Chikina, M., **Dadey, R.E.**, Yano, H., Brunazzi, E.A., Shayan, G., Horne, W., Moskovitz, J.M., Kolls, J.K., Sanders, C., Shuai, Y., Normolle, D.P., Kirkwood, J.M., Ferris, R.L., Delgoffe, G.M., Bruno, T.C., Workman, C.J., Vignali, D.A.A. (2017) Interferon-γ Drives Treg fragility to Promote Anti-Tumor Immunity. *Cell* 169:1130-1141

3.) Scharping, N.E., Menk, A.V., Moreci, R.S., Whetsone, R.D., **Dadey, R.E.**, Watkins, S.C., Ferris, R.L., Delgoffe, G.M. (2016). The Tumor Microenvironment Represses T Cell Mitochondrial Biogenesis to Drive Intratumoral T Cell Metabolic

Insufficiency and Dysfunction. *Immunity* 45: 374-388.

Appendix C.3 Grants, Fellowships, Awards, and Presentations at External Meetings

Grants and Fellowships

National Cancer Institute

a. NIH F31 CA236337 (07/2019-02/2021)
b. NIH T32 CA082084, University of Pittsburgh School of Medicine Cancer Immunology Training Grant (07/2017-07/2019)

Awards

Biomedical Graduate Student Association (BGSA)

a. Travel Award (2020)
b. Best Poster Award at BGSA Symposium (2018)
c. Best Poster Award at BGSA Symposium (2016)

American Association of Immunology

a. Travel Award (2020), cancelled due to COVID19

Cold Spring Harbor

a. Travel Award (2019)

University of Pittsburgh Department of Immunology

a. Best Poster Award at Immunology Retreat (2017)

Presentations at external meetings

1.) Dadey, R.E., Grebinoski, S., Zhang, Q., Gocher, A., Tabib, T., Lafayatis, R., Brunazzi, E., Andrew, L.P., Burton, A., Workman, C.J. Vignali, D.A.A. 2020. Treg-restricted deletion of TRAIL (*Tnfsf10*) reduces autoimmune diabetes. American Association of Immunologists, 2020. *Speaker and Poster*, cancelled due to COVID19

2.) **Dadey, R.E.,** Grebinoski, S., Zhang, Q., Gocher, A., Tabib, T., Lafayatis, R., Brunazzi, E., Andrew, L.P., Burton, A., Workman, C.J. Vignali, D.A.A. 2020. Treg-restricted deletion of TRAIL (*Tnfsf10*) reduces autoimmune diabetes. Translational Research Cancer Centers Consortium, 2020. *Poster*

3.) **Dadey, R.E.,** Overacre-Delgoffe, A.E., Wang, T., Zhang, R., Chen, W.,

Rittenhouse, N., Poholek, A., Tabib, T., Lafyatis, R., Workman, C.J., Vignali, D.A.A. 2018. The Epigenetic Underpinnings of Regulatory T cell Fragility in the Tumor Microenvironment. Society of Immunotherapy for Cancer (SITC). Washington D.C. *Poster*

4.) **Dadey, R.E.,** Overacre-Delgoffe, A.E., Wang, T., Sun, Z., Chen, W., Workman, C.J., Vignali, D.A.A. 2018. The Epigenetic Status of Regulatory T cells in the Tumor Microenvironment. Translational Research Cancer Centers Consortium, Seven Springs, PA 2018. Seven Springs, PA. *Poster and Speaker*

References

1 Togashi, Y., Shitara, K. & Nishikawa, H. Regulatory T cells in cancer immunosuppression - implications for anticancer therapy. *Nat Rev Clin Oncol* **16**, 356-371, doi:10.1038/s41571-019-0175-7 (2019).

2 Paluskievicz, C. M. *et al.* T Regulatory Cells and Priming the Suppressive Tumor Microenvironment. *Front Immunol* **10**, 2453, doi:10.3389/fimmu.2019.02453 (2019).

3 Abbas, A. K. *et al.* Regulatory T cells: recommendations to simplify the nomenclature. *Nat Immunol* **14**, 307-308, doi:10.1038/ni.2554 (2013).

4 Shevach, E. M. & Thornton, A. M. tTregs, pTregs, and iTregs: similarities and differences. *Immunol Rev* **259**, 88-102, doi:10.1111/imr.12160 (2014).

5 Xie, X. *et al.* The Regulatory T Cell Lineage Factor Foxp3 Regulates Gene Expression through Several Distinct Mechanisms Mostly Independent of Direct DNA Binding. *PLoS Genet* **11**, e1005251, doi:10.1371/journal.pgen.1005251 (2015).

6 Marson, A. *et al.* Foxp3 occupancy and regulation of key target genes during T-cell stimulation. *Nature* **445**, 931-935, doi:10.1038/nature05478 (2007).

7 Zheng, Y. *et al.* Genome-wide analysis of Foxp3 target genes in developing and mature regulatory T cells. *Nature* **445**, 936-940, doi:10.1038/nature05563 (2007).

8 Lopes, J. E. *et al.* Analysis of FOXP3 reveals multiple domains required for its function as a transcriptional repressor. *J Immunol* **177**, 3133-3142, doi:10.4049/jimmunol.177.5.3133 (2006).

9 Rudensky, A. Y., Gavin, M. & Zheng, Y. FOXP3 and NFAT: partners in tolerance. *Cell* **126**, 253-256, doi:10.1016/j.cell.2006.07.005 (2006).

10 Hill, J. A. *et al.* Foxp3 transcription-factor-dependent and -independent regulation of the regulatory T cell transcriptional signature. *Immunity* **27**, 786-800, doi:10.1016/j.immuni.2007.09.010 (2007).

11 Williams, L. M. & Rudensky, A. Y. Maintenance of the Foxp3-dependent developmental program in mature regulatory T cells requires continued expression of Foxp3. *Nat Immunol* **8**, 277-284, doi:10.1038/ni1437 (2007).

12 Zheng, Y. & Rudensky, A. Y. Foxp3 in control of the regulatory T cell lineage. *Nat Immunol* **8**, 457-462, doi:10.1038/ni1455 (2007).

13 Burchill, M. A., Yang, J., Vogtenhuber, C., Blazar, B. R. & Farrar, M. A. IL-2 receptor beta-dependent STAT5 activation is required for the development of Foxp3+ regulatory T cells. *J Immunol* **178**, 280-290, doi:10.4049/jimmunol.178.1.280 (2007).

14 Yao, Z. *et al.* Nonredundant roles for Stat5a/b in directly regulating Foxp3. *Blood* **109**, 4368-4375, doi:10.1182/blood-2006-11-055756 (2007).

15 Dikiy, S. *et al.* A distal Foxp3 enhancer enables interleukin-2 dependent thymic Treg cell lineage commitment for robust immune tolerance. *Immunity* **54**, 931-946 e911, doi:10.1016/j.immuni.2021.03.020 (2021).

16 Passerini, L. *et al.* STAT5-signaling cytokines regulate the expression of FOXP3 in CD4+CD25+ regulatory T cells and CD4+CD25- effector T cells. *Int Immunol* **20**, 421-431, doi:10.1093/intimm/dxn002 (2008).

17 Chinen, T. *et al.* An essential role for the IL-2 receptor in Treg cell function. *Nature immunology* **17**, 1322-1333, doi:10.1038/ni.3540 (2016).

18 Toomer, K. H. *et al.* Essential and non-overlapping IL-2Ralpha-dependent processes for thymic development and peripheral homeostasis of regulatory T cells. *Nat Commun* **10**, 1037, doi:10.1038/s41467-019-08960-1 (2019).

19 Pandiyan, P., Zheng, L., Ishihara, S., Reed, J. & Lenardo, M. J. CD4+CD25+Foxp3+ regulatory T cells induce cytokine deprivation-mediated apoptosis of effector CD4+ T cells. *Nat Immunol* **8**, 1353-1362, doi:10.1038/ni1536 (2007).

20 Sawant, D. V. *et al.* Adaptive plasticity of IL-10(+) and IL-35(+) Treg cells cooperatively promotes tumor T cell exhaustion. *Nat Immunol* **20**, 724-735, doi:10.1038/s41590-019-0346-9 (2019).

21 Turnis, M. E. *et al.* Interleukin-35 Limits Anti-Tumor Immunity. *Immunity* **44**, 316-329, doi:10.1016/j.immuni.2016.01.013 (2016).

22 Sawant, D. V., Hamilton, K. & Vignali, D. A. Interleukin-35: Expanding Its Job Profile. *J Interferon Cytokine Res* **35**, 499-512, doi:10.1089/jir.2015.0015 (2015).

23 Osinska, I., Popko, K. & Demkow, U. Perforin: an important player in immune response. *Cent Eur J Immunol* **39**, 109-115, doi:10.5114/ceji.2014.42135 (2014).

24 Bots, M. & Medema, J. P. Granzymes at a glance. *J Cell Sci* **119**, 5011-5014, doi:10.1242/jcs.03239 (2006).

25 Grossman, W. J. *et al.* Differential expression of granzymes A and B in human cytotoxic lymphocyte subsets and T regulatory cells. *Blood* **104**, 2840-2848, doi:10.1182/blood-2004-03-0859 (2004).

26 Gondek, D. C., Lu, L. F., Quezada, S. A., Sakaguchi, S. & Noelle, R. J. Cutting edge: contact-mediated suppression by CD4+CD25+ regulatory cells involves a granzyme B-dependent, perforin-independent mechanism. *J Immunol* **174**, 1783-1786, doi:10.4049/jimmunol.174.4.1783 (2005).

27 Krummel, M. F. & Allison, J. P. CTLA-4 engagement inhibits IL-2 accumulation and cell cycle progression upon activation of resting T cells. *J Exp Med* **183**, 2533-2540, doi:10.1084/jem.183.6.2533 (1996).

28 Workman, C. J., Dugger, K. J. & Vignali, D. A. Cutting edge: molecular analysis of the negative regulatory function of lymphocyte activation gene-3. *J Immunol* **169**, 5392-5395, doi:10.4049/jimmunol.169.10.5392 (2002).

29 Workman, C. J. *et al.* Lymphocyte activation gene-3 (CD223) regulates the size of the expanding T cell population following antigen activation in vivo. *J Immunol* **172**, 5450-5455, doi:10.4049/jimmunol.172.9.5450 (2004).

30 Andrews, L. P., Marciscano, A. E., Drake, C. G. & Vignali, D. A. LAG3 (CD223) as a cancer immunotherapy target. *Immunol Rev* **276**, 80-96, doi:10.1111/imr.12519 (2017).

31 Vignali, D. A., Collison, L. W. & Workman, C. J. How regulatory T cells work. *Nat Rev Immunol* **8**, 523-532, doi:10.1038/nri2343 (2008).

32 Corthay, A. How do regulatory T cells work? *Scand J Immunol* **70**, 326-336, doi:10.1111/j.1365-3083.2009.02308.x (2009).

33 Miyara, M. *et al.* Functional delineation and differentiation dynamics of human CD4+ T cells expressing the FoxP3 transcription factor. *Immunity* **30**, 899-911, doi:10.1016/j.immuni.2009.03.019 (2009).

34 Schmidt, A., Oberle, N. & Krammer, P. H. Molecular mechanisms of treg-mediated T cell suppression. *Front Immunol* **3**, 51, doi:10.3389/fimmu.2012.00051 (2012).

35 Vignali, D. A. Mechanisms of T(reg) Suppression: Still a Long Way to Go. *Front Immunol* **3**, 191, doi:10.3389/fimmu.2012.00191 (2012).

36 Liu, C., Workman, C. J. & Vignali, D. A. Targeting regulatory T cells in tumors. *FEBS J* **283**, 2731-2748, doi:10.1111/febs.13656 (2016).

37 Pandiyan, P. & Lenardo, M. J. The control of CD4+CD25+Foxp3+ regulatory T cell survival. *Biol Direct* **3**, 6, doi:10.1186/1745-6150-3-6 (2008).

38 Janeway, C. A., Jr. Travers, P., Walport, M., et. al. in *Immunobiology: The Immune System in Health and Disease* (New York: Garland Science, 2001).

39 Sung, H. *et al.* Global cancer statistics 2020: GLOBOCAN estimates of incidence and mortality worldwide for 36 cancers in 185 countries. *CA Cancer J Clin*, doi:10.3322/caac.21660 (2021).

40 Cancer Tomorrow. *Available from https://gco.iarc.fr/* ([cited 2021]).

41 *Diabetes Facts and Figures*, <https://idf.org/aboutdiabetes/what-is-diabetes/facts-figures.html> (2020).

42 Cancer Statistics. *Available from: https://www.cancer.gov/about-cancer/understanding/statistics* ([cited 2021]).

43 Siegel, R. L., Miller, K. D., Fuchs, H. E. & Jemal, A. Cancer Statistics, 2021. *CA Cancer J Clin* **71**, 7-33, doi:10.3322/caac.21654 (2021).

44 Mariotto, A. B., Yabroff, K. R., Shao, Y., Feuer, E. J. & Brown, M. L. Projections of the cost of cancer care in the United States: 2010-2020. *J Natl Cancer Inst* **103**, 117-128, doi:10.1093/jnci/djq495 (2011).

45 Park, J. & Look, K. A. Health Care Expenditure Burden of Cancer Care in the United States. *Inquiry* **56**, 46958019880696, doi:10.1177/0046958019880696 (2019).

46 Stratton, M. R., Campbell, P. J. & Futreal, P. A. The cancer genome. *Nature* **458**, 719-724, doi:10.1038/nature07943 (2009).

47 Hanahan, D. & Weinberg, R. A. The hallmarks of cancer. *Cell* **100**, 57-70, doi:10.1016/s0092-8674(00)81683-9 (2000).

48 Hanahan, D. & Weinberg, R. A. Hallmarks of cancer: the next generation. *Cell* **144**, 646-674, doi:10.1016/j.cell.2011.02.013 (2011).

49 Cooper, G. M. in *The Cell: A Molecular Approach* Vol. 2nd edition (ed Sunderland) (Sinauer Associates, 2000).

50 Dunn, G. P., Old, L. J. & Schreiber, R. D. The three Es of cancer immunoediting. *Annu Rev Immunol* **22**, 329-360, doi:10.1146/annurev.immunol.22.012703.104803 (2004).

51 Dighe, A. S., Richards, E., Old, L. J. & Schreiber, R. D. Enhanced in vivo growth and resistance to rejection of tumor cells expressing dominant negative IFN gamma receptors. *Immunity* **1**, 447-456, doi:10.1016/1074-7613(94)90087-6 (1994).

52 Kaplan, D. H. *et al.* Demonstration of an interferon gamma-dependent tumor surveillance system in immunocompetent mice. *Proc Natl Acad Sci U S A* **95**, 7556-7561, doi:10.1073/pnas.95.13.7556 (1998).

53 Street, S. E., Cretney, E. & Smyth, M. J. Perforin and interferon-gamma activities independently control tumor initiation, growth, and metastasis. *Blood* **97**, 192-197, doi:10.1182/blood.v97.1.192 (2001).

54 Smyth, M. J. *et al.* Nature's TRAIL--on a path to cancer immunotherapy. *Immunity* **18**, 1-6, doi:10.1016/s1074-7613(02)00502-2 (2003).

55 Takeda, K. *et al.* Critical role for tumor necrosis factor-related apoptosis-inducing ligand in immune surveillance against tumor development. *J Exp Med* **195**, 161-169, doi:10.1084/jem.20011171 (2002).

56 Cretney, E. *et al.* Increased susceptibility to tumor initiation and metastasis in TNF-related apoptosis-inducing ligand-deficient mice. *J Immunol* **168**, 1356-1361, doi:10.4049/jimmunol.168.3.1356 (2002).

57 Chin, Y. E. *et al.* Cell growth arrest and induction of cyclin-dependent kinase inhibitor p21 WAF1/CIP1 mediated by STAT1. *Science* **272**, 719-722, doi:10.1126/science.272.5262.719 (1996).

58 Bromberg, J. F., Horvath, C. M., Wen, Z., Schreiber, R. D. & Darnell, J. E., Jr. Transcriptionally active Stat1 is required for the antiproliferative effects of both interferon alpha and interferon gamma. *Proc Natl Acad Sci U S A* **93**, 7673-7678, doi:10.1073/pnas.93.15.7673 (1996).

59 Chin, Y. E., Kitagawa, M., Kuida, K., Flavell, R. A. & Fu, X. Y. Activation of the STAT signaling pathway can cause expression of caspase 1 and apoptosis. *Mol Cell Biol* **17**, 5328-5337, doi:10.1128/mcb.17.9.5328 (1997).

60 Girardi, M. *et al.* Regulation of cutaneous malignancy by gammadelta T cells. *Science* **294**, 605-609, doi:10.1126/science.1063916 (2001).

61 Ostroumov, D., Fekete-Drimusz, N., Saborowski, M., Kuhnel, F. & Woller, N. CD4 and CD8 T lymphocyte interplay in controlling tumor growth. *Cell Mol Life Sci* **75**, 689-713, doi:10.1007/s00018-017-2686-7 (2018).

62 Penn, I. & Starzl, T. E. Malignant lymphomas in transplantation patients: a review of the world experience. *Int Z Klin Pharmakol Ther Toxikol* **3**, 49-54 (1970).

63 Gatti, R. A. & Good, R. A. Occurrence of malignancy in immunodeficiency diseases. A literature review. *Cancer* **28**, 89-98, doi:10.1002/1097-0142(197107)28:1<89::aid-cncr2820280117>3.0.co;2-q (1971).

64 Boshoff, C. & Weiss, R. AIDS-related malignancies. *Nat Rev Cancer* **2**, 373-382, doi:10.1038/nrc797 (2002).

65 Loeb, L. A., Loeb, K. R. & Anderson, J. P. Multiple mutations and cancer. *Proc Natl Acad Sci U S A* **100**, 776-781, doi:10.1073/pnas.0334858100 (2003).

66 Khong, H. T. & Restifo, N. P. Natural selection of tumor variants in the generation of "tumor escape" phenotypes. *Nat Immunol* **3**, 999-1005, doi:10.1038/ni1102-999 (2002).

67 Long, S. A. & Buckner, J. H. CD4+FOXP3+ T regulatory cells in human autoimmunity: more than a numbers game. *J Immunol* **187**, 2061-2066, doi:10.4049/jimmunol.1003224 (2011).

68 Facciabene, A., Motz, G. T. & Coukos, G. T-regulatory cells: key players in tumor immune escape and angiogenesis. *Cancer Res* **72**, 2162-2171, doi:10.1158/0008-5472.CAN-11-3687 (2012).

69 Romano, M., Fanelli, G., Albany, C. J., Giganti, G. & Lombardi, G. Past, Present, and Future of Regulatory T Cell Therapy in Transplantation and Autoimmunity. *Front Immunol* **10**, 43, doi:10.3389/fimmu.2019.00043 (2019).

70 Ohue, Y. & Nishikawa, H. Regulatory T (Treg) cells in cancer: Can Treg cells be a new therapeutic target? *Cancer Sci* **110**, 2080-2089, doi:10.1111/cas.14069 (2019).

71 Nishikawa, H. & Sakaguchi, S. Regulatory T cells in tumor immunity. *Int J Cancer* **127**, 759-767, doi:10.1002/ijc.25429 (2010).

72 Onizuka, S. *et al.* Tumor rejection by in vivo administration of anti-CD25 (interleukin-2 receptor alpha) monoclonal antibody. *Cancer Res* **59**, 3128-3133 (1999).

73 Shimizu, J., Yamazaki, S. & Sakaguchi, S. Induction of tumor immunity by removing CD25+CD4+ T cells: a common basis between tumor immunity and autoimmunity. *J Immunol* **163**, 5211-5218 (1999).

74 Kim, J. M., Rasmussen, J. P. & Rudensky, A. Y. Regulatory T cells prevent catastrophic autoimmunity throughout the lifespan of mice. *Nat Immunol* **8**, 191-197, doi:10.1038/ni1428 (2007).

75 Kim, J. *et al.* Cutting edge: depletion of Foxp3+ cells leads to induction of autoimmunity by specific ablation of regulatory T cells in genetically targeted mice. *J Immunol* **183**, 7631-7634, doi:10.4049/jimmunol.0804308 (2009).

76 Delgoffe, G. M. *et al.* Stability and function of regulatory T cells is maintained by a neuropilin-1-semaphorin-4a axis. *Nature* **501**, 252-256, doi:10.1038/nature12428 (2013).

77 Overacre-Delgoffe, A. E. *et al.* Interferon-gamma Drives Treg Fragility to Promote Anti-tumor Immunity. *Cell* **169**, 1130-1141 e1111, doi:10.1016/j.cell.2017.05.005 (2017).

78 Durgeau, A., Virk, Y., Corgnac, S. & Mami-Chouaib, F. Recent Advances in Targeting CD8 T-Cell Immunity for More Effective Cancer Immunotherapy. *Front Immunol* **9**, 14, doi:10.3389/fimmu.2018.00014 (2018).

79 Boon, T., Coulie, P. G. & Van den Eynde, B. Tumor antigens recognized by T cells. *Immunol Today* **18**, 267-268, doi:10.1016/s0167-5699(97)80020-5 (1997).

80 Echchakir, H. *et al.* Evidence for in situ expansion of diverse antitumor-specific cytotoxic T lymphocyte clones in a human large cell carcinoma of the lung. *Int Immunol* **12**, 537-546, doi:10.1093/intimm/12.4.537 (2000).

81 Karanikas, V. *et al.* High frequency of cytolytic T lymphocytes directed against a tumor-specific mutated antigen detectable with HLA tetramers in the blood of a lung carcinoma patient with long survival. *Cancer Res* **61**, 3718-3724 (2001).

82 Slingluff, C. L., Jr. *et al.* Cytotoxic T-lymphocyte response to autologous human squamous cell cancer of the lung: epitope reconstitution with peptides extracted from HLA-Aw68. *Cancer Res* **54**, 2731-2737 (1994).

83 Weynants, P. *et al.* Derivation of tumor-specific cytolytic T-cell clones from two lung cancer patients with long survival. *Am J Respir Crit Care Med* **159**, 55-62, doi:10.1164/ajrccm.159.1.9805073 (1999).

84 Crispin, J. C. & Tsokos, G. C. Cancer immunosurveillance by CD8 T cells. *F1000Res* **9**, doi:10.12688/f1000research.21150.1 (2020).

85 Bruni, D., Angell, H. K. & Galon, J. The immune contexture and Immunoscore in cancer prognosis and therapeutic efficacy. *Nat Rev Cancer* **20**, 662-680, doi:10.1038/s41568-020-0285-7 (2020).

86 Wherry, E. J. & Kurachi, M. Molecular and cellular insights into T cell exhaustion. *Nat Rev Immunol* **15**, 486-499, doi:10.1038/nri3862 (2015).

87 Blank, C. U. *et al.* Defining 'T cell exhaustion'. *Nat Rev Immunol* **19**, 665-674, doi:10.1038/s41577-019-0221-9 (2019).

88 Mukherjee, S. *The emperor of all maladies : a biography of cancer*. 1st Scribner hardcover edn, (Scribner, 2010).

89 Dobosz, P. & Dzieciatkowski, T. The Intriguing History of Cancer Immunotherapy. *Front Immunol* **10**, 2965, doi:10.3389/fimmu.2019.02965 (2019).

90 Waldman, A. D., Fritz, J. M. & Lenardo, M. J. A guide to cancer immunotherapy: from T cell basic science to clinical practice. *Nat Rev Immunol* **20**, 651-668, doi:10.1038/s41577-020-0306-5 (2020).

91 Decker, W. K. & Safdar, A. Bioimmunoadjuvants for the treatment of neoplastic and infectious disease: Coley's legacy revisited. *Cytokine Growth Factor Rev* **20**, 271-281, doi:10.1016/j.cytogfr.2009.07.004 (2009).

92 Couzin-Frankel, J. Breakthrough of the year 2013. Cancer immunotherapy. *Science* **342**, 1432-1433, doi:10.1126/science.342.6165.1432 (2013).

93 Leach, D. R., Krummel, M. F. & Allison, J. P. Enhancement of antitumor immunity by CTLA-4 blockade. *Science* **271**, 1734-1736, doi:10.1126/science.271.5256.1734 (1996).

94 Egen, J. G., Kuhns, M. S. & Allison, J. P. CTLA-4: new insights into its biological function and use in tumor immunotherapy. *Nat Immunol* **3**, 611-618, doi:10.1038/ni0702-611 (2002).

95 Ishida, Y., Agata, Y., Shibahara, K. & Honjo, T. Induced expression of PD-1, a novel member of the immunoglobulin gene superfamily, upon programmed cell death. *EMBO J* **11**, 3887-3895 (1992).

96 Kwon, E. D. *et al.* Manipulation of T cell costimulatory and inhibitory signals for immunotherapy of prostate cancer. *Proc Natl Acad Sci U S A* **94**, 8099-8103, doi:10.1073/pnas.94.15.8099 (1997).

97 Nishimura, H., Nose, M., Hiai, H., Minato, N. & Honjo, T. Development of lupus-like autoimmune diseases by disruption of the PD-1 gene encoding an ITIM motif-carrying immunoreceptor. *Immunity* **11**, 141-151, doi:10.1016/s1074-7613(00)80089-8 (1999).

98 Freeman, G. J. *et al.* Engagement of the PD-1 immunoinhibitory receptor by a novel B7 family member leads to negative regulation of lymphocyte activation. *J Exp Med* **192**, 1027-1034, doi:10.1084/jem.192.7.1027 (2000).

99 Iwai, Y., Terawaki, S. & Honjo, T. PD-1 blockade inhibits hematogenous spread of poorly immunogenic tumor cells by enhanced recruitment of effector T cells. *Int Immunol* **17**, 133-144, doi:10.1093/intimm/dxh194 (2005).

100 Hodi, F. S. *et al.* Biologic activity of cytotoxic T lymphocyte-associated antigen 4 antibody blockade in previously vaccinated metastatic melanoma and ovarian carcinoma patients. *Proc Natl Acad Sci U S A* **100**, 4712-4717, doi:10.1073/pnas.0830997100 (2003).

101 Buchbinder, E. I. & Desai, A. CTLA-4 and PD-1 Pathways: Similarities, Differences, and Implications of Their Inhibition. *Am J Clin Oncol* **39**, 98-106, doi:10.1097/COC.0000000000000239 (2016).

102 Tivol, E. A. *et al.* Loss of CTLA-4 leads to massive lymphoproliferation and fatal multiorgan tissue destruction, revealing a critical negative regulatory role of CTLA-4. *Immunity* **3**, 541-547, doi:10.1016/1074-7613(95)90125-6 (1995).

103 Read, S., Malmstrom, V. & Powrie, F. Cytotoxic T lymphocyte-associated antigen 4 plays an essential role in the function of CD25(+)CD4(+) regulatory cells that control intestinal inflammation. *J Exp Med* **192**, 295-302, doi:10.1084/jem.192.2.295 (2000).

104 Takahashi, T. *et al.* Immunologic self-tolerance maintained by CD25(+)CD4(+) regulatory T cells constitutively expressing cytotoxic T lymphocyte-associated antigen 4. *J Exp Med* **192**, 303-310, doi:10.1084/jem.192.2.303 (2000).

105 Chambers, C. A., Kuhns, M. S., Egen, J. G. & Allison, J. P. CTLA-4-mediated inhibition in regulation of T cell responses: mechanisms and manipulation in tumor immunotherapy. *Annu Rev Immunol* **19**, 565-594, doi:10.1146/annurev.immunol.19.1.565 (2001).

106 Wing, K. *et al.* CTLA-4 control over Foxp3+ regulatory T cell function. *Science* **322**, 271-275, doi:10.1126/science.1160062 (2008).

107 Ovcinnikovs, V. *et al.* CTLA-4-mediated transendocytosis of costimulatory molecules primarily targets migratory dendritic cells. *Sci Immunol* **4**, doi:10.1126/sciimmunol.aaw0902 (2019).

108 Grohmann, U. *et al.* CTLA-4-Ig regulates tryptophan catabolism in vivo. *Nature immunology* **3**, 1097-1101, doi:10.1038/ni846 (2002).

109 Fallarino, F. *et al.* Modulation of tryptophan catabolism by regulatory T cells. *Nat Immunol* **4**, 1206-1212, doi:10.1038/ni1003 (2003).

110 Mellor, A. L. & Munn, D. H. IDO expression by dendritic cells: tolerance and tryptophan catabolism. *Nat Rev Immunol* **4**, 762-774, doi:10.1038/nri1457 (2004).

111 Munn, D. H. *et al.* Inhibition of T cell proliferation by macrophage tryptophan catabolism. *J Exp Med* **189**, 1363-1372, doi:10.1084/jem.189.9.1363 (1999).

112 Fallarino, F. *et al.* T cell apoptosis by tryptophan catabolism. *Cell Death Differ* **9**, 1069-1077, doi:10.1038/sj.cdd.4401073 (2002).

113 Lee, G. K. *et al.* Tryptophan deprivation sensitizes activated T cells to apoptosis prior to cell division. *Immunology* **107**, 452-460, doi:10.1046/j.1365-2567.2002.01526.x (2002).

114 Platten, M., Wick, W. & Van den Eynde, B. J. Tryptophan catabolism in cancer: beyond IDO and tryptophan depletion. *Cancer Res* **72**, 5435-5440, doi:10.1158/0008-5472.CAN-12-0569 (2012).

115 Mokyr, M. B., Kalinichenko, T., Gorelik, L. & Bluestone, J. A. Realization of the therapeutic potential of CTLA-4 blockade in low-dose chemotherapy-treated tumor-bearing mice. *Cancer Res* **58**, 5301-5304 (1998).

116 Hodi, F. S. *et al.* Improved survival with ipilimumab in patients with metastatic melanoma. *N Engl J Med* **363**, 711-723, doi:10.1056/NEJMoa1003466 (2010).

117 Callahan, M. K., Postow, M. A. & Wolchok, J. D. CTLA-4 and PD-1 Pathway Blockade: Combinations in the Clinic. *Front Oncol* **4**, 385, doi:10.3389/fonc.2014.00385 (2014).

118 Larkin, J. *et al.* Five-Year Survival with Combined Nivolumab and Ipilimumab in Advanced Melanoma. *N Engl J Med* **381**, 1535-1546, doi:10.1056/NEJMoa1910836 (2019).

119 Price, K. D., Simutis, F., Fletcher, A., Ramaiah,L., Srour,R., Kozlosky, J., Sathish, J., Engelhardt, J., Capozzi, A., Crona, J., Newsome, C., Wheeler, J., Szatkowski, D., Thekkumthala, A., Wang, B., Freebern, W., Haggerty,H., Bunch, T., and Graziano, M. Abstract LB-B33: Nonclinical safety evaluation of two distinct second generation variants of anti-CTLA4 monoclonal antibody, ipilimumab, in monkeys. *AACR-NCI-EORTC International Conference: Molecular Targets and Cancer Therapeutics* (2018).

120 Engelhardt, J., Akter, R., Loffredo, J., Bezman, N., So, P., Tipton, K., Irving, B., West, J., Freebern, W., Bunch, T., Price, K. in *AACR Annual Meeting 2020* (Philadelphia, PA, 2020).

121 Qin, W. *et al.* The Diverse Function of PD-1/PD-L Pathway Beyond Cancer. *Front Immunol* **10**, 2298, doi:10.3389/fimmu.2019.02298 (2019).

122 Mazanet, M. M. & Hughes, C. C. B7-H1 is expressed by human endothelial cells and suppresses T cell cytokine synthesis. *J Immunol* **169**, 3581-3588, doi:10.4049/jimmunol.169.7.3581 (2002).

123 Salmaninejad, A. *et al.* PD-1/PD-L1 pathway: Basic biology and role in cancer immunotherapy. *J Cell Physiol* **234**, 16824-16837, doi:10.1002/jcp.28358 (2019).

124 Topalian, S. L., Drake, C. G. & Pardoll, D. M. Targeting the PD-1/B7-H1(PD-L1) pathway to activate anti-tumor immunity. *Curr Opin Immunol* **24**, 207-212, doi:10.1016/j.coi.2011.12.009 (2012).

125 Wu, X. *et al.* Application of PD-1 Blockade in Cancer Immunotherapy. *Comput Struct Biotechnol J* **17**, 661-674, doi:10.1016/j.csbj.2019.03.006 (2019).

126 Weber, J. S. *et al.* Nivolumab versus chemotherapy in patients with advanced melanoma who progressed after anti-CTLA-4 treatment (CheckMate 037): a randomised, controlled, open-label, phase 3 trial. *Lancet Oncol* **16**, 375-384, doi:10.1016/S1470-2045(15)70076-8 (2015).

127 Robert, C. *et al.* Nivolumab in previously untreated melanoma without BRAF mutation. *N Engl J Med* **372**, 320-330, doi:10.1056/NEJMoa1412082 (2015).

128 Robert, C. *et al.* Anti-programmed-death-receptor-1 treatment with pembrolizumab in ipilimumab-refractory advanced melanoma: a randomised dose-comparison cohort of a phase 1 trial. *Lancet* **384**, 1109-1117, doi:10.1016/S0140-6736(14)60958-2 (2014).

129 Overman, M. J., Ernstoff, M. S. & Morse, M. A. Where We Stand With Immunotherapy in Colorectal Cancer: Deficient Mismatch Repair, Proficient Mismatch Repair, and Toxicity Management. *Am Soc Clin Oncol Educ Book* **38**, 239-247, doi:10.1200/EDBK_200821 (2018).

130 Hargadon, K. M., Johnson, C. E. & Williams, C. J. Immune checkpoint blockade therapy for cancer: An overview of FDA-approved immune checkpoint inhibitors. *Int Immunopharmacol* **62**, 29-39, doi:10.1016/j.intimp.2018.06.001 (2018).

131 Darvin, P., Toor, S. M., Sasidharan Nair, V. & Elkord, E. Immune checkpoint inhibitors: recent progress and potential biomarkers. *Exp Mol Med* **50**, 165, doi:10.1038/s12276-018-0191-1 (2018).

132 Triebel, F. *et al.* LAG-3, a novel lymphocyte activation gene closely related to CD4. *J Exp Med* **171**, 1393-1405, doi:10.1084/jem.171.5.1393 (1990).

133 Workman, C. J. & Vignali, D. A. The CD4-related molecule, LAG-3 (CD223), regulates the expansion of activated T cells. *Eur J Immunol* **33**, 970-979, doi:10.1002/eji.200323382 (2003).

134 Workman, C. J. & Vignali, D. A. Negative regulation of T cell homeostasis by lymphocyte activation gene-3 (CD223). *J Immunol* **174**, 688-695, doi:10.4049/jimmunol.174.2.688 (2005).

135 Woo, S. R. *et al.* Immune inhibitory molecules LAG-3 and PD-1 synergistically regulate T-cell function to promote tumoral immune escape. *Cancer Res* **72**, 917-927, doi:10.1158/0008-5472.CAN-11-1620 (2012).

136 Huang, C. T. *et al.* Role of LAG-3 in regulatory T cells. *Immunity* **21**, 503-513, doi:10.1016/j.immuni.2004.08.010 (2004).

137 Liang, B. *et al.* Regulatory T cells inhibit dendritic cells by lymphocyte activation gene-3 engagement of MHC class II. *J Immunol* **180**, 5916-5926, doi:10.4049/jimmunol.180.9.5916 (2008).

138 Andrews, L. P., Yano, H. & Vignali, D. A. A. Inhibitory receptors and ligands beyond PD-1, PD-L1 and CTLA-4: breakthroughs or backups. *Nat Immunol* **20**, 1425-1434, doi:10.1038/s41590-019-0512-0 (2019).

139 Smyth, M. J. & Teng, M. W. 2018 Nobel Prize in physiology or medicine. *Clin Transl Immunology* **7**, e1041, doi:10.1002/cti2.1041 (2018).

140 Redondo, M. J., Steck, A. K. & Pugliese, A. Genetics of type 1 diabetes. *Pediatr Diabetes* **19**, 346-353, doi:10.1111/pedi.12597 (2018).

141 Los, E. & Wilt, A. S. in *StatPearls* (2021).

142 Patterson, C. C. *et al.* Worldwide estimates of incidence, prevalence and mortality of type 1 diabetes in children and adolescents: Results from the International Diabetes Federation Diabetes Atlas, 9th edition. *Diabetes Res Clin Pract* **157**, 107842, doi:10.1016/j.diabres.2019.107842 (2019).

143 *Type 1 Diabetes Facts*, <https://www.jdrf.org/t1d-resources/about/facts/> (

144 American Diabetes, A. Economic Costs of Diabetes in the U.S. in 2017. *Diabetes Care* **41**, 917-928, doi:10.2337/dci18-0007 (2018).

145 Tao, B., Pietropaolo, M., Atkinson, M., Schatz, D. & Taylor, D. Estimating the cost of type 1 diabetes in the U.S.: a propensity score matching method. *PLoS One* **5**, e11501, doi:10.1371/journal.pone.0011501 (2010).

146 Simmons, K. M. & Michels, A. W. Type 1 diabetes: A predictable disease. *World J Diabetes* **6**, 380-390, doi:10.4239/wjd.v6.i3.380 (2015).

147 *National Diabetes Statistics Report* <https://www.cdc.gov/diabetes/pdfs/data/statistics/national-diabetes-statistics-report.pdf> (2020).

148 Dabelea, D. *et al.* Prevalence of type 1 and type 2 diabetes among children and adolescents from 2001 to 2009. *JAMA* **311**, 1778-1786, doi:10.1001/jama.2014.3201 (2014).

149 DiMeglio, L. A., Evans-Molina, C. & Oram, R. A. Type 1 diabetes. *Lancet* **391**, 2449-2462, doi:10.1016/S0140-6736(18)31320-5 (2018).

150 Rich, S. S. *et al.* The Type 1 Diabetes Genetics Consortium. *Ann N Y Acad Sci* **1079**, 1-8, doi:10.1196/annals.1375.001 (2006).

151 Noble, J. A. Immunogenetics of type 1 diabetes: A comprehensive review. *J Autoimmun* **64**, 101-112, doi:10.1016/j.jaut.2015.07.014 (2015).

152 Barrett, J. C. *et al.* Genome-wide association study and meta-analysis find that over 40 loci affect risk of type 1 diabetes. *Nat Genet* **41**, 703-707, doi:10.1038/ng.381 (2009).

153 Todd, J. A. *et al.* Robust associations of four new chromosome regions from genome-wide analyses of type 1 diabetes. *Nat Genet* **39**, 857-864, doi:10.1038/ng2068 (2007).

154 Atkinson, M. A. The pathogenesis and natural history of type 1 diabetes. *Cold Spring Harb Perspect Med* **2**, doi:10.1101/cshperspect.a007641 (2012).

155 Gamble, D. R., Kinsley, M. L., FitzGerald, M. G., Bolton, R. & Taylor, K. W. Viral antibodies in diabetes mellitus. *Br Med J* **3**, 627-630, doi:10.1136/bmj.3.5671.627 (1969).

156 Yoon, J. W., Austin, M., Onodera, T. & Notkins, A. L. Isolation of a virus from the pancreas of a child with diabetic ketoacidosis. *N Engl J Med* **300**, 1173-1179, doi:10.1056/NEJM197905243002102 (1979).

157 Hober, D. & Sane, F. Enteroviral pathogenesis of type 1 diabetes. *Discov Med* **10**, 151-160 (2010).

158 Andreoletti, L. *et al.* Detection of coxsackie B virus RNA sequences in whole blood samples from adult patients at the onset of type I diabetes mellitus. *J Med Virol* **52**, 121-127, doi:10.1002/(sici)1096-9071(199706)52:2<121::aid-jmv1>3.0.co;2-5 (1997).

159 Chehadeh, W. *et al.* Increased level of interferon-alpha in blood of patients with insulin-dependent diabetes mellitus: relationship with coxsackievirus B infection. *J Infect Dis* **181**, 1929-1939, doi:10.1086/315516 (2000).

160 Huang, X. *et al.* Interferon expression in the pancreases of patients with type I diabetes. *Diabetes* **44**, 658-664, doi:10.2337/diab.44.6.658 (1995).

161 Foulis, A. K., Farquharson, M. A. & Meager, A. Immunoreactive alpha-interferon in insulin-secreting beta cells in type 1 diabetes mellitus. *Lancet* **2**, 1423-1427, doi:10.1016/s0140-6736(87)91128-7 (1987).

162 Li, Q. & McDevitt, H. O. The role of interferon alpha in initiation of type I diabetes in the NOD mouse. *Clin Immunol* **140**, 3-7, doi:10.1016/j.clim.2011.04.010 (2011).

163 Ferreira, R. C. *et al.* A type I interferon transcriptional signature precedes autoimmunity in children genetically at risk for type 1 diabetes. *Diabetes* **63**, 2538-2550, doi:10.2337/db13-1777 (2014).

164 Fabris, P. *et al.* Development of type 1 diabetes mellitus during interferon alfa therapy for chronic HCV hepatitis. *Lancet* **340**, 548, doi:10.1016/0140-6736(92)91744-s (1992).

165 Hao, W. *Early Diagnosis and Intervention for Type 1 Diabetes (T1D) -Progress from T1D TrialNet*,

<https://professional.diabetes.org/sites/professional.diabetes.org/files/media/hao_wa2016.pdf> (2016).

166 Shapiro, A. M. *et al.* International trial of the Edmonton protocol for islet transplantation. *N Engl J Med* **355**, 1318-1330, doi:10.1056/NEJMoa061267 (2006).

167 Esmeijer, K. *et al.* Superior Long-term Survival for Simultaneous Pancreas-Kidney Transplantation as Renal Replacement Therapy: 30-Year Follow-up of a Nationwide Cohort. *Diabetes Care* **43**, 321-328, doi:10.2337/dc19-1580 (2020).

168 Anderson, M. S. & Bluestone, J. A. The NOD mouse: a model of immune dysregulation. *Annu Rev Immunol* **23**, 447-485, doi:10.1146/annurev.immunol.23.021704.115643 (2005).

169 Feuerer, M., Shen, Y., Littman, D. R., Benoist, C. & Mathis, D. How punctual ablation of regulatory T cells unleashes an autoimmune lesion within the pancreatic islets. *Immunity* **31**, 654-664, doi:10.1016/j.immuni.2009.08.023 (2009).

170 Vandenbark, A. A. & Offner, H. Critical evaluation of regulatory T cells in autoimmunity: are the most potent regulatory specificities being ignored? *Immunology* **125**, 1-13, doi:10.1111/j.1365-2567.2008.02900.x (2008).

171 Lindley, S. *et al.* Defective suppressor function in CD4(+)CD25(+) T-cells from patients with type 1 diabetes. *Diabetes* **54**, 92-99, doi:10.2337/diabetes.54.1.92 (2005).

172 Hull, C. M., Peakman, M. & Tree, T. I. M. Regulatory T cell dysfunction in type 1 diabetes: what's broken and how can we fix it? *Diabetologia* **60**, 1839-1850, doi:10.1007/s00125-017-4377-1 (2017).

173 Pugliese, A. Insulitis in the pathogenesis of type 1 diabetes. *Pediatr Diabetes* **17 Suppl 22**, 31-36, doi:10.1111/pedi.12388 (2016).

174 Coppieters, K. T. *et al.* Demonstration of islet-autoreactive CD8 T cells in insulitic lesions from recent onset and long-term type 1 diabetes patients. *J Exp Med* **209**, 51-60, doi:10.1084/jem.20111187 (2012).

175 Willcox, A., Richardson, S. J., Bone, A. J., Foulis, A. K. & Morgan, N. G. Analysis of islet inflammation in human type 1 diabetes. *Clin Exp Immunol* **155**, 173-181, doi:10.1111/j.1365-2249.2008.03860.x (2009).

176 Shimizu, J., Kanagawa, O. & Unanue, E. R. Presentation of beta-cell antigens to CD4+ and CD8+ T cells of non-obese diabetic mice. *J Immunol* **151**, 1723-1730 (1993).

177 Wang, B., Gonzalez, A., Benoist, C. & Mathis, D. The role of CD8+ T cells in the initiation of insulin-dependent diabetes mellitus. *Eur J Immunol* **26**, 1762-1769, doi:10.1002/eji.1830260815 (1996).

178 Katz, J., Benoist, C. & Mathis, D. Major histocompatibility complex class I molecules are required for the development of insulitis in non-obese diabetic mice. *Eur J Immunol* **23**, 3358-3360, doi:10.1002/eji.1830231244 (1993).

179 Serreze, D. V., Leiter, E. H., Christianson, G. J., Greiner, D. & Roopenian, D. C. Major histocompatibility complex class I-deficient NOD-B2mnull mice are diabetes and insulitis resistant. *Diabetes* **43**, 505-509, doi:10.2337/diab.43.3.505 (1994).

180 Serreze, D. V. *et al.* Initiation of autoimmune diabetes in NOD/Lt mice is MHC class I-dependent. *J Immunol* **158**, 3978-3986 (1997).

181 DiLorenzo, T. P. *et al.* Major histocompatibility complex class I-restricted T cells are required for all but the end stages of diabetes development in nonobese diabetic mice and use a prevalent T cell receptor alpha chain gene rearrangement. *Proc Natl Acad Sci U S A* **95**, 12538-12543, doi:10.1073/pnas.95.21.12538 (1998).

182 Nagata, M., Santamaria, P., Kawamura, T., Utsugi, T. & Yoon, J. W. Evidence for the role of CD8+ cytotoxic T cells in the destruction of pancreatic beta-cells in nonobese diabetic mice. *J Immunol* **152**, 2042-2050 (1994).

183 Trivedi, P. *et al.* Perforin facilitates beta cell killing and regulates autoreactive CD8+ T-cell responses to antigen in mouse models of type 1 diabetes. *Immunol Cell Biol* **94**, 334-341, doi:10.1038/icb.2015.89 (2016).

184 Kagi, D. *et al.* Cytotoxicity mediated by T cells and natural killer cells is greatly impaired in perforin-deficient mice. *Nature* **369**, 31-37, doi:10.1038/369031a0 (1994).

185 Kagi, D. *et al.* Reduced incidence and delayed onset of diabetes in perforin-deficient nonobese diabetic mice. *J Exp Med* **186**, 989-997, doi:10.1084/jem.186.7.989 (1997).

186 Thomas, H. E., Trapani, J. A. & Kay, T. W. The role of perforin and granzymes in diabetes. *Cell Death Differ* **17**, 577-585, doi:10.1038/cdd.2009.165 (2010).

187 Amrani, A. *et al.* Perforin-independent beta-cell destruction by diabetogenic CD8(+) T lymphocytes in transgenic nonobese diabetic mice. *J Clin Invest* **103**, 1201-1209, doi:10.1172/JCI6266 (1999).

188 Tsompana, M. & Buck, M. J. Chromatin accessibility: a window into the genome. *Epigenetics Chromatin* **7**, 33, doi:10.1186/1756-8935-7-33 (2014).

189 Weinhold, B. Epigenetics: the science of change. *Environ Health Perspect* **114**, A160-167, doi:10.1289/ehp.114-a160 (2006).

190 Hamilton, J. P. Epigenetics: principles and practice. *Dig Dis* **29**, 130-135, doi:10.1159/000323874 (2011).

191 Frenkel, D. A new TRAIL in Alzheimer's disease therapy. *Brain* **138**, 8-10, doi:10.1093/brain/awu334 (2015).

192 Thorburn, A. Tumor necrosis factor-related apoptosis-inducing ligand (TRAIL) pathway signaling. *J Thorac Oncol* **2**, 461-465, doi:10.1097/JTO.0b013e31805fea64 (2007).

193 Dubuisson, A. & Micheau, O. Antibodies and Derivatives Targeting DR4 and DR5 for Cancer Therapy. *Antibodies (Basel)* **6**, doi:10.3390/antib6040016 (2017).

194 Wiley, S. R. *et al.* Identification and characterization of a new member of the TNF family that induces apoptosis. *Immunity* **3**, 673-682, doi:10.1016/1074-7613(95)90057-8 (1995).

195 Pitti, R. M. *et al.* Induction of apoptosis by Apo-2 ligand, a new member of the tumor necrosis factor cytokine family. *J Biol Chem* **271**, 12687-12690, doi:10.1074/jbc.271.22.12687 (1996).

196 Schneider, P. *et al.* Characterization of two receptors for TRAIL. *FEBS Lett* **416**, 329-334, doi:10.1016/s0014-5793(97)01231-3 (1997).

197 Naval, J., de Miguel, D., Gallego-Lleyda, A., Anel, A. & Martinez-Lostao, L. Importance of TRAIL Molecular Anatomy in Receptor Oligomerization and

Signaling. Implications for Cancer Therapy. *Cancers (Basel)* **11**, doi:10.3390/cancers11040444 (2019).

198 Wang, S. & El-Deiry, W. S. TRAIL and apoptosis induction by TNF-family death receptors. *Oncogene* **22**, 8628-8633, doi:10.1038/sj.onc.1207232 (2003).

199 Cohen, G. M. Caspases: the executioners of apoptosis. *Biochem J* **326 (Pt 1)**, 1-16, doi:10.1042/bj3260001 (1997).

200 Pan, G. *et al.* The receptor for the cytotoxic ligand TRAIL. *Science* **276**, 111-113, doi:10.1126/science.276.5309.111 (1997).

201 Yasukochi, A., Kawakubo, T., Nakamura, S. & Yamamoto, K. Cathepsin E enhances anticancer activity of doxorubicin on human prostate cancer cells showing resistance to TRAIL-mediated apoptosis. *Biol Chem* **391**, 947-958, doi:10.1515/BC.2010.087 (2010).

202 Kawakubo, T. *et al.* Cathepsin E prevents tumor growth and metastasis by catalyzing the proteolytic release of soluble TRAIL from tumor cell surface. *Cancer Res* **67**, 10869-10878, doi:10.1158/0008-5472.CAN-07-2048 (2007).

203 Kayagaki, N. *et al.* Involvement of TNF-related apoptosis-inducing ligand in human CD4+ T cell-mediated cytotoxicity. *J Immunol* **162**, 2639-2647 (1999).

204 Jeremias, I., Herr, I., Boehler, T. & Debatin, K. M. TRAIL/Apo-2-ligand-induced apoptosis in human T cells. *Eur J Immunol* **28**, 143-152, doi:10.1002/(SICI)1521-4141(199801)28:01<143::AID-IMMU143>3.0.CO;2-3 (1998).

205 Falschlehner, C., Schaefer, U. & Walczak, H. Following TRAIL's path in the immune system. *Immunology* **127**, 145-154, doi:10.1111/j.1365-2567.2009.03058.x (2009).

206 Kayagaki, N. *et al.* Expression and function of TNF-related apoptosis-inducing ligand on murine activated NK cells. *J Immunol* **163**, 1906-1913 (1999).

207 Takeda, K. *et al.* Involvement of tumor necrosis factor-related apoptosis-inducing ligand in surveillance of tumor metastasis by liver natural killer cells. *Nat Med* **7**, 94-100, doi:10.1038/83416 (2001).

208 Kayagaki, N. *et al.* Type I interferons (IFNs) regulate tumor necrosis factor-related apoptosis-inducing ligand (TRAIL) expression on human T cells: A novel mechanism for the antitumor effects of type I IFNs. *J Exp Med* **189**, 1451-1460, doi:10.1084/jem.189.9.1451 (1999).

209 Ehrlich, S., Infante-Duarte, C., Seeger, B. & Zipp, F. Regulation of soluble and surface-bound TRAIL in human T cells, B cells, and monocytes. *Cytokine* **24**, 244-253, doi:10.1016/s1043-4666(03)00094-2 (2003).

210 Halaas, O., Vik, R., Ashkenazi, A. & Espevik, T. Lipopolysaccharide induces expression of APO2 ligand/TRAIL in human monocytes and macrophages. *Scand J Immunol* **51**, 244-250, doi:10.1046/j.1365-3083.2000.00671.x (2000).

211 Fanger, N. A., Maliszewski, C. R., Schooley, K. & Griffith, T. S. Human dendritic cells mediate cellular apoptosis via tumor necrosis factor-related apoptosis-inducing ligand (TRAIL). *J Exp Med* **190**, 1155-1164, doi:10.1084/jem.190.8.1155 (1999).

212 Griffith, T. S. *et al.* Monocyte-mediated tumoricidal activity via the tumor necrosis factor-related cytokine, TRAIL. *J Exp Med* **189**, 1343-1354, doi:10.1084/jem.189.8.1343 (1999).

213 Gura, T. How TRAIL kills cancer cells, but not normal cells. *Science* **277**, 768, doi:10.1126/science.277.5327.768 (1997).

214 Nesterov, A., Nikrad, M., Johnson, T. & Kraft, A. S. Oncogenic Ras sensitizes normal human cells to tumor necrosis factor-alpha-related apoptosis-inducing ligand-induced apoptosis. *Cancer Res* **64**, 3922-3927, doi:10.1158/0008-5472.CAN-03-2219 (2004).

215 Wang, Y., Quon, K. C., Knee, D. A., Nesterov, A. & Kraft, A. S. RAS, MYC, and sensitivity to tumor necrosis factor-alpha-related apoptosis-inducing ligand-induced apoptosis. *Cancer Res* **65**, 1615-1616; author reply 1616-1617, doi:10.1158/0008-5472.CAN-04-2757 (2005).

216 Sedger, L. M. *et al.* Characterization of the in vivo function of TNF-alpha-related apoptosis-inducing ligand, TRAIL/Apo2L, using TRAIL/Apo2L gene-deficient mice. *Eur J Immunol* **32**, 2246-2254, doi:10.1002/1521-4141(200208)32:8<2246::AID-IMMU2246>3.0.CO;2-6 (2002).

217 Zerafa, N. *et al.* Cutting edge: TRAIL deficiency accelerates hematological malignancies. *J Immunol* **175**, 5586-5590, doi:10.4049/jimmunol.175.9.5586 (2005).

218 Finnberg, N., Klein-Szanto, A. J. & El-Deiry, W. S. TRAIL-R deficiency in mice promotes susceptibility to chronic inflammation and tumorigenesis. *J Clin Invest* **118**, 111-123, doi:10.1172/JCI29900 (2008).

219 Grosse-Wilde, A. *et al.* TRAIL-R deficiency in mice enhances lymph node metastasis without affecting primary tumor development. *J Clin Invest* **118**, 100-110, doi:10.1172/JCI33061 (2008).

220 Rossin, A., Miloro, G. & Hueber, A. O. TRAIL and FasL Functions in Cancer and Autoimmune Diseases: Towards an Increasing Complexity. *Cancers (Basel)* **11**, doi:10.3390/cancers11050639 (2019).

221 Smyth, M. J. *et al.* Tumor necrosis factor-related apoptosis-inducing ligand (TRAIL) contributes to interferon gamma-dependent natural killer cell protection from tumor metastasis. *J Exp Med* **193**, 661-670, doi:10.1084/jem.193.6.661 (2001).

222 Sag, D., Ayyildiz, Z. O., Gunalp, S. & Wingender, G. The Role of TRAIL/DRs in the Modulation of Immune Cells and Responses. *Cancers (Basel)* **11**, doi:10.3390/cancers11101469 (2019).

223 Rubtsov, Y. P. *et al.* Regulatory T cell-derived interleukin-10 limits inflammation at environmental interfaces. *Immunity* **28**, 546-558, doi:10.1016/j.immuni.2008.02.017 (2008).

224 Zhou, X. *et al.* Selective miRNA disruption in T reg cells leads to uncontrolled autoimmunity. *J Exp Med* **205**, 1983-1991, doi:10.1084/jem.20080707 (2008).

225 Liu, P., Jenkins, N. A. & Copeland, N. G. A highly efficient recombineering-based method for generating conditional knockout mutations. *Genome Res* **13**, 476-484, doi:10.1101/gr.749203 (2003).

226 Zhang, Q. *et al.* LAG3 limits regulatory T cell proliferation and function in autoimmune diabetes. *Sci Immunol* **2**, doi:10.1126/sciimmunol.aah4569 (2017).

227 Bettini, M. *et al.* Cutting edge: accelerated autoimmune diabetes in the absence of LAG-3. *J Immunol* **187**, 3493-3498, doi:10.4049/jimmunol.1100714 (2011).

228 Leiter, E. H., Prochazka, M. & Coleman, D. L. The non-obese diabetic (NOD) mouse. *Am J Pathol* **128**, 380-383 (1987).

229 Leiter, E. H. The NOD mouse: a model for insulin-dependent diabetes mellitus. *Curr Protoc Immunol* **Chapter 15**, Unit 15 19, doi:10.1002/0471142735.im1509s24 (2001).

230 Lennon, G. P. *et al.* T cell islet accumulation in type 1 diabetes is a tightly regulated, cell-autonomous event. *Immunity* **31**, 643-653, doi:10.1016/j.immuni.2009.07.008 (2009).

231 Workman, C. J. *et al.* In vivo Treg suppression assays. *Methods Mol Biol* **707**, 119-156, doi:10.1007/978-1-61737-979-6_9 (2011).

232 Do, J. *et al.* Treg-specific IL-27Ralpha deletion uncovers a key role for IL-27 in Treg function to control autoimmunity. *Proc Natl Acad Sci U S A* **114**, 10190-10195, doi:10.1073/pnas.1703100114 (2017).

233 Baird, J. R. *et al.* Immune-mediated regression of established B16F10 melanoma by intratumoral injection of attenuated Toxoplasma gondii protects against rechallenge. *J Immunol* **190**, 469-478, doi:10.4049/jimmunol.1201209 (2013).

234 Wei, S. C. *et al.* Distinct Cellular Mechanisms Underlie Anti-CTLA-4 and Anti-PD-1 Checkpoint Blockade. *Cell* **170**, 1120-1133 e1117, doi:10.1016/j.cell.2017.07.024 (2017).

235 Binder, R. J. CD40-independent engagement of mammalian hsp70 by antigen-presenting cells. *J Immunol* **182**, 6844-6850, doi:10.4049/jimmunol.0900026 (2009).

236 Liu, C. *et al.* Treg Cells Promote the SREBP1-Dependent Metabolic Fitness of Tumor-Promoting Macrophages via Repression of CD8(+) T Cell-Derived

Interferon-gamma. *Immunity* **51**, 381-397 e386, doi:10.1016/j.immuni.2019.06.017 (2019).

237 Andrews, S. FastQC: a quality control tool for high throughput sequence data. *Babraham Bioinformatics* (2013).

238 Anders, S., Pyl, P. T. & Huber, W. HTSeq--a Python framework to work with high-throughput sequencing data. *Bioinformatics* **31**, 166-169, doi:10.1093/bioinformatics/btu638 (2015).

239 Love, M. I., Huber, W. & Anders, S. Moderated estimation of fold change and dispersion for RNA-seq data with DESeq2. *Genome Biol* **15**, 550, doi:10.1186/s13059-014-0550-8 (2014).

240 Team, R. C. R: A Language and Environment for Statistical Computing. (2019).

241 Subramanian, A. *et al.* Gene set enrichment analysis: a knowledge-based approach for interpreting genome-wide expression profiles. *Proc Natl Acad Sci U S A* **102**, 15545-15550, doi:10.1073/pnas.0506580102 (2005).

242 Collison, L. W. & Vignali, D. A. In vitro Treg suppression assays. *Methods Mol Biol* **707**, 21-37, doi:10.1007/978-1-61737-979-6_2 (2011).

243 Teh, P. P., Vasanthakumar, A. & Kallies, A. Development and Function of Effector Regulatory T Cells. *Prog Mol Biol Transl Sci* **136**, 155-174, doi:10.1016/bs.pmbts.2015.08.005 (2015).

244 Dias, S. *et al.* Effector Regulatory T Cell Differentiation and Immune Homeostasis Depend on the Transcription Factor Myb. *Immunity* **46**, 78-91, doi:10.1016/j.immuni.2016.12.017 (2017).

245 Chao, J. L. & Savage, P. A. Unlocking the Complexities of Tumor-Associated Regulatory T Cells. *J Immunol* **200**, 415-421, doi:10.4049/jimmunol.1701188 (2018).

246 Sasada, T., Kimura, M., Yoshida, Y., Kanai, M. & Takabayashi, A. CD4+CD25+ regulatory T cells in patients with gastrointestinal malignancies: possible involvement of regulatory T cells in disease progression. *Cancer* **98**, 1089-1099, doi:10.1002/cncr.11618 (2003).

247 Curiel, T. J. *et al.* Specific recruitment of regulatory T cells in ovarian carcinoma fosters immune privilege and predicts reduced survival. *Nat Med* **10**, 942-949, doi:10.1038/nm1093 (2004).

248 Sato, E. *et al.* Intraepithelial CD8+ tumor-infiltrating lymphocytes and a high CD8+/regulatory T cell ratio are associated with favorable prognosis in ovarian cancer. *Proc Natl Acad Sci U S A* **102**, 18538-18543, doi:10.1073/pnas.0509182102 (2005).

249 Bates, G. J. *et al.* Quantification of regulatory T cells enables the identification of high-risk breast cancer patients and those at risk of late relapse. *J Clin Oncol* **24**, 5373-5380, doi:10.1200/JCO.2006.05.9584 (2006).

250 Deng, G. Tumor-infiltrating regulatory T cells: origins and features. *Am J Clin Exp Immunol* **7**, 81-87 (2018).

251 Watson, M. J. *et al.* Metabolic support of tumour-infiltrating regulatory T cells by lactic acid. *Nature* **591**, 645-651, doi:10.1038/s41586-020-03045-2 (2021).

252 Arvey, A. *et al.* Inflammation-induced repression of chromatin bound by the transcription factor Foxp3 in regulatory T cells. *Nat Immunol* **15**, 580-587, doi:10.1038/ni.2868 (2014).

253 Klemm, S. L., Shipony, Z. & Greenleaf, W. J. Chromatin accessibility and the regulatory epigenome. *Nat Rev Genet* **20**, 207-220, doi:10.1038/s41576-018-0089-8 (2019).

254 Klein, D. C. & Hainer, S. J. Genomic methods in profiling DNA accessibility and factor localization. *Chromosome Res* **28**, 69-85, doi:10.1007/s10577-019-09619-9 (2020).

255 Bediaga, N. G. *et al.* Multi-level remodelling of chromatin underlying activation of human T cells. *Sci Rep* **11**, 528, doi:10.1038/s41598-020-80165-9 (2021).

256 Calderon, D. *et al.* Landscape of stimulation-responsive chromatin across diverse human immune cells. *Nat Genet* **51**, 1494-1505, doi:10.1038/s41588-019-0505-9 (2019).

257 Kong, X. *et al.* Dynamic chromatin accessibility profiling reveals changes in host genome organization in response to baculovirus infection. *PLoS Pathog* **16**, e1008633, doi:10.1371/journal.ppat.1008633 (2020).

258 Buenrostro, J. D., Wu, B., Chang, H. Y. & Greenleaf, W. J. ATAC-seq: A Method for Assaying Chromatin Accessibility Genome-Wide. *Curr Protoc Mol Biol* **109**, 21 29 21-21 29 29, doi:10.1002/0471142727.mb2129s109 (2015).

259 Ou, J. *et al.* ATACseqQC: a Bioconductor package for post-alignment quality assessment of ATAC-seq data. *BMC Genomics* **19**, 169, doi:10.1186/s12864-018-4559-3 (2018).

260 van der Veeken, J. *et al.* Memory of Inflammation in Regulatory T Cells. *Cell* **166**, 977-990, doi:10.1016/j.cell.2016.07.006 (2016).

261 Pacella, I. *et al.* Fatty acid metabolism complements glycolysis in the selective regulatory T cell expansion during tumor growth. *Proc Natl Acad Sci U S A* **115**, E6546-E6555, doi:10.1073/pnas.1720113115 (2018).

262 Smith, P. M. *et al.* The microbial metabolites, short-chain fatty acids, regulate colonic Treg cell homeostasis. *Science* **341**, 569-573, doi:10.1126/science.1241165 (2013).

263 Sinclair, L. V. *et al.* Control of amino-acid transport by antigen receptors coordinates the metabolic reprogramming essential for T cell differentiation. *Nat Immunol* **14**, 500-508, doi:10.1038/ni.2556 (2013).

264 Beyer, M. *et al.* Repression of the genome organizer SATB1 in regulatory T cells is required for suppressive function and inhibition of effector differentiation. *Nat Immunol* **12**, 898-907, doi:10.1038/ni.2084 (2011).

265 McInnes, N. *et al.* FOXP3 and FOXP3-regulated microRNAs suppress SATB1 in breast cancer cells. *Oncogene* **31**, 1045-1054, doi:10.1038/onc.2011.293 (2012).

266 Ortega-Francisco, S. *et al.* TbetaRIII is induced by TCR signaling and downregulated in FoxP3(+) regulatory T cells. *Biochem Biophys Res Commun* **494**, 82-87, doi:10.1016/j.bbrc.2017.10.081 (2017).

267 Overacre-Delgoffe, A. E. & Vignali, D. A. A. Treg Fragility: A Prerequisite for Effective Antitumor Immunity? *Cancer Immunol Res* **6**, 882-887, doi:10.1158/2326-6066.CIR-18-0066 (2018).

268 Yoshida, K. *et al.* Anti-PD-1 antibody decreases tumour-infiltrating regulatory T cells. *BMC Cancer* **20**, 25, doi:10.1186/s12885-019-6499-y (2020).

269 Baecher-Allan, C., Brown, J. A., Freeman, G. J. & Hafler, D. A. CD4+CD25+ regulatory cells from human peripheral blood express very high levels of CD25 ex vivo. *Novartis Found Symp* **252**, 67-88; discussion 88-91, 106-114, doi:10.1002/0470871628.ch6 (2003).

270 Krupnick, A. S. *et al.* Murine vascular endothelium activates and induces the generation of allogeneic CD4+25+Foxp3+ regulatory T cells. *J Immunol* **175**, 6265-6270, doi:10.4049/jimmunol.175.10.6265 (2005).

271 Wang, L. *et al.* Programmed death 1 ligand signaling regulates the generation of adaptive Foxp3+CD4+ regulatory T cells. *Proc Natl Acad Sci U S A* **105**, 9331-9336, doi:10.1073/pnas.0710441105 (2008).

272 Francisco, L. M. *et al.* PD-L1 regulates the development, maintenance, and function of induced regulatory T cells. *J Exp Med* **206**, 3015-3029, doi:10.1084/jem.20090847 (2009).

273 Zhang, B., Chikuma, S., Hori, S., Fagarasan, S. & Honjo, T. Nonoverlapping roles of PD-1 and FoxP3 in maintaining immune tolerance in a novel autoimmune pancreatitis mouse model. *Proc Natl Acad Sci U S A* **113**, 8490-8495, doi:10.1073/pnas.1608873113 (2016).

274 Stathopoulou, C. *et al.* PD-1 Inhibitory Receptor Downregulates Asparaginyl Endopeptidase and Maintains Foxp3 Transcription Factor Stability in Induced Regulatory T Cells. *Immunity* **49**, 247-263 e247, doi:10.1016/j.immuni.2018.05.006 (2018).

275 Park, H. J. *et al.* PD-1 upregulated on regulatory T cells during chronic virus infection enhances the suppression of CD8+ T cell immune response via the interaction with PD-L1 expressed on CD8+ T cells. *J Immunol* **194**, 5801-5811, doi:10.4049/jimmunol.1401936 (2015).

276 Park, H. J. *et al.* Correction: PD-1 Upregulated on Regulatory T Cells during Chronic Virus Infection Enhances the Suppression of CD8+ T Cell Immune Response via the Interaction with PD-L1 Expressed on CD8+ T Cells. *J Immunol* **195**, 5841-5842, doi:10.4049/jimmunol.1502256 (2015).

277 Kamada, T. *et al.* PD-1(+) regulatory T cells amplified by PD-1 blockade promote hyperprogression of cancer. *Proc Natl Acad Sci U S A* **116**, 9999-10008, doi:10.1073/pnas.1822001116 (2019).

278 Garris, C. S. *et al.* Successful Anti-PD-1 Cancer Immunotherapy Requires T Cell-Dendritic Cell Crosstalk Involving the Cytokines IFN-gamma and IL-12. *Immunity* **49**, 1148-1161 e1147, doi:10.1016/j.immuni.2018.09.024 (2018).

279 Koutrolos, M., Berer, K., Kawakami, N., Wekerle, H. & Krishnamoorthy, G. Treg cells mediate recovery from EAE by controlling effector T cell proliferation and motility in the CNS. *Acta Neuropathol Commun* **2**, 163, doi:10.1186/s40478-014-0163-1 (2014).

280 Pillai, M. R. *et al.* The plasticity of regulatory T cell function. *J Immunol* **187**, 4987-4997, doi:10.4049/jimmunol.1102173 (2011).

281 Ren, X. *et al.* Involvement of cellular death in TRAIL/DR5-dependent suppression induced by CD4(+)CD25(+) regulatory T cells. *Cell Death Differ* **14**, 2076-2084, doi:10.1038/sj.cdd.4402220 (2007).

282 Mariani, S. M. & Krammer, P. H. Surface expression of TRAIL/Apo-2 ligand in activated mouse T and B cells. *Eur J Immunol* **28**, 1492-1498, doi:10.1002/(SICI)1521-4141(199805)28:05<1492::AID-IMMU1492>3.0.CO;2-X (1998).

283 Haynes, N. M. *et al.* CD11c+ dendritic cells and B cells contribute to the tumoricidal activity of anti-DR5 antibody therapy in established tumors. *J Immunol* **185**, 532-541, doi:10.4049/jimmunol.0903624 (2010).

284 Chyuan, I. T., Tsai, H. F., Wu, C. S., Sung, C. C. & Hsu, P. N. TRAIL-Mediated Suppression of T Cell Receptor Signaling Inhibits T Cell Activation and Inflammation in Experimental Autoimmune Encephalomyelitis. *Front Immunol* **9**, 15, doi:10.3389/fimmu.2018.00015 (2018).

285 Lehnert, C. *et al.* TRAIL-receptor costimulation inhibits proximal TCR signaling and suppresses human T cell activation and proliferation. *J Immunol* **193**, 4021-4031, doi:10.4049/jimmunol.1303242 (2014).

286 Chyuan, I. T., Tsai, H. F., Wu, C. S. & Hsu, P. N. TRAIL suppresses gut inflammation and inhibits colitogeic T-cell activation in experimental colitis via an apoptosis-independent pathway. *Mucosal Immunol* **12**, 980-989, doi:10.1038/s41385-019-0168-y (2019).

287 Lunemann, J. D. *et al.* Death ligand TRAIL induces no apoptosis but inhibits activation of human (auto)antigen-specific T cells. *J Immunol* **168**, 4881-4888, doi:10.4049/jimmunol.168.10.4881 (2002).

288 Diao, Z. *et al.* TRAIL suppresses tumor growth in mice by inducing tumor-infiltrating CD4(+)CD25 (+) Treg apoptosis. *Cancer Immunol Immunother* **62**, 653-663, doi:10.1007/s00262-012-1370-x (2013).

289 Zhang, X. R. *et al.* Reciprocal expression of TRAIL and CD95L in Th1 and Th2 cells: role of apoptosis in T helper subset differentiation. *Cell Death Differ* **10**, 203-210, doi:10.1038/sj.cdd.4401138 (2003).

290 Ikeda, T. *et al.* Dual effects of TRAIL in suppression of autoimmunity: the inhibition of Th1 cells and the promotion of regulatory T cells. *J Immunol* **185**, 5259-5267, doi:10.4049/jimmunol.0902797 (2010).

291 Janssen, E. M. *et al.* CD4+ T-cell help controls CD8+ T-cell memory via TRAIL-mediated activation-induced cell death. *Nature* **434**, 88-93, doi:10.1038/nature03337 (2005).

292 Bossi, F., Bernardi, S., Zauli, G., Secchiero, P. & Fabris, B. TRAIL modulates the immune system and protects against the development of diabetes. *J Immunol Res* **2015**, 680749, doi:10.1155/2015/680749 (2015).

293 Liu, Z., Kim, J. H., Falo, L. D., Jr. & You, Z. Tumor regulatory T cells potently abrogate antitumor immunity. *J Immunol* **182**, 6160-6167, doi:10.4049/jimmunol.0802664 (2009).

294 Magnuson, A. M. *et al.* Identification and validation of a tumor-infiltrating Treg transcriptional signature conserved across species and tumor types. *Proc Natl Acad Sci U S A* **115**, E10672-E10681, doi:10.1073/pnas.1810580115 (2018).

295 Mi, Q. S. *et al.* Blockade of tumor necrosis factor-related apoptosis-inducing ligand exacerbates type 1 diabetes in NOD mice. *Diabetes* **52**, 1967-1975, doi:10.2337/diabetes.52.8.1967 (2003).

296 Ou, D. *et al.* TNF-related apoptosis-inducing ligand death pathway-mediated human beta-cell destruction. *Diabetologia* **45**, 1678-1688, doi:10.1007/s00125-002-0926-2 (2002).

297 Ishizuka, N. *et al.* Tumor necrosis factor alpha signaling pathway and apoptosis in pancreatic beta cells. *Metabolism* **48**, 1485-1492, doi:10.1016/s0026-0495(99)90234-2 (1999).

298 Knight, R. R. *et al.* Human beta-cell killing by autoreactive preproinsulin-specific CD8 T cells is predominantly granule-mediated with the potency dependent upon T-cell receptor avidity. *Diabetes* **62**, 205-213, doi:10.2337/db12-0315 (2013).

299 Kang, S., Park, S. Y., Lee, H. J. & Yoo, Y. H. TRAIL upregulates decoy receptor 1 and mediates resistance to apoptosis in insulin-secreting INS-1 cells. *Biochem Biophys Res Commun* **396**, 731-735, doi:10.1016/j.bbrc.2010.05.004 (2010).

300 Dirice, E. *et al.* TRAIL and DcR1 expressions are differentially regulated in the pancreatic islets of STZ- versus CY-applied NOD mice. *Exp Diabetes Res* **2011**, 625813, doi:10.1155/2011/625813 (2011).

301 Iyori, M., Zhang, T., Pantel, H., Gagne, B. A. & Sentman, C. L. TRAIL/DR5 plays a critical role in NK cell-mediated negative regulation of dendritic cell cross-priming of T cells. *J Immunol* **187**, 3087-3095, doi:10.4049/jimmunol.1003879 (2011).

302 Hilliard, B. *et al.* Roles of TNF-related apoptosis-inducing ligand in experimental autoimmune encephalomyelitis. *J Immunol* **166**, 1314-1319, doi:10.4049/jimmunol.166.2.1314 (2001).

303 Lamhamedi-Cherradi, S. E., Zheng, S., Tisch, R. M. & Chen, Y. H. Critical roles of tumor necrosis factor-related apoptosis-inducing ligand in type 1 diabetes. *Diabetes* **52**, 2274-2278, doi:10.2337/diabetes.52.9.2274 (2003).

304 Zauli, G. *et al.* Treatment with recombinant tumor necrosis factor-related apoptosis-inducing ligand alleviates the severity of streptozotocin-induced diabetes. *Diabetes* **59**, 1261-1265, doi:10.2337/db09-1771 (2010).

305 Atkinson, M. A., Eisenbarth, G. S. & Michels, A. W. Type 1 diabetes. *Lancet* **383**, 69-82, doi:10.1016/S0140-6736(13)60591-7 (2014).

306 Rojas, J. *et al.* Pancreatic Beta Cell Death: Novel Potential Mechanisms in Diabetes Therapy. *J Diabetes Res* **2018**, 9601801, doi:10.1155/2018/9601801 (2018).

307 Porter, A. G. & Janicke, R. U. Emerging roles of caspase-3 in apoptosis. *Cell Death Differ* **6**, 99-104, doi:10.1038/sj.cdd.4400476 (1999).

308 Shepard, B. D. & Badley, A. D. The Biology of TRAIL and the Role of TRAIL-Based Therapeutics in Infectious Diseases. *Antiinfect Agents Med Chem* **8**, 87-101, doi:10.2174/187152109787846060 (2009).

309 Kang, S. *et al.* Systemic delivery of TNF-related apoptosis-inducing ligand (TRAIL) elevates levels of tissue inhibitor of metalloproteinase-1 (TIMP-1) and prevents type 1 diabetes in nonobese diabetic mice. *Endocrinology* **151**, 5638-5646, doi:10.1210/en.2009-0478 (2010).

310 Lamhamedi-Cherradi, S. E., Zheng, S. J., Maguschak, K. A., Peschon, J. & Chen, Y. H. Defective thymocyte apoptosis and accelerated autoimmune diseases in TRAIL-/- mice. *Nat Immunol* **4**, 255-260, doi:10.1038/ni894 (2003).

311 Dadey, R. E. *et al.* Regulatory T Cell-Derived TRAIL Is Not Required for Peripheral Tolerance. *Immunohorizons* **5**, 48-58, doi:10.4049/immunohorizons.2000098 (2021).

312 Zakharov, P. N., Hu, H., Wan, X. & Unanue, E. R. Single-cell RNA sequencing of murine islets shows high cellular complexity at all stages of autoimmune diabetes. *J Exp Med* **217**, doi:10.1084/jem.20192362 (2020).

313 Papageorgiou, A., Dinney, C. P. & McConkey, D. J. Interferon-alpha induces TRAIL expression and cell death via an IRF-1-dependent mechanism in human bladder cancer cells. *Cancer Biol Ther* **6**, 872-879, doi:10.4161/cbt.6.6.4088 (2007).

314 Betterle, C. *et al.* Islet cell and insulin autoantibodies in organ-specific autoimmune patients. Their behaviour and predictive value for the development of type 1 (insulin-dependent) diabetes mellitus. A 10-year follow-up study. *Diabetologia* **30**, 292-297, doi:10.1007/BF00299020 (1987).

315 Hartwig, T. *et al.* The TRAIL-Induced Cancer Secretome Promotes a Tumor-Supportive Immune Microenvironment via CCR2. *Mol Cell* **65**, 730-742 e735, doi:10.1016/j.molcel.2017.01.021 (2017).

316 von Karstedt, S. *et al.* Cancer cell-autonomous TRAIL-R signaling promotes KRAS-driven cancer progression, invasion, and metastasis. *Cancer Cell* **27**, 561-573, doi:10.1016/j.ccell.2015.02.014 (2015).

317 Cheung, S. S. *et al.* Tumor necrosis factor-related apoptosis-inducing ligand and CD56 expression in patients with type 1 diabetes mellitus. *Pancreas* **30**, 105-114, doi:10.1097/01.mpa.0000148515.77497.4b (2005).

318 Qaisar, N., Jurczyk, A. & Wang, J. P. Potential role of type I interferon in the pathogenic process leading to type 1 diabetes. *Curr Opin Endocrinol Diabetes Obes* **25**, 94-100, doi:10.1097/MED.0000000000000399 (2018).

319 Li, Q. *et al.* Interferon-alpha initiates type 1 diabetes in nonobese diabetic mice. *Proc Natl Acad Sci U S A* **105**, 12439-12444, doi:10.1073/pnas.0806439105 (2008).

320 Zhou, X., Bailey-Bucktrout, S., Jeker, L. T. & Bluestone, J. A. Plasticity of CD4(+) FoxP3(+) T cells. *Curr Opin Immunol* **21**, 281-285, doi:10.1016/j.coi.2009.05.007 (2009).

321 Lin, W. *et al.* Allergic dysregulation and hyperimmunoglobulinemia E in Foxp3 mutant mice. *J Allergy Clin Immunol* **116**, 1106-1115, doi:10.1016/j.jaci.2005.08.046 (2005).

322 Rubtsov, Y. P. *et al.* Stability of the regulatory T cell lineage in vivo. *Science* **329**, 1667-1671, doi:10.1126/science.1191996 (2010).

323 Korn, T. & Muschaweckh, A. Stability and Maintenance of Foxp3(+) Treg Cells in Non-lymphoid Microenvironments. *Front Immunol* **10**, 2634, doi:10.3389/fimmu.2019.02634 (2019).

324 Hanks, B. A. *et al.* Type III TGF-beta receptor downregulation generates an immunotolerant tumor microenvironment. *J Clin Invest* **123**, 3925-3940, doi:10.1172/JCI65745 (2013).

325 Skene, P. J. & Henikoff, S. An efficient targeted nuclease strategy for high-resolution mapping of DNA binding sites. *Elife* **6**, doi:10.7554/eLife.21856 (2017).

326 Delacher, M. *et al.* Single-cell chromatin accessibility landscape identifies tissue repair program in human regulatory T cells. *Immunity* **54**, 702-720 e717, doi:10.1016/j.immuni.2021.03.007 (2021).

327 Jing, X. *et al.* Role of hypoxia in cancer therapy by regulating the tumor microenvironment. *Mol Cancer* **18**, 157, doi:10.1186/s12943-019-1089-9 (2019).

328 Jones, W. & Bianchi, K. Aerobic glycolysis: beyond proliferation. *Front Immunol* **6**, 227, doi:10.3389/fimmu.2015.00227 (2015).

329 Zheng, J. Energy metabolism of cancer: Glycolysis versus oxidative phosphorylation (Review). *Oncol Lett* **4**, 1151-1157, doi:10.3892/ol.2012.928 (2012).

330 Nadzialek, S. *et al.* Understanding the gap between the estrogenicity of an effluent and its real impact into the wild. *Sci Total Environ* **408**, 812-821, doi:10.1016/j.scitotenv.2009.09.002 (2010).

331 Chang, C. H. *et al.* Metabolic Competition in the Tumor Microenvironment Is a Driver of Cancer Progression. *Cell* **162**, 1229-1241, doi:10.1016/j.cell.2015.08.016 (2015).

332 Jiang, B. Aerobic glycolysis and high level of lactate in cancer metabolism and microenvironment. *Genes Dis* **4**, 25-27, doi:10.1016/j.gendis.2017.02.003 (2017).

333 Sugiura, A. & Rathmell, J. C. Metabolic Barriers to T Cell Function in Tumors. *J Immunol* **200**, 400-407, doi:10.4049/jimmunol.1701041 (2018).

334 Brand, A. *et al.* LDHA-Associated Lactic Acid Production Blunts Tumor Immunosurveillance by T and NK Cells. *Cell Metab* **24**, 657-671, doi:10.1016/j.cmet.2016.08.011 (2016).

335 Angelin, A. *et al.* Foxp3 Reprograms T Cell Metabolism to Function in Low-Glucose, High-Lactate Environments. *Cell Metab* **25**, 1282-1293 e1287, doi:10.1016/j.cmet.2016.12.018 (2017).

336 Pacella, I. & Piconese, S. Immunometabolic Checkpoints of Treg Dynamics: Adaptation to Microenvironmental Opportunities and Challenges. *Front Immunol* **10**, 1889, doi:10.3389/fimmu.2019.01889 (2019).

337 Clambey, E. T. *et al.* Hypoxia-inducible factor-1 alpha-dependent induction of FoxP3 drives regulatory T-cell abundance and function during inflammatory hypoxia of the mucosa. *Proc Natl Acad Sci U S A* **109**, E2784-2793, doi:10.1073/pnas.1202366109 (2012).

338 Wang, Y. A. *et al.* Effects of tumor metabolic microenvironment on regulatory T cells. *Mol Cancer* **17**, 168, doi:10.1186/s12943-018-0913-y (2018).

339 Scharping, N. E., Menk, A. V., Whetstone, R. D., Zeng, X. & Delgoffe, G. M. Efficacy of PD-1 Blockade Is Potentiated by Metformin-Induced Reduction of Tumor Hypoxia. *Cancer Immunol Res* **5**, 9-16, doi:10.1158/2326-6066.CIR-16-0103 (2017).

340 Chulpanova, D. S., Kitaeva, K. V., Rutland, C. S., Rizvanov, A. A. & Solovyeva, V. V. Mouse Tumor Models for Advanced Cancer Immunotherapy. *Int J Mol Sci* **21**, doi:10.3390/ijms21114118 (2020).

341 Li, E., Lin, L., Chen, C. W. & Ou, D. L. Mouse Models for Immunotherapy in Hepatocellular Carcinoma. *Cancers (Basel)* **11**, doi:10.3390/cancers11111800 (2019).

342 Shackleton, M., Quintana, E., Fearon, E. R. & Morrison, S. J. Heterogeneity in cancer: cancer stem cells versus clonal evolution. *Cell* **138**, 822-829, doi:10.1016/j.cell.2009.08.017 (2009).

343 Aktary, Z., Corvelo, A., Estrin, C. & Larue, L. Sequencing two Tyr::CreER(T2) transgenic mouse lines. *Pigment Cell Melanoma Res* **33**, 426-434, doi:10.1111/pcmr.12842 (2020).

344 Dankort, D. *et al.* Braf(V600E) cooperates with Pten loss to induce metastatic melanoma. *Nat Genet* **41**, 544-552, doi:10.1038/ng.356 (2009).

345 Schreiber, T. H. & Podack, E. R. A critical analysis of the tumour immunosurveillance controversy for 3-MCA-induced sarcomas. *Br J Cancer* **101**, 381-386, doi:10.1038/sj.bjc.6605198 (2009).

346 Chiba, K. FTY720, a new class of immunomodulator, inhibits lymphocyte egress from secondary lymphoid tissues and thymus by agonistic activity at sphingosine 1-phosphate receptors. *Pharmacol Ther* **108**, 308-319, doi:10.1016/j.pharmthera.2005.05.002 (2005).

347 Brinkmann, V., Cyster, J. G. & Hla, T. FTY720: sphingosine 1-phosphate receptor-1 in the control of lymphocyte egress and endothelial barrier function. *Am J Transplant* **4**, 1019-1025, doi:10.1111/j.1600-6143.2004.00476.x (2004).

348 Mognol, G. P. *et al.* Exhaustion-associated regulatory regions in CD8(+) tumor-infiltrating T cells. *Proc Natl Acad Sci U S A* **114**, E2776-E2785, doi:10.1073/pnas.1620498114 (2017).

349 Pauken, K. E. *et al.* Epigenetic stability of exhausted T cells limits durability of reinvigoration by PD-1 blockade. *Science* **354**, 1160-1165, doi:10.1126/science.aaf2807 (2016).

350 Zappasodi, R. *et al.* Rational design of anti-GITR-based combination immunotherapy. *Nat Med* **25**, 759-766, doi:10.1038/s41591-019-0420-8 (2019).

351 Ko, K. *et al.* Treatment of advanced tumors with agonistic anti-GITR mAb and its effects on tumor-infiltrating Foxp3+CD25+CD4+ regulatory T cells. *J Exp Med* **202**, 885-891, doi:10.1084/jem.20050940 (2005).

352 Cohen, A. D. *et al.* Agonist anti-GITR monoclonal antibody induces melanoma tumor immunity in mice by altering regulatory T cell stability and intra-tumor accumulation. *PLoS One* **5**, e10436, doi:10.1371/journal.pone.0010436 (2010).

353 Turk, M. J. *et al.* Concomitant tumor immunity to a poorly immunogenic melanoma is prevented by regulatory T cells. *J Exp Med* **200**, 771-782, doi:10.1084/jem.20041130 (2004).

354 Finnberg, N. *et al.* DR5 knockout mice are compromised in radiation-induced apoptosis. *Mol Cell Biol* **25**, 2000-2013, doi:10.1128/MCB.25.5.2000-2013.2005 (2005).

355 Yuan, X. *et al.* Developing TRAIL/TRAIL death receptor-based cancer therapies. *Cancer Metastasis Rev* **37**, 733-748, doi:10.1007/s10555-018-9728-y (2018).

356 Schneider, P. *et al.* Identification of a new murine tumor necrosis factor receptor locus that contains two novel murine receptors for tumor necrosis factor-related apoptosis-inducing ligand (TRAIL). *J Biol Chem* **278**, 5444-5454, doi:10.1074/jbc.M210783200 (2003).

357 LeBlanc, H. N. & Ashkenazi, A. Apo2L/TRAIL and its death and decoy receptors. *Cell Death Differ* **10**, 66-75, doi:10.1038/sj.cdd.4401187 (2003).

358 Mbongue, J. C., Nieves, H. A., Torrez, T. W. & Langridge, W. H. The Role of Dendritic Cell Maturation in the Induction of Insulin-Dependent Diabetes Mellitus. *Front Immunol* **8**, 327, doi:10.3389/fimmu.2017.00327 (2017).

359 Wherry, E. J. T cell exhaustion. *Nat Immunol* **12**, 492-499, doi:10.1038/ni.2035 (2011).

360 Young, A., Nguyen, V., Mehdizadeh, S., Sheehan, K.C.F., Serreze, D.V., Schreiber, R.D., Bluestone, J.A. Development of syngeneic NOD tumor models to study tumor immunity in autoimmune-prone mice. *J Immunol* **178** (2018).

361 Brincks, E. L., Katewa, A., Kucaba, T. A., Griffith, T. S. & Legge, K. L. CD8 T cells utilize TRAIL to control influenza virus infection. *J Immunol* **181**, 4918-4925, doi:10.4049/jimmunol.181.7.4918 (2008).

362 Shrestha, B., Pinto, A. K., Green, S., Bosch, I. & Diamond, M. S. CD8+ T cells use TRAIL to restrict West Nile virus pathogenesis by controlling infection in neurons. *J Virol* **86**, 8937-8948, doi:10.1128/JVI.00673-12 (2012).

363 Schmidt, M. E. & Varga, S. M. The CD8 T Cell Response to Respiratory Virus Infections. *Front Immunol* **9**, 678, doi:10.3389/fimmu.2018.00678 (2018).

364 Matsuoka, Y., Lamirande, E. W. & Subbarao, K. The mouse model for influenza. *Curr Protoc Microbiol* **Chapter 15**, Unit 15G 13, doi:10.1002/9780471729259.mc15g03s13 (2009).

365 Abdel-Hakeem, M. S. Viruses Teaching Immunology: Role of LCMV Model and Human Viral Infections in Immunological Discoveries. *Viruses* **11**, doi:10.3390/v11020106 (2019).

366 Prochazka, M., Serreze, D. V., Frankel, W. N. & Leiter, E. H. NOR/Lt mice: MHC-matched diabetes-resistant control strain for NOD mice. *Diabetes* **41**, 98-106, doi:10.2337/diab.41.1.98 (1992).

367 Rivadeneira, D. B. *et al.* Oncolytic Viruses Engineered to Enforce Leptin Expression Reprogram Tumor-Infiltrating T Cell Metabolism and Promote Tumor Clearance. *Immunity* **51**, 548-560 e544, doi:10.1016/j.immuni.2019.07.003 (2019).

368 Najjar, Y. G. *et al.* Tumor cell oxidative metabolism as a barrier to PD-1 blockade immunotherapy in melanoma. *JCI Insight* **4**, doi:10.1172/jci.insight.124989 (2019).

369 Williams, R. *et al.* Preclinical models of HPV+ and HPV- HNSCC in mice: an immune clearance of HPV+ HNSCC. *Head Neck* **31**, 911-918, doi:10.1002/hed.21040 (2009).

370 Lechner, M. G. *et al.* Immunogenicity of murine solid tumor models as a defining feature of in vivo behavior and response to immunotherapy. *J Immunother* **36**, 477-489, doi:10.1097/01.cji.0000436722.46675.4a (2013).

371 Overwijk, W. W. & Restifo, N. P. B16 as a mouse model for human melanoma. *Curr Protoc Immunol* **Chapter 20**, Unit 20 21, doi:10.1002/0471142735.im2001s39 (2001).

372 Rosenberg, S. A., Spiess, P. & Lafreniere, R. A new approach to the adoptive immunotherapy of cancer with tumor-infiltrating lymphocytes. *Science* **233**, 1318-1321, doi:10.1126/science.3489291 (1986).

373 Vallera, D. A., Taylor, P. A., Aukerman, S. L. & Blazar, B. R. Antitumor protection from the murine T-cell leukemia/lymphoma EL4 by the continuous subcutaneous coadministration of recombinant macrophage-colony stimulating factor and interleukin-2. *Cancer Res* **53**, 4273-4280 (1993).

374 Vermeer, D. W. *et al.* Metastatic model of HPV+ oropharyngeal squamous cell carcinoma demonstrates heterogeneity in tumor metastasis. *Oncotarget* **7**, 24194-24207, doi:10.18632/oncotarget.8254 (2016).

375 Johnstone, C. N. *et al.* Functional and molecular characterisation of EO771.LMB tumours, a new C57BL/6-mouse-derived model of spontaneously metastatic mammary cancer. *Dis Model Mech* **8**, 237-251, doi:10.1242/dmm.017830 (2015).

376 Than, N. G., Hahn, S., Rossi, S. W. & Szekeres-Bartho, J. Editorial: Fetal-Maternal Immune Interactions in Pregnancy. *Front Immunol* **10**, 2729, doi:10.3389/fimmu.2019.02729 (2019).

377 Samstein, R. M., Josefowicz, S. Z., Arvey, A., Treuting, P. M. & Rudensky, A. Y. Extrathymic generation of regulatory T cells in placental mammals mitigates maternal-fetal conflict. *Cell* **150**, 29-38, doi:10.1016/j.cell.2012.05.031 (2012).